SURFACE POTENTIAL AND INFRARED SPECTROSCOPIC STUDIES IN HETEROGENEOUS CATALYSIS

A thesis submitted for the degree of

Doctor of Philosophy

of the University of London

by

Dr. rer. nat. Hansjürgen HEYNE

Dipl. Chem.

Department of Chemistry,

Imperial College,

London, S.W.7.

April 1965

ABSTRACT

The chemisorption of carbon monoxide on platinum has been investigated by means of infrared spectroscopy (1) and surface potential measurements (2).

The infrared investigations show that only the linear chemisorbed CO species is present on a platinum surface.

The CO stretching band of this species is observed at about 2070 cm^{-1}.

Its apparent extinction coefficient has been found to be

$$k_a = 2 \times 10^{-18} \text{ cm}^2 \times \text{molecules}^{-1}$$

$$= 12 \times 10^2 \text{ litre} \times \text{mole}^{-1} \times \text{cm}^{-1}$$

The apparent integrated absorption intensity B of this band has been found to be

$$B = 680 \text{ to } 1260 \times 10^2 \text{ litre} \times \text{mole}^{-1} \times \text{cm}^{-2}$$

decreasing with increasing coverage.

On oxidized platinum surfaces two new CO stretching bands have been observed.

They have been attributed to the surface species

"Pt^{++} - CO" : band position at 2120 cm^{-1} and

"Pt^{++++} - CO" : band position at 2170 cm^{-1}.

The values for the apparent extinction coefficient and the apparent integrated absorption intensity for the CO stretching band of carbon monoxide chemisorbed by Pt^{2+}-ions have been found to be

$$k_a = 0.4 \text{ to } 0.5 \times 10^{-18} \text{ cm}^2 \times \text{molecules}^{-1}$$

$$= 2.4 \text{ to } 3.0 \times 10^{2} \text{ litre} \times \text{mole}^{-1} \times \text{cm}^{-1}$$

and

$$B = 290 \times 10^{2} \text{ litre} \times \text{mole}^{-1} \times \text{cm}^{-2}$$

The surface potential of carbon monoxide on platinum has been found to be

Pt/CO; T = 300° K S.P. = 0.00 ± 0.01 volt

T = 77° K S.P. = 0.00 ± 0.01 volt

The final figure for the surface potential of oxygen on platinum is

Pt/O_2; T = 300° K S.P. = - 1.04 ± 0.01 volt

The surface potential of carbon monoxide on palladium has been determined, thus enabling the surface potential figures in the series nickel, palladium, and platinum to be compared.

Ni/CO; T = 293° K S.P. = - 1.09 volt (3)

Pd/CO; T = 300° K S.P. = - 0.84 volt

Pt/CO; T = 300° K S.P. = ⁻ 0.00 volt

The kinetics of the oxidation of chemisorbed carbon monoxide have been investigated by means of infrared technique and surface potential measurements.

The reaction velocity at P_{O_2}:0.5 to 5 mm Hg and T:250 to 370° K can be described by

$$V = k \times \left[CO_a\right]^2 \times P_{O_2} \times f(T, P_{O_2})$$

The following mechanism has been proposed

$$O_{2\ g} \rightleftharpoons O_{2\ ad}$$

$$O_{2\ ad} + CO_a \rightleftharpoons CO_3\ a$$

$$CO_3\ a + CO_a \rightleftharpoons 2\ CO_{2\ g} + Pt_2$$

$$Pt_2 + O_{2\ g} \longrightarrow 2\ O_a$$

(suffix a - chemisorbed state;
suffix ad - physically adsorbed state).

The experimental velocities have been explained

in terms of the basic collision theory; a steric factor of $P \sim 0.1$ has been derived.

The experimental activation energy has been found to be about 10 K cal $mole^{-1}$ depending on the activity of the platinum catalyst.

ACKNOWLEDGEMENTS

I thank Professor R. M. Barrer, F.R.S., for the provision of laboratory facilities in the Department of Physical Chemistry of Imperial College.

I wish to thank most sincerely my supervisor, Professor F. C. Tompkins, F.R.S., whose great enthusiasm and continual interest in my work over the last two years has been a great source of encouragement.

My sincere thanks, too, to Dr. D. O. Hayward for many helpful discussions during the course of this work.

I am most grateful to my friends N. Taylor and C. McManus who were always around me in times of need.

Thanks are also due to the technical staff of the Chemistry Department of Imperial College for their indispensable assistance.

Finally I wish to record my gratitude to the Deutsche Akademische Austauschdienst, Bonn, for the award of a Nato-fellowship.

CONTENTS

PART 1

INFRARED SPECTROSCOPIC STUDIES OF THE PROPERTIES OF CARBON MONOXIDE ON AEROSIL SUPPORTED PLATINUM AND PLATINUM OXIDE SURFACES.

		page
1.1	Introduction	13
1.2	Experimental	15
1.3	Interaction of CO, H_2, N_2, CO_2, A with the Aerosil support material	21
1.4	Interaction of H_2, O_2, N_2, CO_2, A with the Aerosil-supported platinum sample	24
1.5	Determination of the apparent extinction coefficient of the CO stretching band of the chemisorbed carbon monoxide	30

page

1.6 Determination of the apparent integrated absorption intensity of the CO stretching band of the chemisorbed carbon monoxide 37

1.7 Interaction of N_2, CO_2, and A with the chemisorbed carbon monoxide 50

1.8 Interaction of H_2 with the chemisorbed carbon monoxide 52

1.9 Interaction of O_2 with the chemisorbed carbon monoxide 57

1.10 Chemisorption of carbon monoxide on an oxidized platinum surface 59

1.11 Properties of carbon monoxide chemisorbed by Pt^{2+}-ions; deterimination of the apparent extinction coefficient and the apparent integrated

page

absorption intensity of the CO stretching band 71

1.12 Identification of the CO band at 2170 cm^{-1} 79

1.13 Discussion of the chemisorption of carbon monoxide on platinum and platinum ions 83

PART 2

INFRARED SPECTROSCOPIC AND SURFACE POTENTIAL STUDIES OF THE OXIDATION OF CHEMISORBED CARBON MONOXIDE ON PLATINUM.

page

2.1 Introduction 90

2.2 Infrared spectroscopic studies of the kinetic of the oxidation of carbon monoxide chemisorbed on Aerosil-supported platinum 91

2.2.1 Experimental 91

2.2.2 Discussion 100

page

2.3 Surface potential studies of the chemisorption of carbon monoxide and oxygen on platinum films 115

2.3.1 Experimental 115

2.3.2 Chemisorption of carbon monoxide on platinum films at 300° K and 77° K 116

2.3.3 Chemisorption of oxygen on platinum films at 300° K 123

2.4 Surface potential studies of the reaction between chemisorbed carbon monoxide and gaseous oxygen 128

2.5 Surface potential studies of the reaction between chemisorbed oxygen and gaseous carbon monoxide 129

2.6 Surface potential studies of the kinetics of the oxidation of

page

carbon monoxide chemisorbed on platinum films 137

2.7 Discussion of the kinetic results and the mechanism of the oxidation of carbon monoxide chemisorbed on platinum 152

REFERENCES 180

PART 1

INFRARED SPECTROSCOPIC STUDIES OF THE PROPERTIES OF CARBON MONOXIDE CHEMISORBED ON AEROSIL SUPPORTED PLATINUM AND PLATINUM OXIDE SURFACES.

1.1 Introduction

Since the pioneering work of Eischens et al. (1) the I.R. spectroscopic technique has become one of the main tools for studying the surface chemistry of metals (5, 6) and the I.R. work was soon extended to a whole variety of gases which were chemisorbed on the surfaces of transition metals (7, 8, 9, 10, 11).

Among others the I.R. work on the system Pt/H_2 (12) and Ni/N_2 (13) and on the chemisorption of CO on Au (14) provide more interesting information about the bonding of the chemisorbed molecules. It is hoped to get more insight into the bonding of adsorbed molecules by comparing their spectra with those of similar inorganic compounds.

Our work is mainly concerned with the chemisorption of CO on Pt- and Pt-oxide-surfaces.

The system Pt/CO has already been studied by Eischens et al. (10).

New results concerning the I.R. spectra of Pt-carbonyl

compounds (15) and the recent studies of the integrated absorption intensities on a series of transition metal carbonyls and carbonyl-compounds (16) initiated further work.

The application of these results as well as their underlying ideas lead to interesting conclusions upon the bonding structure of the carbon monoxide chemisorbed on Pt- and on oxidized Pt-surfaces.

1.2 Experimental

In this work the technique of silica supported metals first introduced by Eischens et al. (1) is used.

2500 mg "Aerosil"[x] are mixed with an aqueous solution of 500 mg $H_2PtCl_6 \times H_2O$, corresponding to a metal content of 8.4 weight %.

The slurry is then dried in an oven at 160° C for six hours. The substance is powdered in a glass mortar and amounts between 100 and 400 mg are introduced into a die (fig. 1) and pressed to form pellets (Ø = 30 mm). The die is so designed that the pellet (p) is in a metal tubing (t) of stainless steel. This allows easy handling of the pellet and it also improves the thermal contact with the furnace (f) of the direct-transmission-cell (fig. 2) which is connected to the high vacuum apparatus (fig. 3). The metal tubing is kept in its final position by two springs (s).

The furnace (f) can be heated by a Pt-resistance wire up to 350° C. The temperature of the pellet is taken from the inside of the metal tubing by a thermocouple (th).

---

[x] Aerosil (Typ 2491/460) from DEGUSSA, Frankfurt a. M., GERMANY

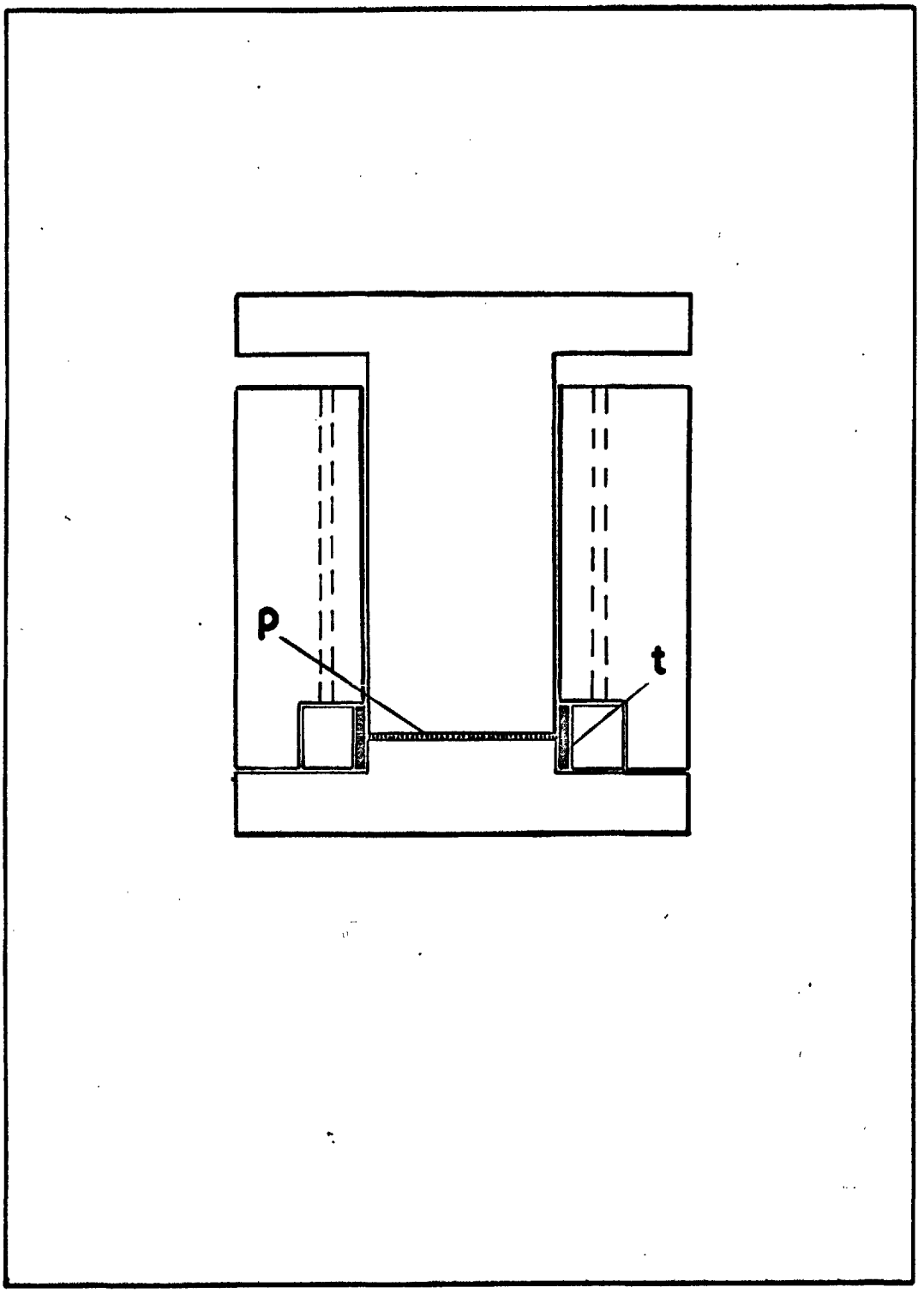


Fig.1. Pellet die

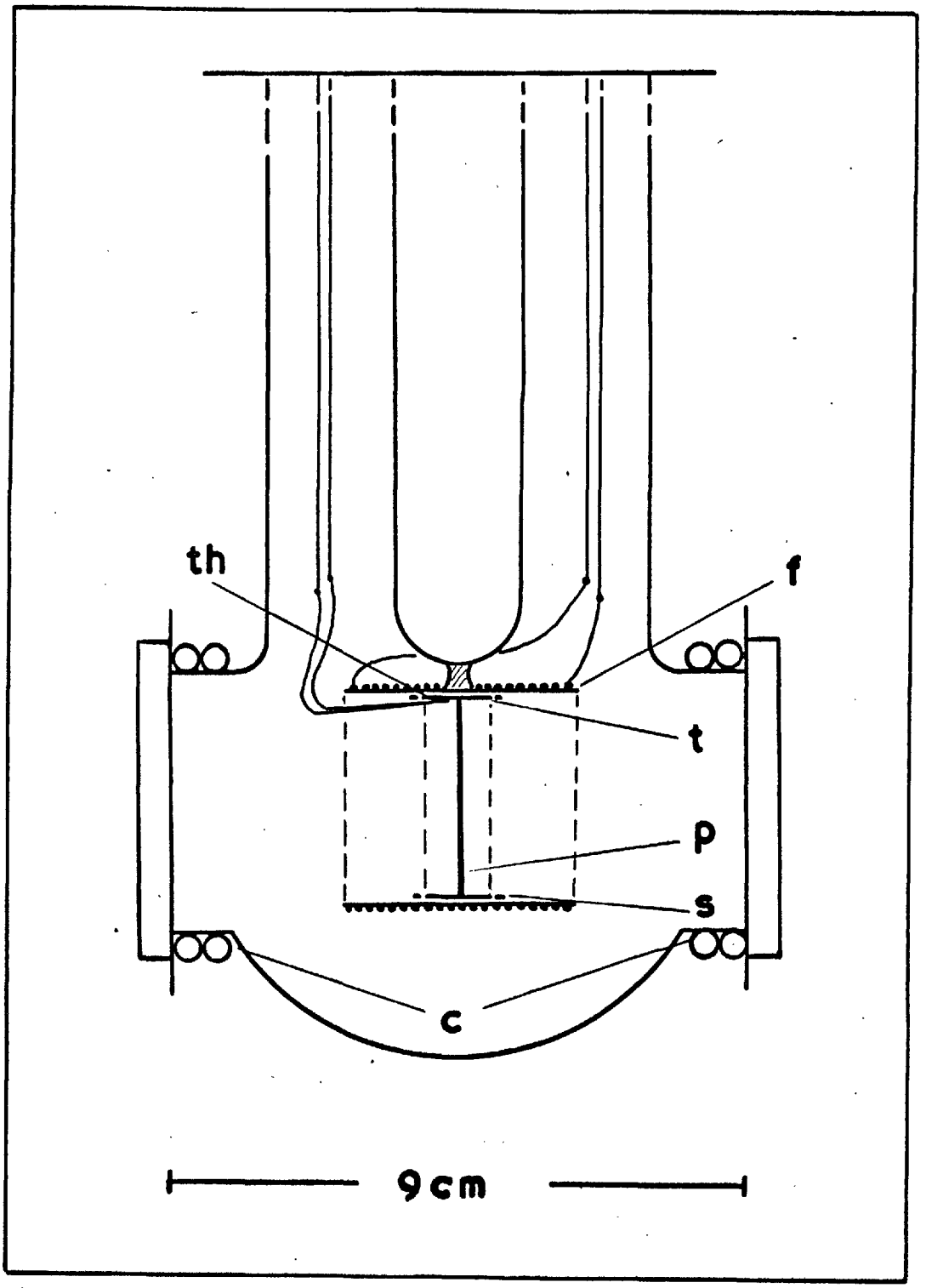


Fig.2. Cell for infrared study of chemisorbed gases

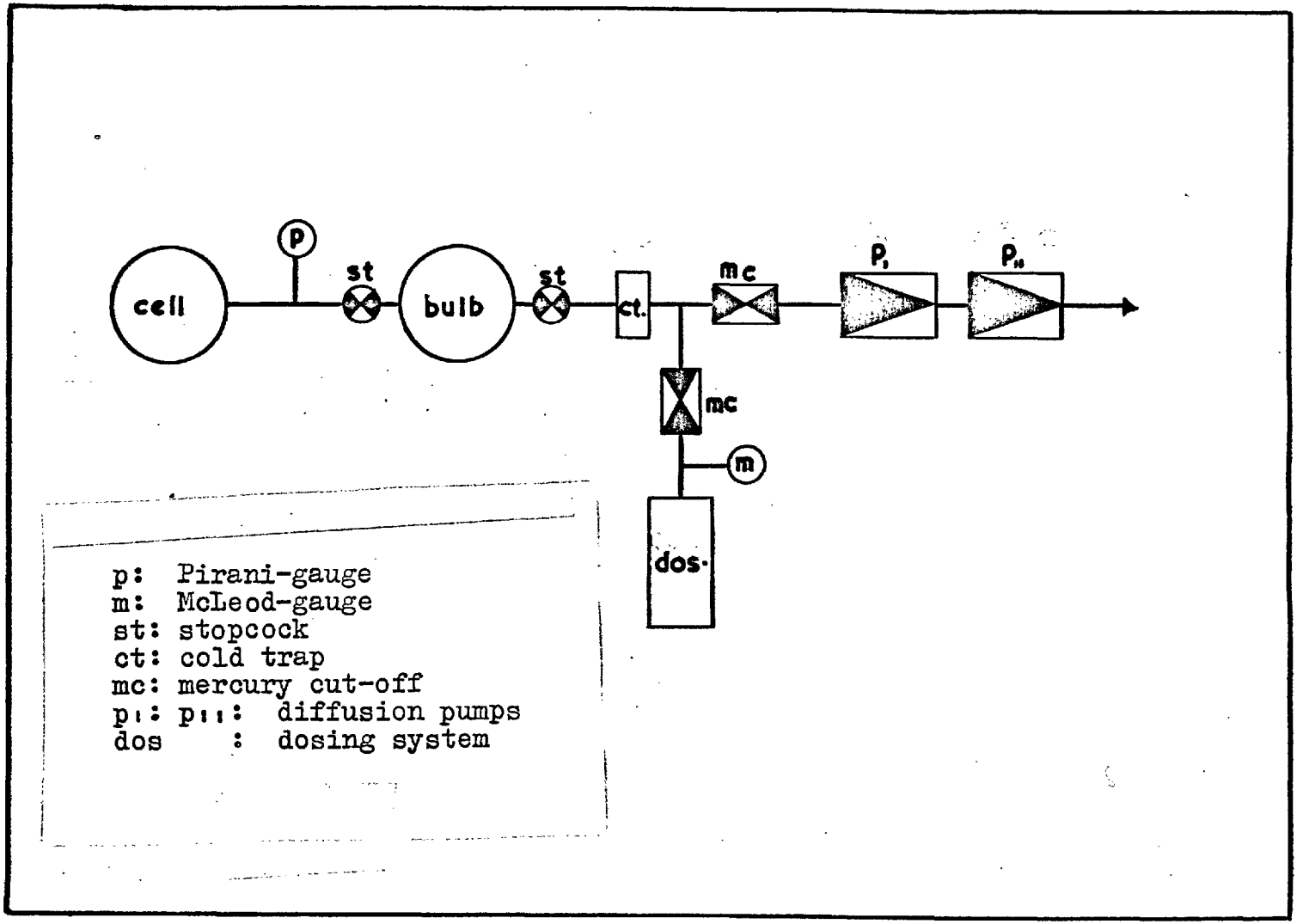


Fig.3. Vacuum apparatus

The CaF_2 windows of the cell are fixed with Picein. They are kept cool by a simple water cooling system, in which Compo-tubings (lead alloy) are used for the coils (c).

The transmission of the I.R. cell with its CaF_2 windows is 85%.

The transmission with a 120 mg pellet is 15 % and with a 400 mg pellet 4% at 2060 cm^{-1}. Under high vacuum conditions the pellet is baked out in the furnace (f) of the cell (fig. 2) for 2-4 hours at 250-300° C. Finally the surface of the deposited Pt-particles is cleaned in an atmosphere of 10 m.m H_2 at 200° C for another 4 hours. The H_2 is renewed 3 to 4 times and is then pumped off and the pellet is degassed for two hours at 200° C. After cooling the Pt-Aerosil-pellet is capable of chemisorbing carbon monoxide.

The I.R. measurements are taken by the usual differential method, i.e., in the reference beam there is another cell with a similar Pt-Aerosil-pellet. The I.R. measurements were made with a Perkin Elmer Infracord Model 137 E. Owing to the large losses of I.R. energy due to Rayleigh scattering and the absorption of the Aerosil and the Pt-particles only 4% of the whole I.R. radiation at about 2060 cm^{-1} is getting into the detector (400 mg-sample). As the size of the Aerosil and Pt-particles is in the order

of 100 Å and, hence, about 1% of the wavelength of the I.R. radiation there are no losses of radiation due to light scattering caused by reflection or refraction.

Because of the small transparency of the sample it was necessary to work with 5 times wider slit widths of the monochromator to bring about 25 times more energy into the detector and to obtain sufficient power for the pen servo system. Further, the method of compensated spectra was used by inserting another I.R. cell with a similar Pt-pellet into the reference beam.

By working with 5 times wider slit widths we are loosing resolution. But this fact is not too serious as we are dealing with the absorption bands of a chemisorbed CO layer with broad absorption bands like those of liquid and solid carbon monoxide. (17).

Our I.R. work was carried out with a spectral slit width of 23 cm^{-1} which is about the half band width of liquid CO (22 cm^{-1} at 80° K) (17). Under our operating conditions the reproducibility of the recorded spectra is $\pm$ 0.5% T (ordinate) and $\pm$ 0.01 μ (abscissa).

1.3 Interaction of CO, H_2, O_2, N_2, CO_2, A with the Aerosil support material

In the region between 4000-1200 cm^{-1} in which our I.R. work was done, Aerosil has the following absorption bands (tab. 1); these are listed with those which Benesi and Jones (17) obtained for their water-silica-system.

The Aerosil spectrum was taken from a sample in the form of a pellet. The bands at 2900 cm^{-1}, 2850 cm^{-1} and 2330 cm^{-1}, which are not contained in the spectra of the silica gel originate from a small hydrocarbon content and from adsorbed carbon dioxide. The adsorbed CO_2 is easily removed by baking out the sample under high vacuum conditions. But the hydrocarbons remain unchanged even after heating for a long time under an oxygen pressure of 10 mm Hg.

The differences in the positions of that two sets of bands (tab. 1) might be caused by different processing of the samples and different particle structures and sizes.

The interaction arising from the adsorption of the different gases on the surface groups of the Aerosil was studied in a separate experiment.

Table 1

Aerosil	Silica-Gel (17)	Assignment
	3730 cm^{-1} (m)	OH-stretching vibration
3450 cm^{-1} (st)	3580 cm^{-1} (m)	OH- " "
2900 cm^{-1} (w)		
2850 cm^{-1} (w)		
2330 cm^{-1} (m)		
1970 cm^{-1} (sh)	2000 cm^{-1} (w)	Si-O combination vibration
1850 cm^{-1} (m)	1875 cm^{-1} (w)	Si-O " "
1620 cm^{-1} (m)	1640 cm^{-1} (w)	Si-O overtone vibration
	1635 cm^{-1} (m)	HOH bending vibration
	1200 cm^{-1} (sh)	SiO stretching vibration
	1095 cm^{-1} (v.st.)	SiO stretching vibration

(w) - weak, (m) - medium, (st) - strong, (v.st.) - very strong,
(sh) - shoulder

140 mg Aerosil were mixed with distilled water and then dried at 160° C in an oven and pressed to form a pellet. The sample was baked out for 3 hours at 250° C under high vacuum conditions until there was no further change in the I.R. spectra of this sample. After cooling to room temperature various gases (CO, H_2, O_2, N_2, CO_2, A) were added (p = 10 mm).

Except for the bands of CO_2 and CO when these gases were present, there were no specific bands observed in this region. The CO_2 and CO bands could be easily removed by pumping.

As there was no change in the position and in the intensities of the Aerosil bands, the adsorption of these gases and their interaction with the surface is of minor importance.

1.4 Interaction of H_2, O_2, N_2, CO_2, A with the Aerosil supported platinum sample

For the following experiment one of our Aerosil supported Pt-pellets (400 mg) is used.

In the region between 2200 and 1300 cm^{-1} there are with the exception of CO and H_2 no specific bands observed when the other gases are introduced. The runs are carried out at room temperature and the gas pressure used is in the range between 10^{-1} and 10 mm Hg. All gases increase the absorption of the SiO combination vibration band at 1850 cm^{-1}, the SiO overtone vibration and HOH bending vibration bands at about 1650 cm^{-1}. The large increase of the absorption above 1400 cm^{-1} is caused by the interaction of these adsorbed gases with the Si-O groups on the Aerosil surface (SiO vibration bands at 1200 cm^{-1} and 1095 cm^{-1}). In the presence of H_2 this effect is remarkably large, probably due to the strong interaction of H_2 with oxygen containing groups on the surface.

In fig. 4 is shown how important this effect is for the different gases. The effect on the SiO combination vibration band is larger than on the SiO-overtone or HOH bending vibration bands both of which cannot be separated

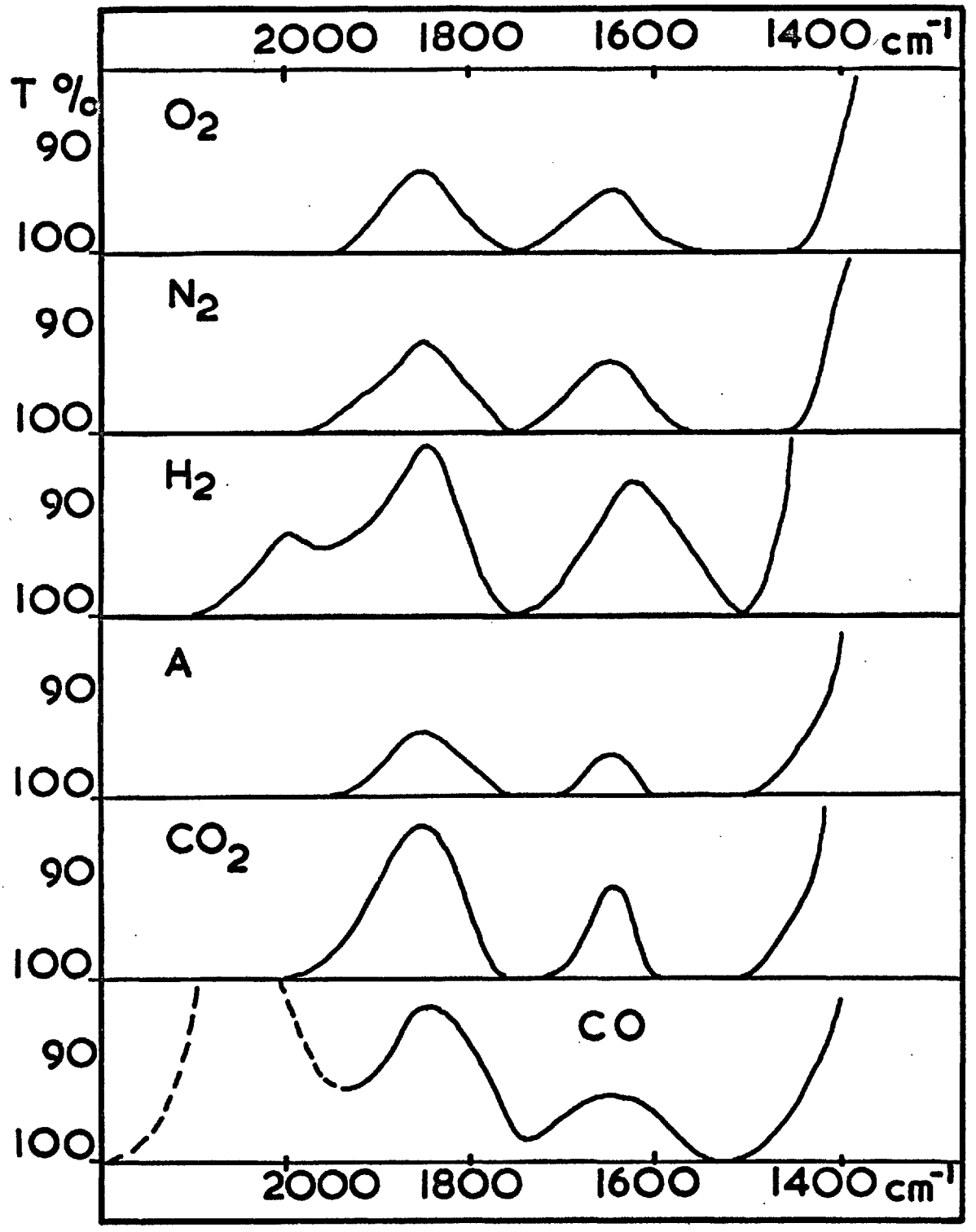


Fig.4. Interaction of various gases with the Aerosil support of the Pt-sample

in our spectra. Fig. 4 also contains the corresponding data for the gas CO whose specific interaction with the Pt metal surface (CO-band at about 2070 cm^{-1}) is discussed later.

According to the magnitude of their effect on the support the series of added gases can be separated into four groups.

I: H_2

II: CO_2, CO

III: N_2, O_2

IV: A

The band at 2000 cm^{-1} in the presence of H_2 may be either attributed to a particular strong interaction of H_2 with the SiO surface groups or, more probably, may be attributed to the band of H_2 chemisorbed on Pt (12). The observed effects on the Aerosil surface groups can be very easily removed by pumping within one or two minutes.

Higher pressure above 10 mm Hg effects a further increase of the absorption of the Aerosil bands. In the case of O_2 it is shown in fig. 5 how the maximum extinction $E_a = \log T_{o/T}$ for the bands at 1850 cm^{-1} and 1650 cm^{-1} depends on the gas pressure. T and T_o are the transparencies with and without the gas phase present in the cell.

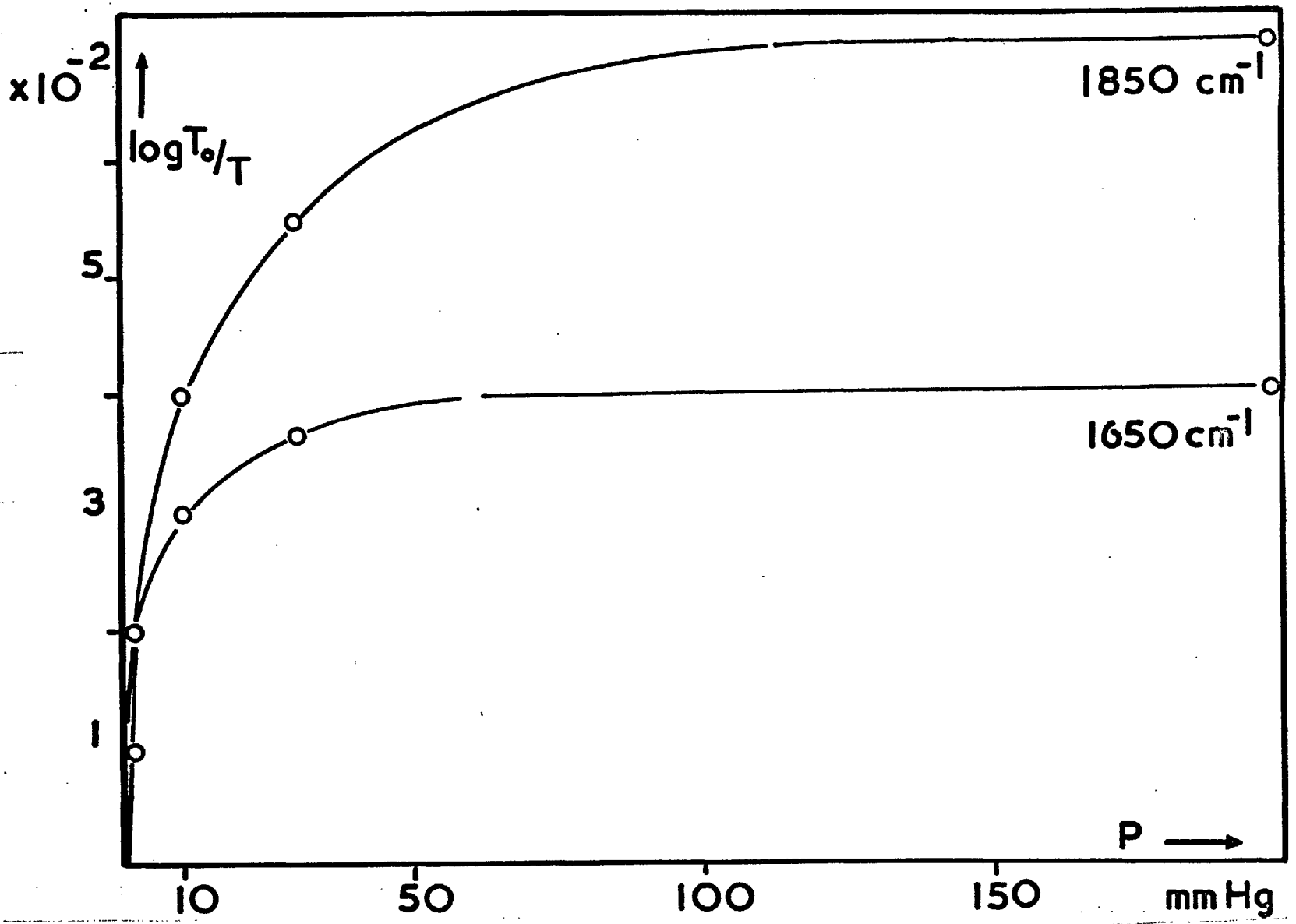


Fig.5. Pressure dependency of the interaction between oxygen and the Aerosil support of the Pt-sample

If one assumes that log T_o/T is proportional to the concentration of the adsorbed gas molecules n_s a curve closely resembling an adsorption isotherm (fig. 5) is obtained.

As the effect also occurs wher the Pt surface has already been covered by CO, H_2 and O_2, the interaction of these gases cannot originate from their adsorption on the Pt-surface.

We therefore assume that their adsorption takes place on the area adjacent to the Pt-particles and that from there the interaction with the surface groups of the Aerosil takes place.

Yaroslavsky and Terenin (18) also studied the interaction of physical adsorbed molecules with the functional groups on the surface of the adsorbent. McDonald (19) thoroughly investigated the interaction of physical adsorbed molecules and the OH-groups of an Aerosil surface.

In the case of N_2 ($T = -190^\circ$ C; $p = 1 - 50$ mm Hg) McDonald found a gradual decrease of the original OH band and a corresponding increase of a new band which was shifted towards lower wave numbers. On condensation of N_2 ($T = -200^\circ$ C; $p = 1$ atm) there was then only this new band there which was more intense than the original OH-band, which again appeared on desorption of N_2. The shift of the OH-band for this particular case was 24 cm^{-1}.

It is possible that similar effects occur with the Aerosil bands.

Under our experimental conditions we would not be able to decide whether a new and slightly red-shifted, but more intense band is appearing or whether there is only the observed increase of the original Aerosil bands. In the case of the OH groups of the Aerosil the observed effect was thought to be caused by the proton-quadrupole interaction between the surface hydroxyl groups and the adsorbed molecules (20).

It is interesting to note at this place that under very different experimental conditions (22), under which Pt was evaporated in an CO atmosphere on a MgO-window, a CO-band at about 1850 cm^{-1} appeared beside the very intense band at 2070 cm^{-1} (23).

But the bonding of this kind of CO species on the Pt surface proved to be unstable. It could be completely removed by pumping, but not be found again after gaseous carbon monoxide has been added to the Pt film (23).

1.5 Determination of the apparent extinction coefficient of the CO stretching band of chemisorbed carbon monoxide

For quantitative investigations of the properties of the chemisorbed carbon monoxide species, it becomes necessary to know the relationship between the intensity of the CO band, measured by the extinction $E_a = \log (T_o/T)$ and the corresponding surface concentration; T_o and T are the apparent intensities of the sample without and with chemisorbed C O on the surface, measured by the height of the corresponding band peak.

For the chemisorption of carbon monoxide on Aerosil supported Pt-powder the conditions for the investigation of such a relationship are relatively favourable as only one CO band at about 2070 cm^{-1} is present. Eischens et al. attributed this band to carbon monoxide chemisorbed in a linear structure (10).

At the end of the reduction process in hydrogen the Pt surface is covered with chemisorbed hydrogen. As it is not possible to achieve a better vacuum than 10^{-6} m.m. Hg with this kind of cell the Pt surface will become partially

covered by oxygen before all the chemisorbed hydrogen can be removed. Hence, the conditions on the Pt surface are undefined before CO can be added.

We therefore have chosen the following surface reaction to determine the apparent extinction coefficient

$$\text{"Pt - O "} + 2CO_g \rightarrow CO_{2g} + \text{"Pt - CO"}$$

We start with a Pt surface which has been covered at room temperature with a layer of chemisorbed oxygen atoms, indicated as "Pt - O". A charge of CO gas is then added.

According to Langmuir (4) almost every collision between gaseous CO and chemisorbed oxygen leads to the formation of CO_2, which then desorbs (24, 4).

On the freed Pt-site carbon monoxide is then chemisorbed. The reaction is generally completed within a minute. The gas phase over the pellet consists completely of CO_2, which can be demonstrated by freezing it down in a cold trap filled with liquid nitrogen.

The amount of the chemisorbed carbon monoxide can then be found by the difference.

More CO can be added to the system and the relationship between E_a and C_{CO} which one finds is shown in fig. 6.

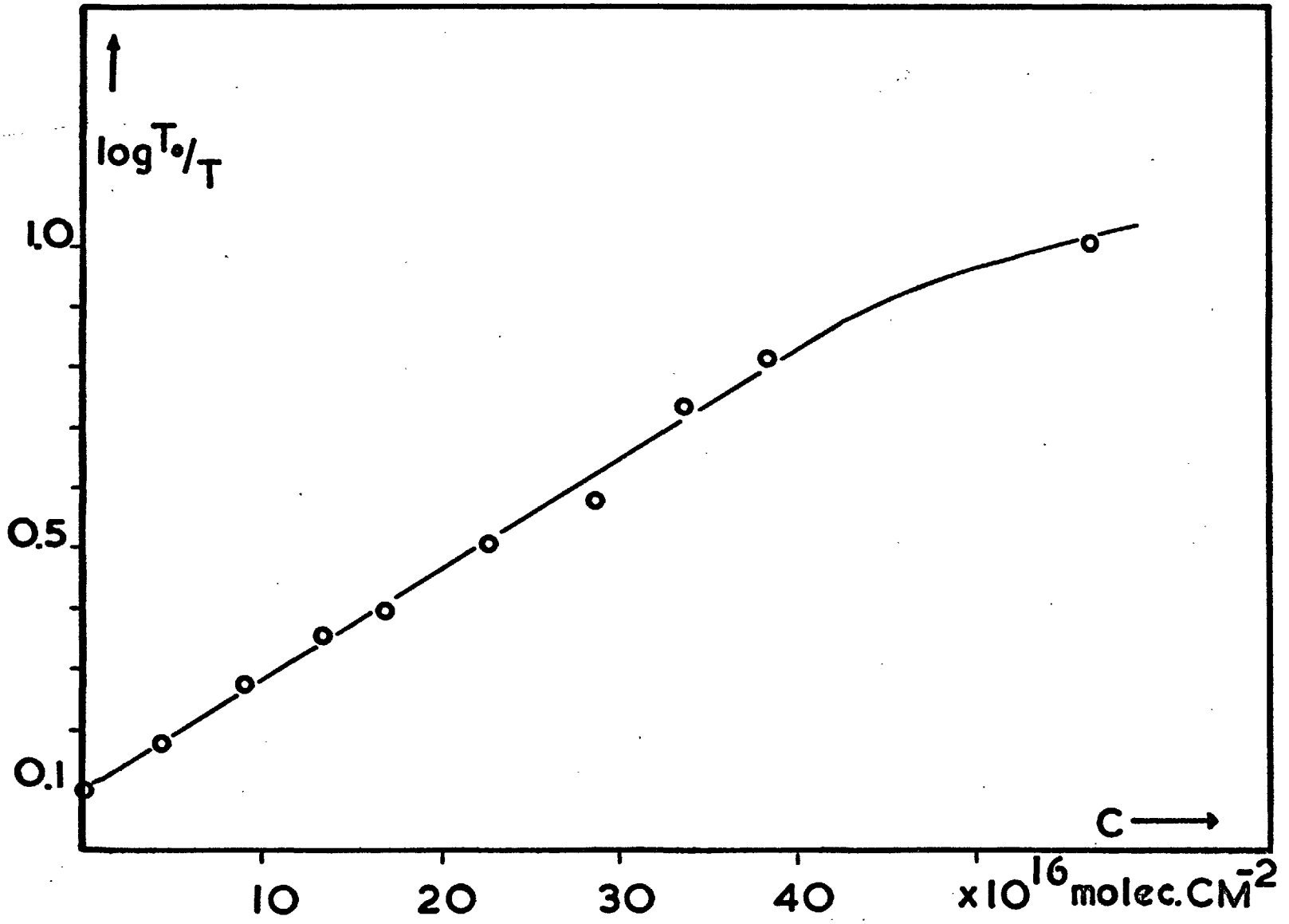


Fig.6. Apparent extinction as a function of coverage

The function does not go through the origin. This is due to the fact that the experiment was started with a small CO concentration already there on the Pt surface.

Up to 40×10^{16} molecules CM^{-2} geometric pellet area the relation is linear. At higher surface concentrations the slope decreases.

It is interesting to note that carbon monoxide exceeding a concentration of 40×10^{16} molecules CM^{-2} is relatively weakly held by the surface and can be pumped off quite easily as demonstrated in fig. 7.

The apparent extinction coefficient is given by the slop in fig. 6 and amounts in the linear region to

$$k_a = 2 \times 10^{-18} \text{ cm}^2/\text{molecules}$$

which correspond to

$$k_a = 12 \times 10^2 \text{ litre} \times \text{mole}^{-1} \times \text{cm}^{-1}$$

The relative error is within $\pm$ 10% (4 runs).

At the end of the coverage experiment the chemisorbed carbon monoxide can be oxidized in an oxygen atmosphere at room temperature. Charges of carbon monoxide then can be added again after the gaseous oxygen has been pumped off.

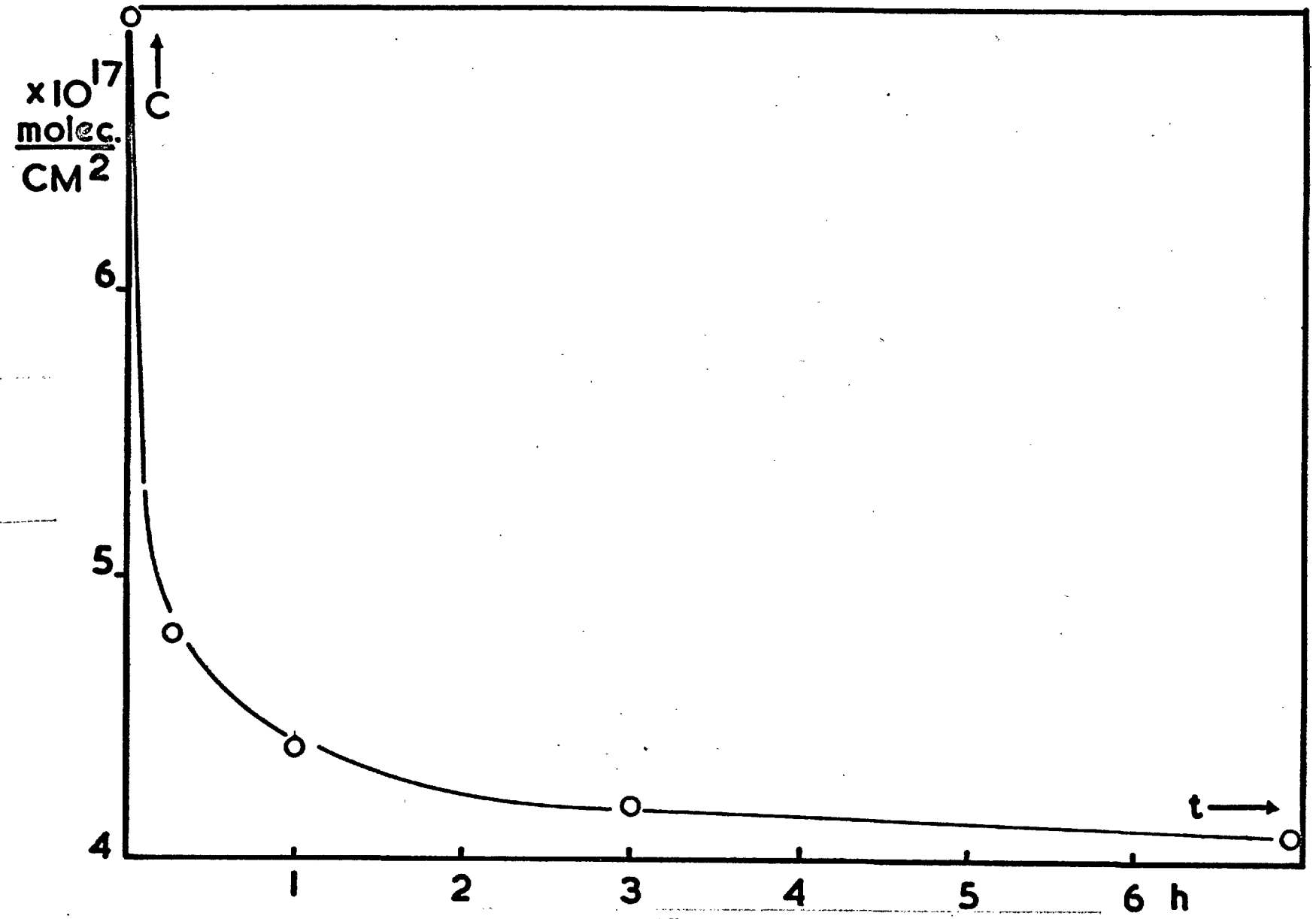


Fig.7. Removability of the chemisorbed CO

The apparent extinction coefficient for CO on Pt has been previously determined by Eischens et al (10). They were using the stepwise oxidation of the chemisorbed carbon monoxide by adding small amounts of oxygen to the carbon monoxide covered sample.

They had to heat up the sample to about 200° C so that the velocity of the oxidation of the chemisorbed CO became reasonably high. But at these high temperatures a desorption of the chemisorbed CO could cause inaccuracies (4).

These authors found an extinction coefficient $k = 3 \times 10^{-18}$ cm^2/molecules ($\theta < 0.66$).

The increase of the extinction coefficient for $\theta > 0.66$ which they found was not observed by us.

As previously found by Eischens et al (10) the peak of the CO band is shifted towards higher wave-numbers as the surface concentration increases.

Fig. 8 demonstrates this effect, which we reproduced. The shift amounts to about 30 cm^{-1} when the surface concentration increases from 4×10^{16} to 40×10^{16} molecules CM^{-2} geometric pellet area.

This shift is about one third of that which one observes when carbon monoxide is chemisorbed from the gas phase (2143 cm^{-1} → 2040 cm^{-1}).

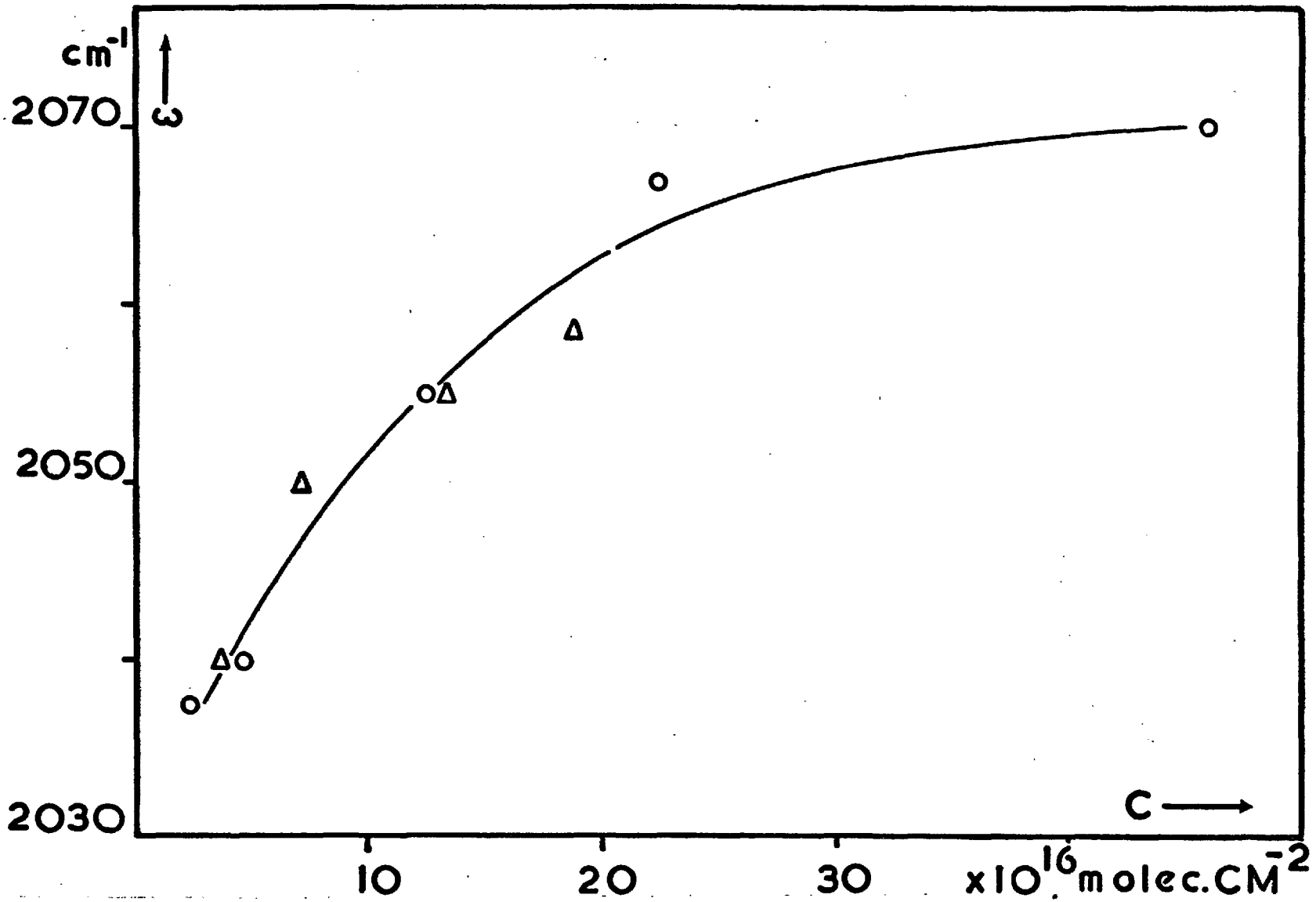


Fig.8. Variation of the wave number ω of the band centre with surface concentration of chemisorbed carbon monoxide

1.6 Determination of the apparent integrated absorption intensity of the CO stretching band of the chemisorbed carbon monoxide

Discussion of I.R. results of the chemisorption of gases like carbon monoxide on silica supported metal surfaces has been mainly limited to the frequencies of the bands of the chemisorbed surface species and on such information as force constants and bonding distances which could be derived from the frequency figures.

No attempt has been made so far to determine the integrated absorption intensities of chemisorbed species and to use these figures to provide additional information about the bonding structure of the species concerned.

The importance of the integrated absorption intensity as a measure for studying the structure of organic molecules has been pointed out by Lippert and Mecke (25).

Recently Noack determined the true integrated absorption intensities A of various metal carbonyls and a series of Fe-carbonyl-compounds (16).

The experimental conditions for such quantitative work are not favourable for chemisorbed CO species on Aerosil

supported metals for reasons which we stated in the experimental part (1.2). As we are not working with strictly monochromatic light and because of the interaction of the chemisorbed CO species on the Pt-surface only the apparent integrated absorption intensity B can be determined from our experimental results

$$B = \frac{1}{c \times d} \int_{band} \log_e \frac{T_o}{T} \cdot \times d\omega$$

c - concentration in moles litre^{-1}

d - length of the cell in cm,

T_o, T - apparent intensities of the sample without and with chemisorbed CO present on the Pt-surface,

ω - wave number in cm^{-1}

The units of B are in cm^{-2} x mole^{-1} x litre. In adsorption work the product c x d is generally expressed in molecules x cm^{-2}; for conversion into cm^{-2} x mole^{-1} x litre units a factor 6 x 10^{20} is used.

The magnitude of the apparent integrated absorption $F = \int \log_e {}^{T_o}/_T \times d\omega$ is found graphically.

For better accuracy the recorded I.R. bands are photographically magnified 2, 4 and 8 fold, depending on the size of the original I.R. band.

Hence we obtained bands which after magnification cover an area of 10 to 15 cm^2. From these magnified bands the corresponding figures of T and T_o are taken at intervals of 1 mm corresponding to 3.5 to 11 cm^{-1} depending on the magnification of the band. Then $\log_e({}^{T_o}/_T)$ is plotted as a function of $\omega(cm^{-1})$ and the area covered by this function is determined as F.

The figures of the apparent integrated absorption F are then divided by the corresponding surface concentration. For this the known relationship between the extinction of the band peak and surface concentration described in the previous chapter is used. These figures are then converted into $mole^{-1} \times litre^{+1} \times cm^{-2}$ units.

In tab. 2 are listed the figures of the apparent integrated absorption intensity B together with the corresponding surface concentrations and the position of the CO band peak.

These B-figures have then to be corrected according

to the wing correction method (26). From these figures the true integrated absorption intensities A can be evaluated by using the extension of the method of Wilson and Wells, described by Ramsay (26).

One of the essential assumptions of both methods is that the band can be described by a Lorentz curve

$$\log_e \left(\frac{I_o}{I}\right)_\nu = \frac{a}{(\nu - \nu_o)^2 + b^2}$$

where ν_o is the frequency of the peak of the band and a and b are constants.

Another assumption is that the interaction of the molecules concerned only broadens the band so that it can still be described by a Lorentz curve.

The CO bands in the I.R. spectra of the chemisorbed species are slightly asymmetric with a longer wing towards lower frequencies and also the band peak is shifted towards higher frequencies with increasing surface concentration.

Hence, there is an interaction of the chemisorbed CO species with the surface and with each other.

Table 2 (fig. 9, line 1)

wave number ω cm^{-1}	concentration n_s molecules CM^{-2}	$B \times 10^{-2}$ $cm^{-2} \times mole^{-1} \times litre$
2038	0.31×10^{17}	1250
	0.30×10^{17}	1330
2043	0.51×10^{17}	1080
2048	0.80×10^{17}	1130
2053	1.10×10^{17}	1200
2055	1.28×10^{17}	950
2063	2.0×10^{17}	1140
2064	2.1×10^{17}	950
2067	2.7×10^{17}	1070
2070	4.5×10^{17}	980
2089	10×10^{17}	700

n_s - molecules per CM^2 geometric pellet area

For these reasons the resulting corrections are open to discussion, but they give at least some idea of the order of magnitude of which the true corrections would be.

In tab. 3 are listed the estimated figures of the various corrections.

The 'wing' correction amounts for a weak band (2043 cm^{-1}) 31%, where as it is only 17% for an intense CO band (2070 cm^{-1}). The corrections which one has to take into account to get from the 'wing' corrected B figures the true integrated absorption intensities A amount to 23% for the intense band and 10% for the weak one.

The average resulting correction which one has to apply to the uncorrected B-figures (tab. 2) amounts to about 40%.

Table 3

ω	n_s	s/w	corr. 1	corr. 2	S
2043	5.1	1.1	31%	10%	41%
2064	20.0	1.4	21%	13%	34%
2070	45.0	2.0	17%	23%	40%

ω - frequency of the CO band in cm^{-1}

n_s - concentration of the chemisorbed CO molecules

molecules x CM^{-2} x 10^{-16}

s - spectral slit width

w - half band width

corr. 1 - 'wing' correction according to (4)

corr. 2 - correction according to Wilson and Wells (4)

S - resulting correction

In fig. 9 are plotted the data of the uncorrected apparent integrated absorption intensity B as a function of the wave number ω for the linearly chemisorbed CO (0 - 0 - 0).

Within the limits of experimental error the B figures decrease with increasing wave number and, hence (fig. 8), also with increasing CO surface concentration.

Whereas the relationship between the B figures and the wave number can be regarded as approximately linear, the concentration dependency of B is not linear (tab. 2). According to tab. 2 the apparent integrated absorption intensity decreases only to about half its highest known figure when the CO surface concentration increases by a factor of about 30.

Also are plotted in fig. 9 the integrated absorption intensities of CO chemisorbed linearly on Pt^{2+}-ions; the properties of these surface species are discussed in chapter 1.11.

For the terminal CO groups in Fe carbonyls and Fe carbonyl compounds Noack found a similar dependency of the true integrated absorption intensity A with the wave number ω. (16).

The increase of these A-figures with decreasing wave number is shown by line ii. Because of this linear

relationship we have drawn through the figures for the chemisorbed species a straight line i.

For the various carbonyls and carbonyl compounds which have two and more CO stretching bands for the terminal CO group the approximate frequency centres (16) in cm^{-1} are plotted.

Such a relationship between integrated absorption and wave number is well known and has been found for various functional groups in organic compounds (25).

In the case of the phenolic OH groups, for instance, it could be demonstrated that as the absorption band is shifted towards lower wave number the increase in the integrated absorption intensity is accompanied by an increase in the polarity of the OH group and its dissociation constant.

Similar evidence has been found for the CO group in aldehydes and for other functional groups (25).

In terms of the chemisorbed CO species this would mean that at low surface concentrations the polarity of the CO group is bigger than at high surface concentrations.

A linear relationship between integrated absorption intensity and wave number even holds when we plot the A-figures of the terminal CO groups of various metal carbonyls although the symmetry of these metal carbonyls varies (16) (line iii).

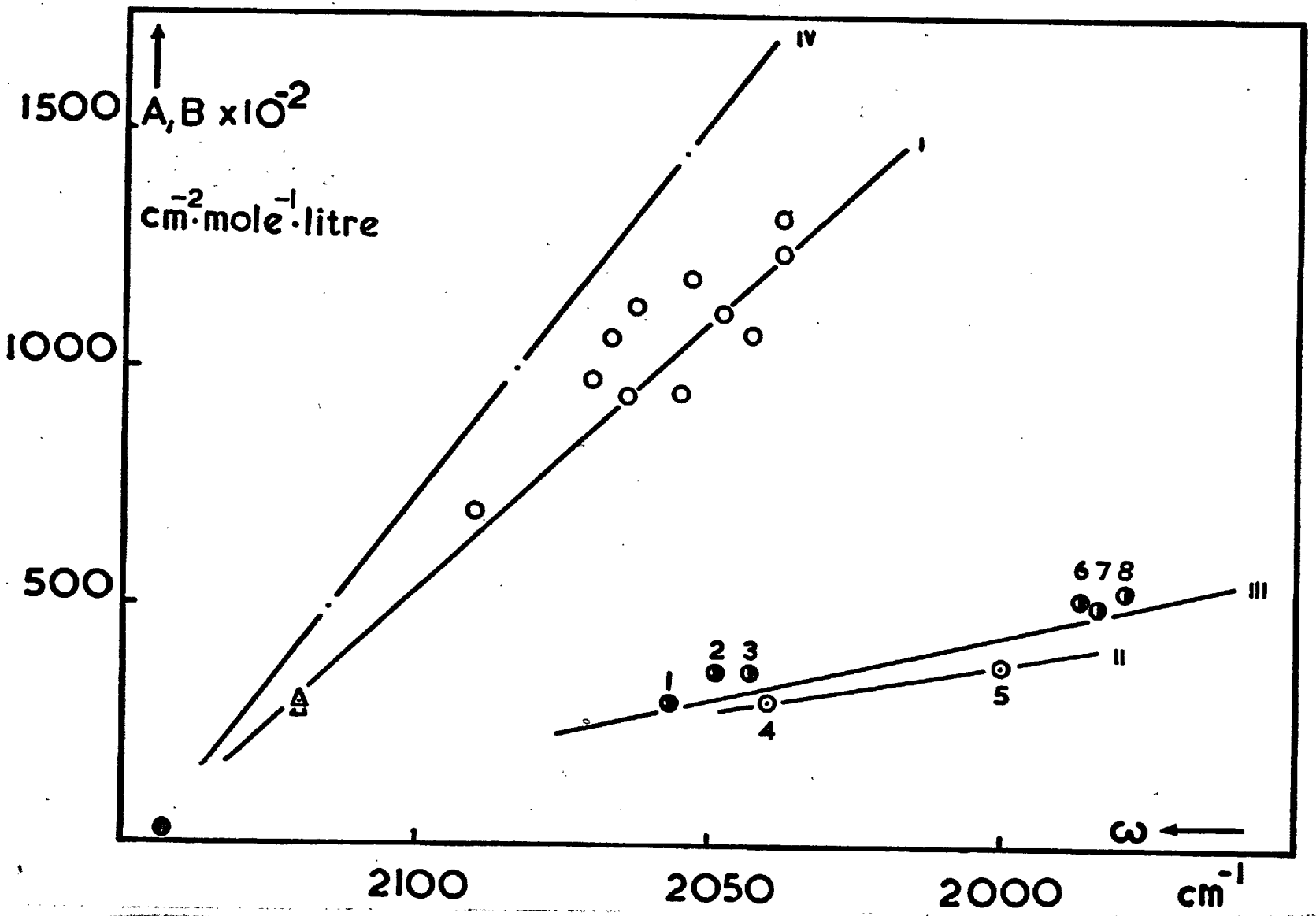


Fig.9. Integrated absorption intensity as a function of wave number

The various metal carbonyls are in fig. 9 (line iii):

1.	$Co_2(CO)_8$	5.	$Fe(CO)_5$
2.	$Co_4(CO)_{12}$	6.	$Mo(CO)_6$
3.	$Ni(CO)_4$	7.	$Cr(CO)_6$
4.	$Fe_3(CO)_{12}$	8.	$W(CO)_6$

In general it seems reasonable to assume that this relationship (fig. 9) which we found for linearly chemisorbed carbon monoxide on Pt and Pt^{++} surface sites also holds for other metal surfaces provided that the CO species were chemisorbed in a linear structure.

For $Co_2(CO)_8$ Noack shows that CO in a bridged structure with its band centre at 1860 cm^{-1} has a mean A-figure of 150 x 10^2 cm^{-2} x $litre^{+1}$ x $mole^{-1}$ instead of a much higher figure of about 850 x 10^2 cm^{-2} x $mole^{-1}$ x litre which one would expect for a terminal CO group at 1860 cm^{-1} according to line iii (fig. 9) (16).

It is reasonable to expect that the difference in the A-figures for terminal and bridged CO groups in carbonyls also holds for the corresponding chemisorbed species. Therefore the determination of the integrated absorption intensity would provide us with an experimental means to give an experimental answer in the present controversy whether chemisorbed CO species with CO bands within

1850 - 2000 cm^{-1} are due to bridged surface species, according to Eischens, or whether they are due to linearly chemisorbed CO species, too, as it is assumed by Blyholder (27, 28).

When one compares the integrated absorption intensity of terminal CO groups in metal-carbonyls and of chemisorbed CO species at the same position (cm^{-1}) the increase in case of the chemisorbed state in the low wave number region is striking.

At 2050 cm^{-1} the B-figure for the chemisorbed species is increased by a factor of 4 compared with the corresponding A-figure of the metal carbonyl (line iii). In case of the estimated A-figures of the chemisorbed species (line iv) the increase would then become even more significant.

This difference in the figures of the integrated absorption intensities gets smaller as one moves towards higher wave numbers. All lines in fig. 9 seem to cross rather close to the A-figure of gaseous CO at 2143 cm^{-1} position.

The big differences in the integrated absorption intensities in the low wave number region (fig. 9) cannot be attributed to differences in the symmetry of the metal carbonyl species (line iii) and that of the chemisorbed surface state (line i,iv).

We therefore suppose that this effect and the increase of the slope for the B, ω-function of the chemisorbed CO species is due to the interaction of the chemisorbed CO with the metal and metal oxide surfaces.

At present we have not sufficient experimental evidence to explain this effect.

1.7 Interaction of N_2, CO_2 and A with the chemisorbed carbon monoxide

Eischens and Pliskin (10) have previously studied the effect of gases like H_2, NH_3, HCl on carbon monoxide which is chemisorbed on a Pt surface. They noticed a shift of the CO band depending on the nature of the gas added.

In our experiments the Pt-particles were covered by exposure to a CO atmosphere of 1 mm for about 15 minutes. The gas phase CO and the weakly chemisorbed CO (fig. 7, chapter 1.5) were then pumped off (15 minutes) (fig. 7). After this the pressure increase in the cell was less than 10^{-4} mm over a period of half an hour. By adding gases like N_2, CO_2 or A (p = 10 mm.) no change in position, shape or intensity of the CO band could be detected. But the amount of chemisorbed CO removed on evacuation for another 15 minutes is greatly increased.

After treatment with N_2, with A and with CO_2 24%, 13% and 7% of the chemisorbed CO could be removed during the 15 minutes pumping. Without this, the amount of chemisorbed CO which was removed in the second 15 minutes pumping was only about 4% (fig. 7).

We assume that the added gases (p = 10 mm) are adsorbed

on the Pt-area from which the CO was removed during the first 15 minutes pumping. These molecules weaken the metal carbon bond so that the CO is more easily removable.

The weakening of the Me-C bond should result in a shift of the C-O band towards higher frequencies, when one is assuming a similar bonding mechanism as in metal carbonyls (chapter 1.13). This frequency shift would occur in the region where n_s is in the order of 40×10^{16} molecules CM^{-2} pellet area (fig. 8). But here the change of the frequency with coverage is very small and there is little difference between the CO frequency of chemisorbed CO which could be easily removed and that what could not be removed. Thus, it is quite reasonable that no shift could be detected.

The increase of the SiO bands of the support in the presence of these gases ($p = 10$ mm) indicates that some gas is also adsorbed in the area around the Pt-particles. But their influence on the chemisorbed CO molecules should be much smaller than of those molecules which are adsorbed by the Pt-surface.

1.8 Interaction of H_2 with the chemisorbed carbon monoxide

Eischens and Pliskin (10) reported a shift of the CO band to longer wavelength (0.09μ) when hydrogen was added to carbon monoxide chemisorbed on silica supported Pt. They attributed this effect to the electronic interaction of the hydrogen with the chemisorbed CO. The change of the CO band which we observed on addition of hydrogen is mainly characterized by the asymmetric broadening of the original CO band (fig. 10, A) to the side of lower wave numbers (fig. 10, B). There is also a small decrease in the maximum extinction $\log T_o/T$ of the band A on the addition of H_2.

The determination of the apparent integrated absorption intensities B of both bands shows an increase of the integrated absorption intensity by 42% when hydrogen was added (p = 10 mm Hg).

On pumping (15 minutes) there is a decrease of the maximum extinction of band B corresponding to a loss of about 13% of the chemisorbed carbon monoxide. As the broadening of band B essentially remains, we have to assume that the gaseous hydrogen does not interact directly with the chemisorbed CO but is strongly chemisorbed on the Pt-surface.

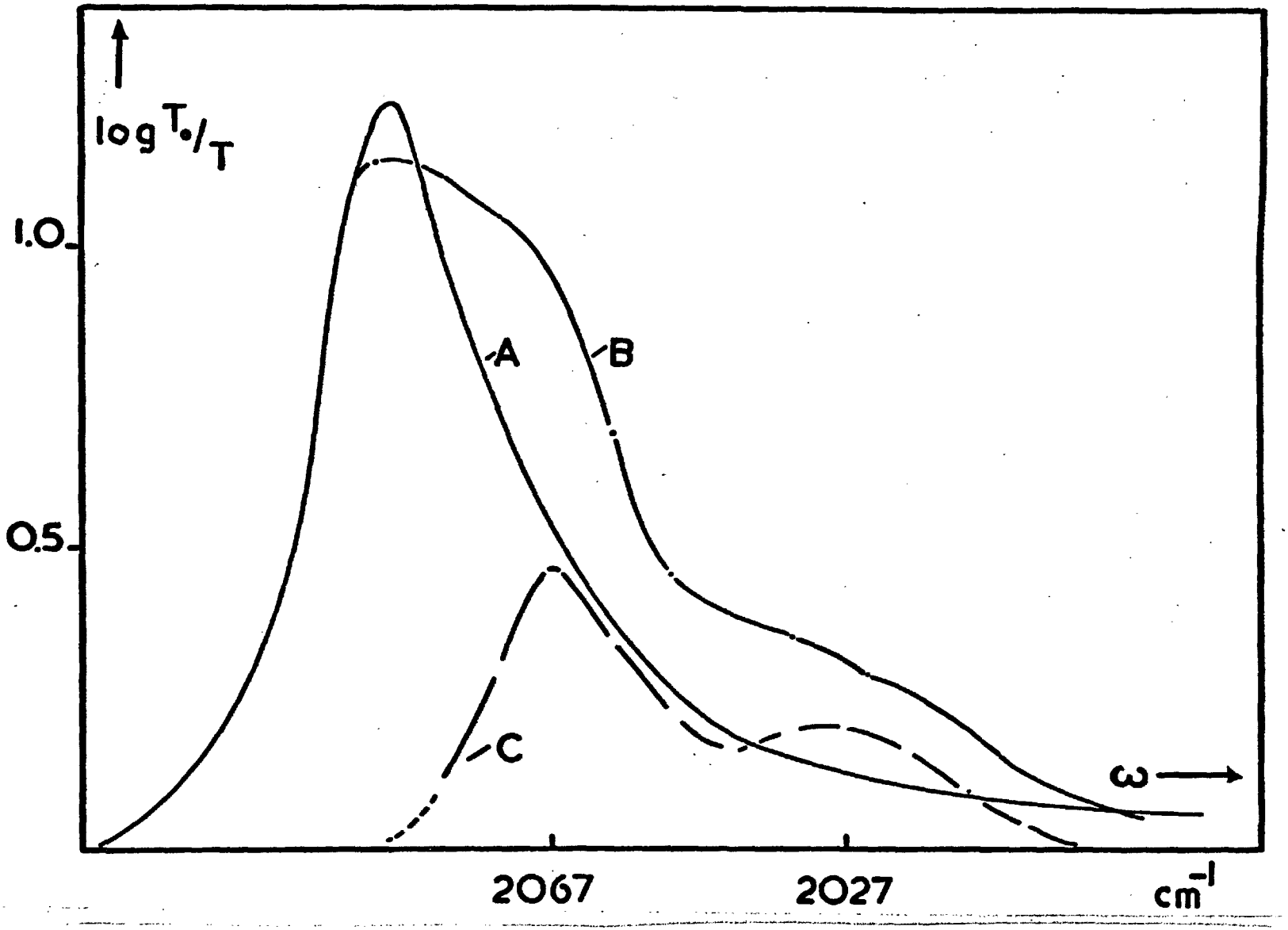


Fig.10. Interaction of H_2 with the CO covered Pt surface

The infrared spectrum of chemisorbed hydrogen on Pt has been reported by Pliskin and Eischens (12). At relatively large pressure (p = 400 mm Hg) two bands at 2057 cm^{-1} and 2109 cm^{-1} occur which are both attributed to the Pt-H vibrations.

The asymmetric shape of band B (fig. 10) and the increase of the integrated absorption intensity by 42% makes it very probable that the broadening of the original CO band A (fig. 10) is caused by the superposition of the corresponding Pt-H-bands.

The subtraction of the integrated absorption intensities of band B and band A provides us with band C in the lower frequency region.

Band C consists of a strong absorption maximum at 2046 cm^{-1} and a weak one at 2006 cm^{-1} position. In this subtraction process the small decrease of band B in the region where this band covers band A was not considered.

When CO covers the Pt surface the metal-hydrogen bands are shifted by 50 cm^{-1} to lower frequencies due to the indirect electronic interaction with the chemisorbed CO, as we assume.

Using a hydrogen pressure of 400 mm Pliskin and Eischens (10) obtained at room temperature a maximum extinction of 0.07 for the Pt-H bands.

In our previous experiments with a CO free Pt-surface we found under our experimental conditions (p_{H_2} = 10 mm Hg, ϑ = 35° C) an extinction figure of 0.04 for the band at about 2000 cm^{-1} position.

In the presence of chemisorbed CO this value shows a marked increase to 0.47 under the same pressure and temperature conditions.

The additional uptake of H_2 in the presence of adsorbed CO seems to be a more general effect. So Sastri and Viswanathen reported an increase of the H_2 uptake on a CO-covered cobalt surface (29).

For two major reasons it is not possible to compare the figures for the maximum extinction quantitatively.

Firstly, we do not know how the CO band is effected merely by interaction with the chemisorbed hydrogen. Hence, the figures which we get for the Pt-H bands (C) are uncertain. But the mere interaction effect could be studied by means of deuterium which would provide Pt-D bands at 1479 cm^{-1} and 1515 cm^{-1} far out of the CO band region at 2000 cm^{-1}.

Secondly we have to consider that the shift of the Pt-H band towards lower frequencies is most probably connected with a marked increase in the values of the integrated absorption intensity.

As we have found for the chemisorption of CO on Pt and

as we know from other examples, i.e. carbonyl compounds and organic compounds, such a shift towards lower frequencies would mean an increase of the Pt-H-dipolmoment when CO is present on the surface.

Further support for the chemisorption of hydrogen on the carbon monoxide covered metal surfaces is provided from the spectra of hydrocarbonyls.

Edgell and Summit (30) report for $HCo(CO)_4$ a band at 1934 cm^{-1} which they attribute to the Co-H vibration and for the compound $H\text{-}Re(CO)_5$ the corresponding Re-H band was found by Beck, Hieber and Braun at 1832 cm^{-1} (31).

The variety of inorganic hydrocarbonyls known (32) makes it possible that metal-hydrogen bands as with Pt occur at other CO-covered metal surfaces. Some evidence for this assumption is given in the experimental results on CO-covered Rh- and Pd surfaces. On adding H_2 to the CO-covered Rh surfaces a band was reported at 2048 cm^{-1} (33) and with Pd in addition to a small shift of the CO band, a broadening of this band to lower frequencies was observed (34).

1.9 Interaction of O_2 with chemisorbed carbon monoxide

By adding oxygen ($p \sim 1$ mm , $\vartheta = 40^\circ$ C) a fairly rapid oxidation of the chemisorbed carbon monoxide is observed.

About 90% of the chemisorbed gas are oxidized within 30 minutes. With diminishing CO concentration there is a shift of the CO band of the remaining chemisorbed CO to lower wave numbers. The reverse effect was observed when the Pt surface was gradually covered by CO.

As in the work of Eischens and Pliskin on oxidation no additional bands occurred in the region between 4000 and 1200 cm^{-1}. With Fe (10), Rh (33), Ni (35), additional bands were reported. An interpretation of the "bands" at 1850 cm^{-1}, 1650 cm^{-1} and 1400 cm^{-1} in terms of CO_3 complexes is in the presence of a gas phase like oxygen (~ 1 mm Hg). meaningless (chapter 1.4).

Recent work done by Kavtaradze and Lygin (34) on silica supported Pd metal has shown that no oxidation of the chemisorbed CO occurs at 25° C and $p_{O_2} = 8$ mm.

This experimental result agrees well with the behaviour of the Pt-catalyst used by Eischens and Pliskin (10) on which rapid oxidation was reported to occur only at about 200° C.

The high activity of our Pt-catalyst might be due not only to energetic differences but also due to impurities on the surface. We can exclude the latter, as oxidation of chemisorbed CO also occurs under similar conditions of temperature and pressure on Pt films which are evaporated under ultra high vacuum conditions (chapter 2.6).

1.10 Chemisorption of carbon monoxide on an oxidized platinum surface

For the following experiments the Aerosil supported Pt pellet had been heated to 250-300° C for 1 hour in an oxygen atmosphere of about 20 mm Hg.

The oxygen was then pumped off and the pellet was cooled to about room temperature.

Recently Weissmantel, Schwabe and Hecht (36) have shown that under these experimental conditions the Pt-surface takes up oxygen with formation of oxide, probably PtO and PtO_2, which process is thermodynamically possible (37).

According to the results of L. Wöhler (38) the formation of PtO should be favoured.

X-ray edge absorption measurements (39) have also provided good evidence that at high temperature Pt oxide is formed in addition to the chemisorption of oxygen on the Pt surface as at room temperature.

If we assume that after 30 minutes pumping ($p < 10^{-6}$ mm) no physically adsorbed oxygen is left on the oxidated Pt surface we have to consider the following adsorption sites Pt^{2+}, Pt^{4+}, O^{2-} in addition to Pt.

The positive and negative charges ascribed to the ions

were chosen for convenience by analogy with the corresponding oxides. The bonding in the transition metal oxides is not purely ionic but has considerable covalent character.

There is also some change in the bonding expected when going from the bulk oxide to its surface layers. Hence, these introduced ion terms can only give a rough qualitative picture of the state of those ions and they provide no information about the bonding between these ions.

From the energic point of view we also expect that the Pt-ions are covered by O^-, O_2^- ions rather than by O^{2-}-ions.

In describing the Pt surface after oxidation we have also to consider that at least some of the surface did not undergo oxide formation so that we have also some chemisorbed O species on top of a Pt-surface. Hence, on adding CO we expect a CO band at about 2070 cm^{-1} corresponding to the chemisorption of CO on Pt. Further, the two different kinds of Pt-ions become also potential bonding partners for the CO.

I.R. - spectra of Pt carbonyl halogenids give evidence for the bonding of the CO to the Pt^{2+}-ion (40).

As the Pt-surface ions are probably covered by different kinds of oxygen species (O^-, O_2^-, O^{2-}) the formation of the different kinds of surface species, i.e. Pt^{2+} - CO,

Pt^{4+} - CO, should largely depend on the velocity with which this oxygen undergoes reaction with the carbon monoxide.

Concerning the oxygen ions on the Pt oxide surface the formation of a $CO_3^{(\delta-)}$-complex (40, 41, 42) on addition of carbon monoxide is likely as discussed by Stone for Cu_2O, NiO, CoO surfaces (43). But due to the interaction of the adsorbed CO gas with the Aerosil support which increases the absorption of the Aerosil bands at about 1850 cm^{-1}, 1650 cm^{-1} and 1400 cm^{-1} (see chapter 1.4) it would become very difficult to observe additional weak bands in this region which might be due to C - O stretching bands of this complex.

Hence, at present this I.R. technique does not provide any experimental evidence for the existence or non-existence for a $CO_3^{(\delta-)}$-complex formed on the Pt oxide layer.

A physical adsorption of the carbon monoxide ($p \sim 10$ mm) on the oxide surface should take place with no activation energy. The corresponding CO band should then also occur at once in its final intensity. Its frequency should not be much out of that of liquid CO (2139 cm^{-1}) (17).

On addition of CO (p = 10 mm Hg) to the oxidized Pt surface three bands occur at about 2070 cm^{-1}, depending on the coverage, at 2120 cm^{-1} and at 2170 cm^{-1} (fig. 11).

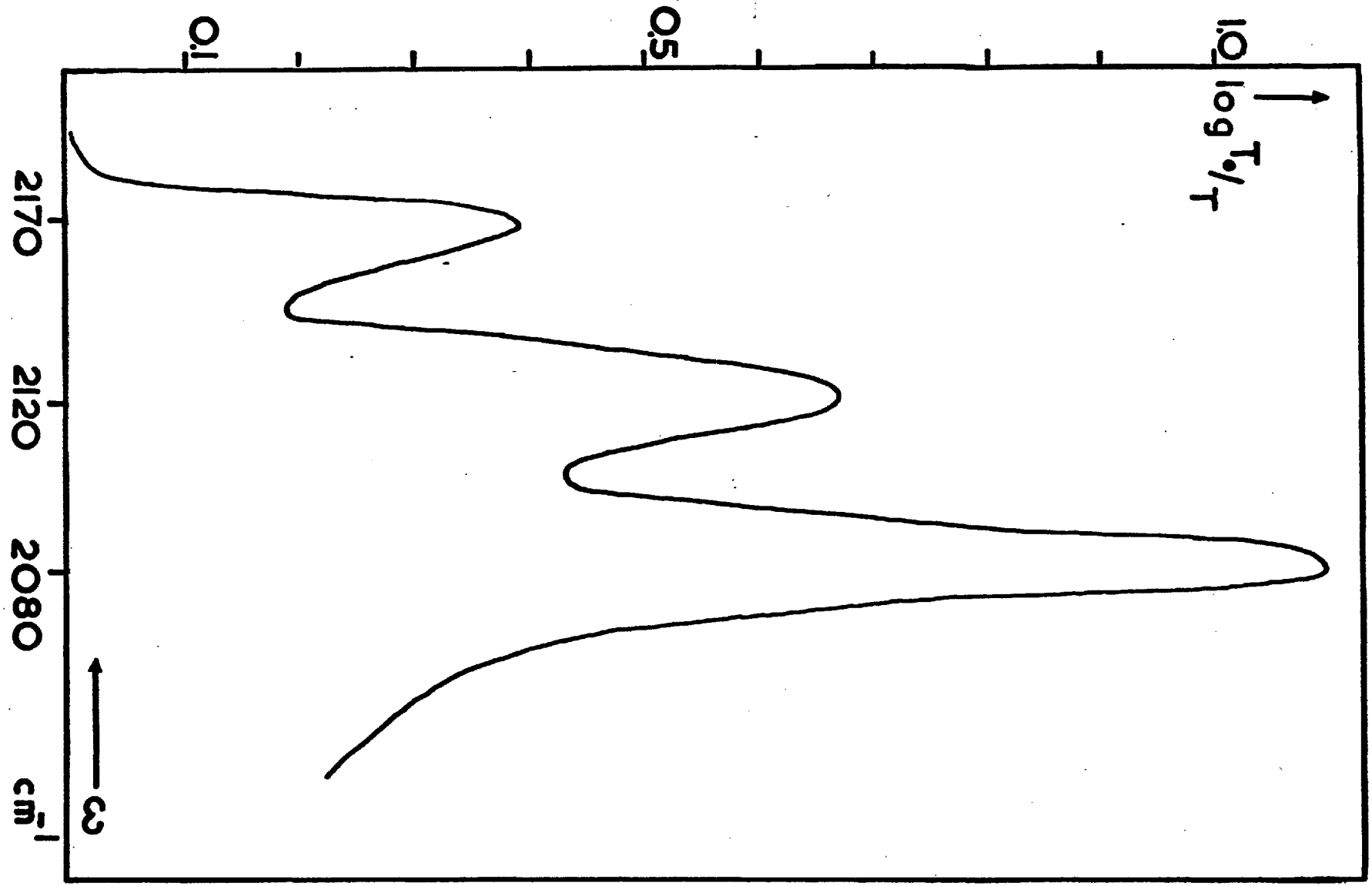


Fig.11. Chemisorption of CO on an oxidized Pt surface; CO-stretching bands at 2070 cm^{-1}, 2120 cm^{-1}, and 2170 cm^{-1}.

Fig. 12 shows how these bands develop in two hours time at about room temperature.

The effects occurring in the earlier stages of the growing of the bands at 2070 cm^{-1} and 2120 cm^{-1} (fig. 12) could not be reproduced. They seem to be connected with the reaction of the CO with the different kinds of oxygen species at the surface.

In tab. 4, 5, 6 we use the maximum extinction of these bands to describe what is happening to them during the following procedures during which the CO is removed and then is added again to the I.R. cell.

Run A and run Z are carried out with the same pellet. The main difference between them is, that in run A the oxidation of the Pt-surface took place in an unsintered state just after the reduction process; in run Z the oxidation was carried out with the pellet in a highly sintered state at the end of a series of other studies concerned with the chemisorption of CO on an oxide free Pt-surface.

We report here the results of run A as they are more suitable because of the more intense bands at 2120 cm^{-1} and 2170 cm^{-1}.

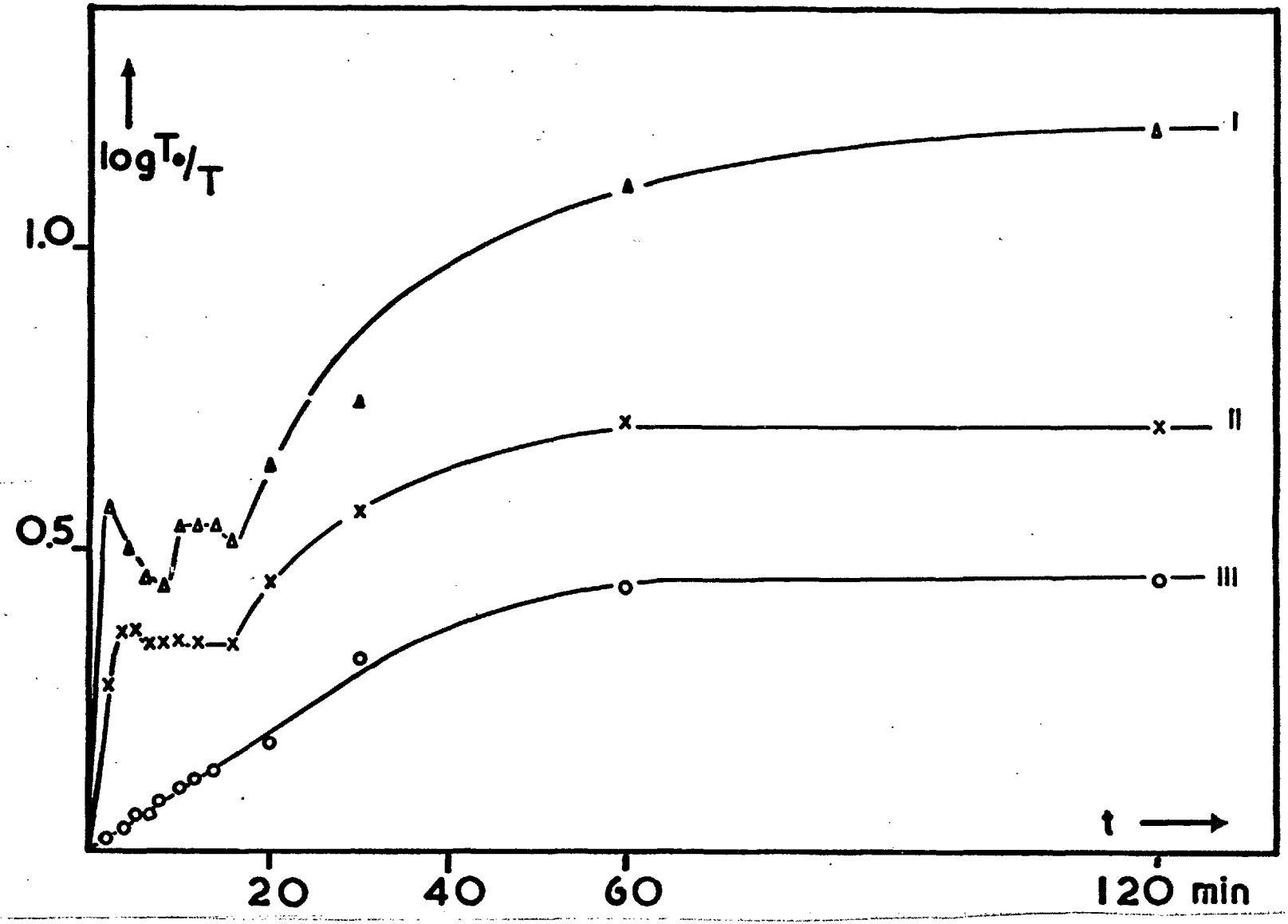


Fig.12. Chemisorption of CO on an oxidized Pt-surface as a function of time

Table 4

Run	p_{co}	t expos.	$\log(T_o/T)_1$	$\log(T_o/T)_2$	$\log(T_o/T)_3$
A	11 mm	2 hours	1.204	0.699	0.448
Z	10 mm	2 hours	1.9	0.08	0.03

suffix 1 - band at 2070 cm^{-1}

2 - band at 2120 cm^{-1}

3 - band at 2170 cm^{-1}

Table 5

	$\log(T_o/T)_1$	$\log(T_o/T)_2$	$\log(T_o/T)_3$
under p_{co} = 10 mm	1.204	0.699	0.448
After 1 hour pumping	0.254	0.549	0.056
After 12 hours pumping	0.206	0.549	0.056
After addition of CO (p = 10 mm)	1.204	0.699	0.414

Table 6

Band:	1	2	3
$\log(T_o/T)$ initial	1.204	0.699	0.448
$\log(T_o/T)_{t_1}$	1.204	0.699	0.333
$\log(T_o/T)_{t_2}$	1.000	0.624	0.222

(p = 10 mm)

The three surface species differ in their ease of removal by pumping. In tab. 5 the figures of their extinction are shown after 1 and 12 hours pumping. This proves that there is no equilibrium between these species, or at least the processes leading to equilibrium are highly activated.

Striking is the comparatively high removability of the band at 2070 cm^{-1}, which we attributed to CO chemisorbed on Pt. The reason for this different behaviour could be the influence of the oxide patches on the chemisorption properties of the residual Pt-surface.

When subsequently CO is added again to the pellet we obtain the same figures for the different bands as before the pumping procedure, (tab. 5). This result indicates that during the long pumping time of 12 hours the heterogeneous nature of the surface remains almost unchanged.

It further proves that the decrease of the different CO species on the surface during pumping is not due to a surface reaction between CO and the different oxygen species.

During the following cycles a decrease of the bands is observed finally (tab. 6). This might be due to slow reduction processes which in turn could cause a decrease in the roughness of the surface. Such reduction processes

were likely to occur, since the sample was kept over night always under a CO pressure of 1-5 mm.

Fig. 13 shows the dependency of the extinction of the three bands on time and pressure. (i: p_{CO} = 0.1 mm Hg; ii: p_{CO} = 2 mm Hg; iii: p_{CO} = 3 mm Hg; iv: p_{CO} = 10 mm Hg). The experimental results are taken during one of the latter stages of these series of experiments. It is interesting that whereas the bands at 2070 cm^{-1} and 2120 cm^{-1} reach almost their final intensities at $p \sim 0.1$ mm, the band at 2170 cm^{-1} needs a pressure of about 10 mm.

A change in the ease of removability of the bands at 2070 cm^{-1} and 2120 cm^{-1} was noticed at the end of these experiments; there was an increase of the removability of the band at 2120 cm^{-1} by 15% whereas the band 2070 cm^{-1} has become less removable by a factor of 0.3.

The interaction of these three surface species with other gases was studied in CO_2, H_2, O_2 atmospheres which always contained some CO due to the high equilibrium pressure of the band at 2170 cm^{-1}.

In an atmosphere of 6 mm H_2 and 1 mm CO the half widths of the bands were decreased and there seemed to be also a slight change in the mutual position of the bands. In a mixture of 30 mm CO_2 and 1 mm CO no interaction with the three bands could be detected.

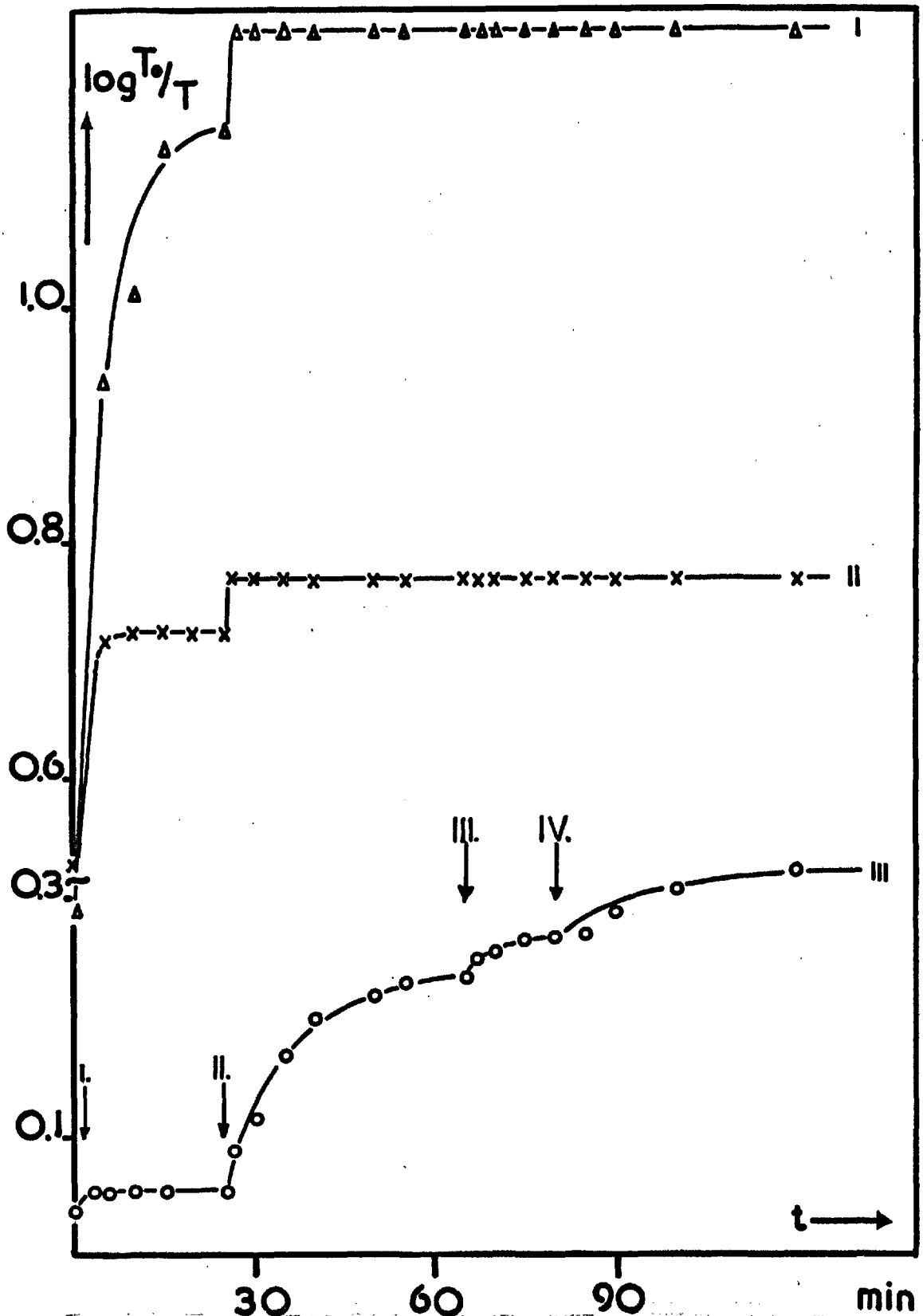


Fig.13. Chemisorption of CO by an oxidized Pt-surface as function of time at different gasphase pressures of CO

Also, in an atmosphere of 6 mm O_2 and 2 mm CO no change in the intensities or the positions of the bands was observed. After 72 hours a small amount of CO_2 ($\log {}^{T_o}/_{T} \sim 0.01$) could be detected in the spectrum.

Previous experiments (see chapter 1.9) have shown that chemisorbed CO ("Pt - CO") can be easily oxidized in an oxygen atmosphere ($\sim$ 1 mm Hg) at about room temperature according to

$$(1) \quad \text{"Pt - CO"} + O_{2g} \rightarrow CO_{2g} + \text{"Pt - O"}$$

The same reaction (1) also takes place when some of the Pt-surface is covered by a layer of Pt-oxide. It can be studied by means of the decrease of the CO stretching band (2070 cm^{-1}), provided no CO is present in the gasphase.

But in the case of a mixed gasphase (p_{O_2} = 6 mm, p_{CO} = 2 mm) no decrease of the concentration of the chemisorbed CO occurs, as the oxidized CO is at once replaced by CO from the gasphase.

This replacement can take place by simple chemisorption of CO from the gasphase on the freed Pt-site. When the Pt-site has already been covered by chemisorbed oxygen ("Pt - O") then reaction between the gaseous CO and this chemisorbed oxygen (4) takes place according to

$$(2) \quad \text{"Pt - O"} + 2\ CO_g \rightarrow CO_{2g} + \text{"Pt - CO"}$$

Both replacement processes require practically no activation energies and, hence, are much faster than reaction (1), for which we determined the activation energy of about 10 K cal.mole^{-1}.

A decrease in the intensities of the bands at 2120 cm^{-1} and 2170 cm^{-1} can be already accelerated when the pellet is heated in a H_2 or CO atmosphere. Thus, within 10-20 minutes the oxide patches can be completely removed and the bands at 2120 cm^{-1} and 2170 cm^{-1} do not appear again when CO is admitted to the system.

According to the chemical behaviour of the chemisorbed species and the frequencies of the corresponding CO stretching bands of the different surface species we attribute the bands at 2070 cm^{-1}, 2120 cm^{-1}, and 2170 cm^{-1}, to CO bonded to Pt, Pt^{2+}, and Pt^{4+}.

The bands at 2120 cm^{-1} and 2170 cm^{-1} and the species they represent are discussed in the next two chapters.

1.11 Properties of carbon monoxide chemisorbed by Pt^{2+}-ions; determination of the apparent integrated absorption intensity of the CO stretching band

Irving and Magnusson (15) studied the CO stretching bands of various Pt (II) carbonyl halogenids. They reported for $\left[Pt(CO)X_2\right]_2$ with X = Cl, Br, I CO frequencies at 2146 cm^{-1}, 2135 cm^{-1}, and 2122 cm^{-1}, respectively.

We have attributed the CO band at 2120 cm^{-1} to CO chemisorbed by Pt^{2+}-ions on the surface of the oxide layer. This agrees also well with the chemical reactivity of this kind of surface species.

The differences in the reactivity of CO chemisorbed on Pt surface atoms (band at about 2070 cm^{-1}) and of CO chemisorbed on Pt^{2+} ions on the surface (2120 cm^{-1}) is clearly demonstrated during the oxidation reaction in an atmosphere of 2 mm Hg oxygen at room temperature.

On addition of oxygen only the band at about 2070 cm^{-1} disappears whereas that at 2120 cm^{-1} remains unchanged. Hence, in agreement with the results on an oxide free Pt sample (chapter 1.9) CO chemisorbed on Pt surface atoms is

oxidized. CO chemisorbed by Pt^{2+}-ions does not react at all under the same experimental conditions.

By this means it is possible to detect very small concentrations of CO chemisorbed by Pt^{2+}-ions in the presence of high concentrations of CO chemisorbed by Pt surface atoms.

After the complete oxidation of the CO chemisorbed on Pt the oxygen was replaced by hydrogen (p = 10 mm Hg). Under these conditions the band at 2120 cm^{-1} gradually disappeared and instead a new band at about 2070 cm^{-1} appeared. The increase of this band was much bigger than the corresponding decrease of the band at 2120 cm^{-1}, which took about 30 minutes to disappear completely (fig. 14).

The linear relationship of the changes of the extinction figures of both bands is demonstrated in fig. 15.

After removing the hydrogen, the new band at about 2070 cm^{-1} could be completely removed by adding oxygen as in the case of CO chemisorbed on Pt.

When after this CO (p = 10 mm Hg) was added again, the hydrogen treated Pt-pellet has the band at 2070 cm^{-1} but not the band at 2120 cm^{-1} and that at 2170 cm^{-1}, both of which were formed with the oxidized Pt-sample.

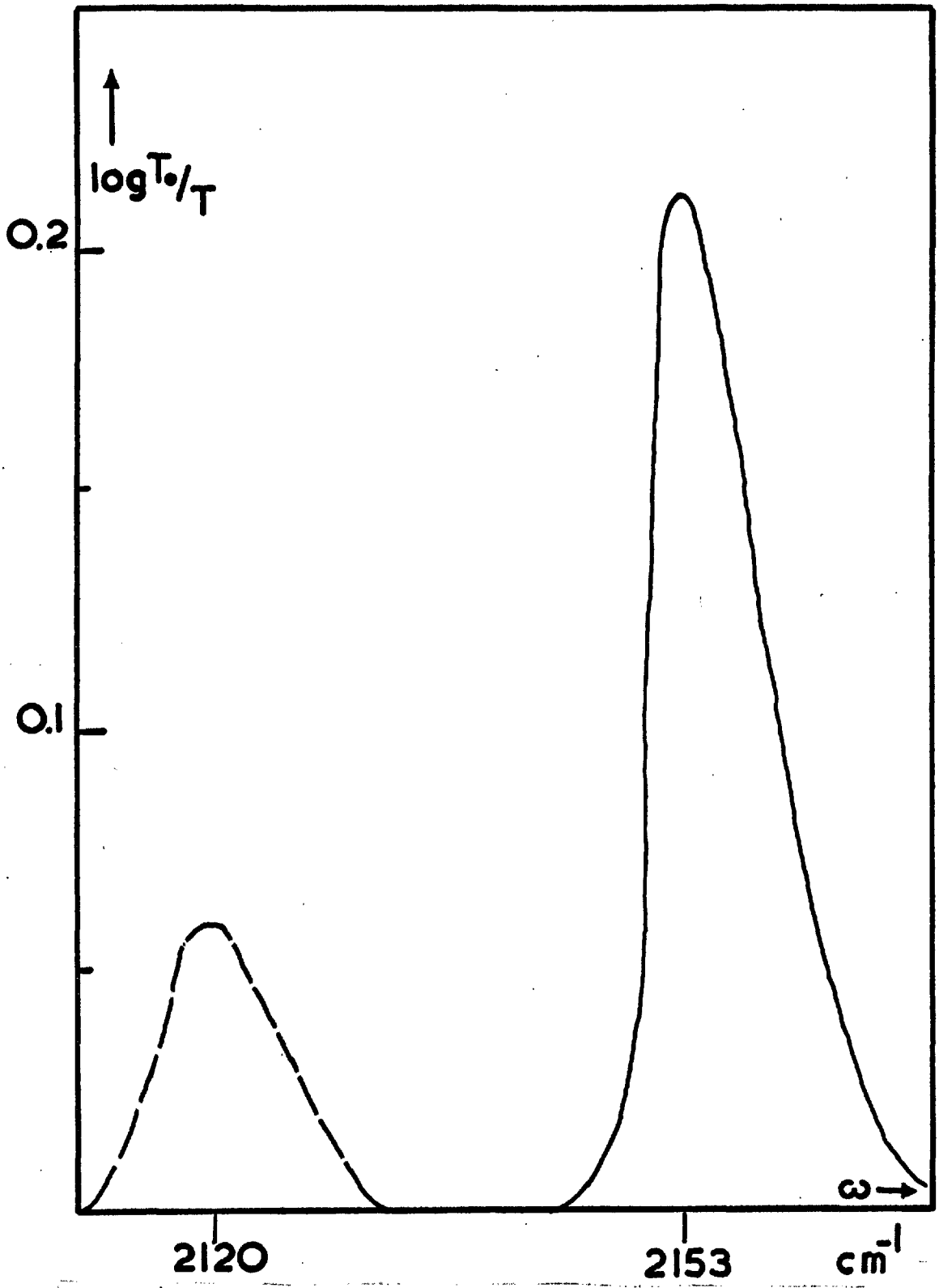


Fig.14. Interaction of H_2 with chemisorbed CO at 2120 cm^{-1} on an oxidized Pt surface

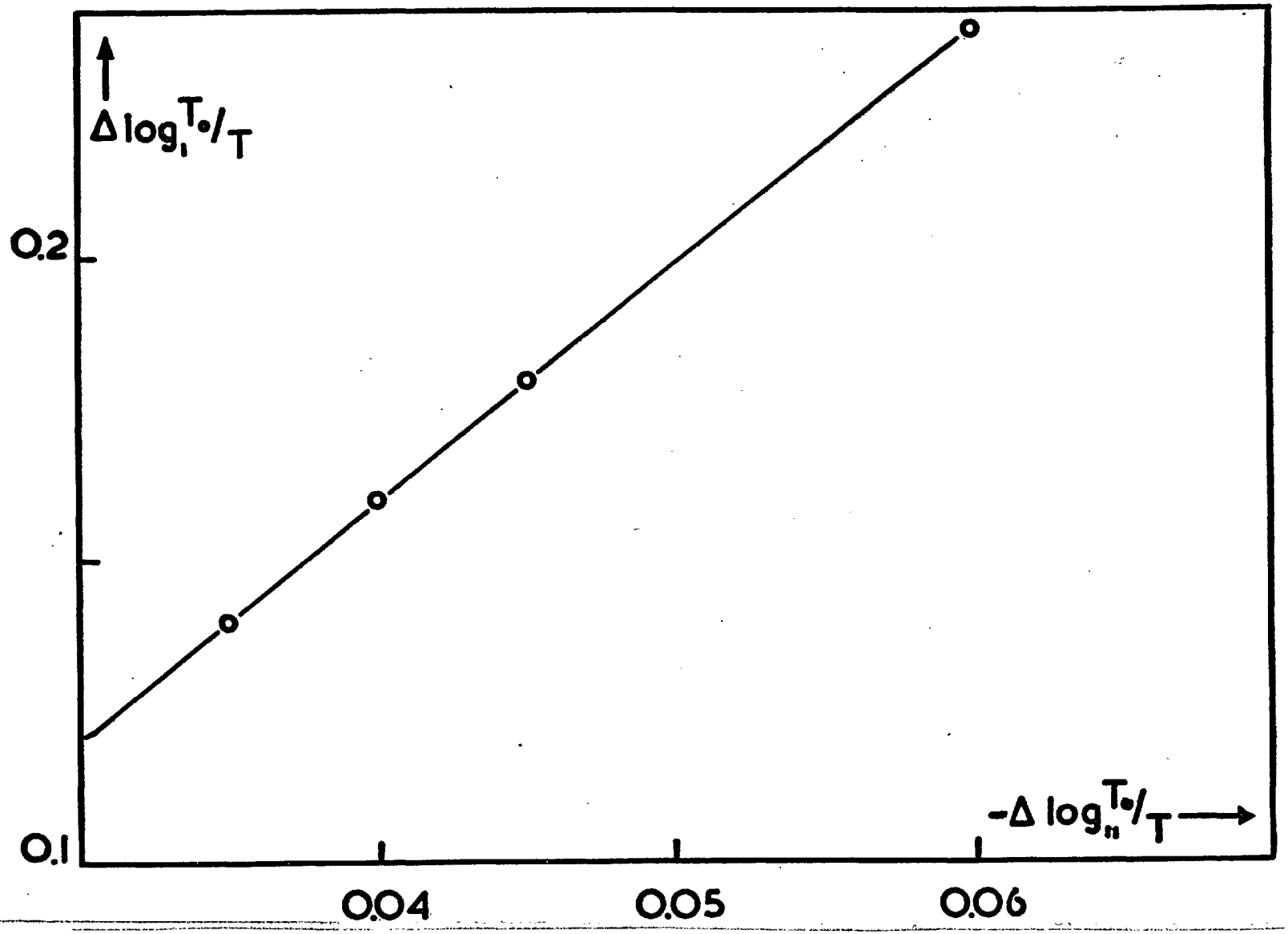


Fig.15. Relationship between the decrease of the extinction of the band at 2120 cm^{-1} and the increase of the extinction of the band at about 2070 cm^{-1}

We interpret the effect of H_2 on the oxidized Pt-sample as a reduction process of oxide patches. During this process the sites of chemisorption of the CO were changed from Pt^{2+}- to Pt-sites, which could be demonstrated by I.R. analysis.

These experiments were carried out with the Pt-pellet oxidized in a highly sintered state. Thus, the bands at 2120 cm^{-1} and 2170 cm^{-1} were not very strong in the presence of a sufficient high CO pressure. But the reactivity of this sample was remarkably high in comparison to the highly oxidized unsintered state of the pellet, in which case no significant changes occurred during the exposure to an H_2, CO atmosphere (chapter 1.10).

In connection with the chemisorption of carbon monoxide on Pt and Pt^{2+} sites on the same Pt sample the question arises, whether the chemisorbed CO species are able to move from one kind of sites to the other.

For carbon monoxide molecules bound by Pt^{2+}-ions it could be demonstrated that during 20 hours at room temperature no surface diffusion of CO from Pt^{2+} to Pt surface sites has taken place.

Concerning the apparent extinction coefficient the slope in fig. 15 indicates a 5 times smaller apparent extinction coefficient for the CO band of carbon monoxide

chemisorbed by Pt^{2+}-ions in comparison with that figure for carbon monoxide chemisorbed on Pt.

This figure is in good agreement with results of the following dosing experiments.

When CO is added in small doses to the sample which has been oxidized at high temperature the CO is chemisorbed by the surface and bands at about 2070 cm^{-1} (Pt - CO) and at 2120 cm^{-1} (Pt^{2+} - CO) are observed.

There is no increase of the band at 2170 cm^{-1} as this band only develops under higher gas pressures ($> 10^{-1}$ mm Hg).

As we know the apparent extinction coefficient for CO chemisorbed on Pt (chapter 1.5) it is possible to calculate the amount of CO which has been chemisorbed by the Pt-surface. The difference between the whole charge of CO and this amount provides us with the amount of CO taken up by the oxide surface forming Pt^{2+} - CO surface species.

In agreement with our previous figure the apparent extinction coefficient of the CO band at 2120 cm^{-1} has been found to be

$$k_a = 0.4 \text{ to } 0.5 \times 10^{-18} \text{ cm}^2/\text{molecules}$$

corresponding to

$$k_a = 2.4 \text{ to } 3.0 \times 10^{2} \text{ litre} \times \text{mole}^{-1} \times \text{cm}^{-1}.$$

As the apparent extinction coefficient for the Pt^{2+} - CO species is known it becomes possible to determine the figures for the corresponding apparent integrated absorption intensity B.

The determination of these figures has been carried out according to the procedure described in chapter 1.6.

The values obtained from two experiments for the apparent integrated absorption intensity B are

$$B_1 = 300 \times 10^2 \text{ cm}^{-2} \cdot \text{mole}^{-1} \cdot \text{litre}$$
$$B_2 = 280 \times 10^2 \quad "$$

Considering the corrections (chapter 1.6) these figures correspond to a mean figure of the true integrated absorption intensity of

$$A = 420 \times 10^2 \text{ cm}^{-2} \text{ mole}^{-1} \text{ litre}.$$

Eischens and Pliskin (10) reported for a CO covered Fe surface a "shift" of the CO band from 1960 cm^{-1} to 2127 cm^{-1} when oxygen was added. A "shift" towards higher frequencies has also been observed by Yang and Garland (33) with Rh, where a "shift" from 2053 cm^{-1} to 2127 cm^{-1} occurs.

There seems to be a direct connection between these results on Fe and Rh and the results of the experiment

where H_2 has been added to an oxidized Pt-sample which contains Pt^{2+} - CO species (2120 cm^{-1}) only. In this particular case we have demonstrated that the "shift" of the CO band at 2120 cm^{-1} towards lower frequencies to about 2070 cm^{-1} is due to the reduction of the Pt-oxide patches.

Hence, we suppose that the "shift" towards higher frequencies for CO covered Fe and Rh surfaces is due to the oxidation of the corresponding metal surfaces and the formation of Fe and Rh ions on which CO is chemisorbed.

With Cu (II) oxide additional to the band at 2127 cm^{-1} a band at 2173 cm^{-1} has been reported (44).

It is of some interest to note that a "shift" towards higher frequencies of the CO band of carbon monoxide chemisorbed on Pt (2070 cm^{-1}) does not occur in the case of Pt on addition of oxygen. This marked difference is due to the fact that at room temperature - as generally assumed - oxygen is in a chemisorbed state rather than in a more ionic one as on Fe and Rh surfaces.

1.12 Identification of the CO band at 2170 cm^{-1}

The previous experiments have shown that this CO band only develops under a relatively large CO pressure ($p > 0.1$ mm Hg) and is very easily removed by pumping.

This indicates a weak bonding of the CO and one might expect a physical adsorption of the CO instead of a chemisorption. But physical adsorption should occur without activation energy and we know from our experiments that it takes about 1 hour to develop the band at 2170 cm^{-1} under a CO gas pressure of 1 to 10 mm. Another argument against physical adsorption of CO is the fact that the CO frequency of the band at 2170 cm^{-1} is shifted by 27 cm^{-1} to higher frequencies in comparison with the frequency of gaseous CO.

For physical adsorption one would expect a CO band near that of liquid CO (2139 cm^{-1}) (17) and not such a big shift which is more than half as large as that which is connected with the ionization of CO to CO^{+} (2184 cm^{-1}) (45).

The results of Irving and Magnusson (15) suggest that the CO might be bonded to a Pt^{2+} ion which already contains a CO molecule. This kind of species could be formed and decomposed by the following mechanism:

$$(i) \qquad Pt^{2+} + 2\,CO \rightleftharpoons Pt^{2+}(CO)_2$$

$$(iia) \qquad Pt^{2+} + CO \rightleftharpoons Pt^{2+}(CO)$$

$$(iib) \qquad Pt^{2+}(CO) + CO \rightleftharpoons Pt^{2+}(CO)_2$$

According to Irving and Magnusson the compound $Pt(CO)_2\,Cl_2$ has two CO bands at 2200 cm^{-1} and 2162 cm^{-1}. These bands are close to the band at 2170 cm^{-1} which we find due to the chemisorption of CO on the oxide surface. The ease of decomposition of the inorganic compound $Pt(CO)_2\,Cl_2$ would correspond well with the high removability of the band at 2170 cm^{-1}.

But there is a serious objection against this idea. No decrease of the band at 2120 cm^{-1} has been observed when the band at 2170 cm^{-1} is formed according to (iib) and there is also no increase of the band at 2120 cm^{-1} when the band at 2170 cm^{-1} is removed by pumping.

There is also no experimental evidence for a reaction according to mechanism (i), because the band at 2170 cm^{-1} occurs at relatively high pressures where all the Pt^{2+}-ions have already chemisorbed one CO molecule according to (iia).

During the oxidation of carbon monoxide over NiO Eischens and Pliskin (35) observed a band whose frequency 2193 cm^{-1} was close to that of the band at 2170 cm^{-1} which we are discussing.

In case of NiO the band was attributed to the asymmetric vibration of a structure of type Me-O-C-O.

On other oxides like ZnO and chromia alumina and alumina (46, 47) bands have been detected at 2174 and 2200 cm^{-1} in the presence of CO.

But as it was impossible in any of these oxides to detect a band which might be due to the corresponding symmetric vibration, we exclude the possibility that the CO is bonded to the oxygen ions on the Pt-oxide surface.

As the formation of Pt (IV) oxide is thermodynamically possible under the experimental conditions we used (37), we assume that the Pt^{4+}-ions are the third chemisorption centres on the surface besides Pt and Pt^{2+}-sites and that the CO band at 2170 cm^{-1} is due to the formation of Pt^{4+} - CO surface species.

The general discussion of the chemisorption of CO on Pt and Pt-ions (chapter 1.13) will show that it is possible to explain why CO is only weakly bound by Pt^{4+}ions and, hence, easily pumped off and why we find the corresponding CO stretching frequency shifted further to higher wave numbers in comparison with the band position for the Pt^{2+}-ions.

For CO bonded to Pt^{4+}-ions it was not possible to determine the apparent extinction coefficient and the

apparent integrated absorption intensity because of its unfavourable high equilibrium pressure.

1.13 Discussion of the chemisorption of carbon monoxide on Pt and Pt-ions

Eischens et al. (48) determined the force constants for the C - O and Pt - C stretching vibrations of linearly chemisorbed CO species by means of the isotopic shift ratio of the C - O stretching vibration of $C^{12}O$ and $C^{13}O$.

Blyholder (50) calculated from the experimental figures of the frequencies of the C - O and Fe - C stretching vibrations of the chemisorbed CO on Fe the corresponding force constants.

The CO force constants of CO linearly chemisorbed on Pt and Fe are close to those figures in metal carbonyls (110). The force constants for the Pt - C and Fe - C vibrations are somewhat bigger than the values in carbonyls, and depend on the mass which one assumes for the "metal surface".

By applying Badger's rule Blyholder (50) calculated the bonding distances for chemisorbed CO species on Fe. These figures as well as those evaluated for Pt are very close to the distance figures in metal carbonyls which were obtained by X-ray analysis and electron diffraction studies.

It is therefore reasonable to assume a similar bonding mechanism for the chemisorption of CO on metal surfaces as

for metal carbonyls, where we have detailed knowledge of the bonding mechanism (51).

In the case of $Ni(CO)_4$ electron diffraction (52), dipolmeasurements (53) and X-ray studies (57) have shown that the CO groups are bonded by the C-atom to the Ni atom in the carbonyl molecule. The same kind of bonding is generally assumed for other transition metal carbonyls and carbonyl compounds and also for CO chemisorbed on transition metal surfaces.

A general molecular orbital approach to the bonding in metal carbonyls has been given by Orgel (51, 55, 56), Ballhausen (57) and Richardson (58). For the chemisorbed CO species Blyholder proposed a molecular orbital view based on Hückel molecular orbitals (28).

The bonding of the carbon monoxide on a Pt atom may be described as a combination of an ordinary dative σ-bonding due to the overlap of the carbon 3σ orbital (59) containing the lone pair of electrons and a 5d 6s $6p^2$ Pt hybrid orbital with a back π-bonding resulting from overlap of a partially filled 5d 6p Pt hybrid orbital with the empty 2π orbitals of the CO molecule.

The back donation of electrons from the metal d, p hybrid orbitals to the 2π orbitals of the CO molecules remove some of the excess charge from the metal atom, built

up by the donor σ bond and allows further σ-bonding to occur. This "synergic interaction" strengthens the Pt - C bond and introduces some double bond character thereby slightly weakening the C - O bond, a result supported by the lowering of the carbonyl infrared stretching frequencies.

Generally, in carbonyls the metal-carbon and the carbon-oxygen bonds are complementary; any effect which increases one necessarily decreases the other (60).

The bonding of CO in a bridged structure can be discussed similarly. One has to consider here all the effects arising from the rehybridization ($sp \rightarrow sp^2$) of the carbon atom (49).

We apply these models mutatis mutandis to the chemisorption of CO in linear and bridged structure on metal surfaces.

In his view of the chemisorption of CO on transition metal surfaces Blyholder interprets the I.R. spectra in terms solely of linear CO species which are adsorbed on metal atoms; the lower frequency bands, generally attributed to bridged CO species, are ascribed in his view to linearly chemisorbed CO bonded to surface metal atoms having less than the maximum number of neighbours.

Among other properties of the chemisorbed CO which Blyholder explains in his m.o. view, he also deals with

the shift of the CO stretching band towards higher wave number with increasing surface coverage. He explains this effect in terms of the competition of an increasing number of CO species for a limited number of metal electrons.

This interpretation is not convincing. It does not take into account the transfer of electrons from the CO molecule to the metal surface and the 'synergic effect' of the metal-carbonyl-bonding.

The effect of the CO concentration on the frequency of the CO stretching band can be studied from data of metal carbonyls where the ratio metal atom to terminal CO groups alters.

According to Noack (16), with $Fe(CO)_4$ and $Fe(CO)_5$, the band centre moves by about 35 cm^{-1} to lower frequencies when the concentration of the terminal CO groups is increasing from 4:1 to 5:1.

A smaller shift of 10 cm^{-1} but in the same direction has been observed in $Co_4(CO)_{12}$ and $Co_2(CO)_8$ when the number of terminal CO groups per metal atom increases.

According to these results one should expect a shift towards lower frequencies with increasing CO coverage rather than a shift towards higher frequencies as experimentally observed (chapter 1.5); (10).

As we mentioned above, the metal-carbon and the

carbon-oxygen bonds are roughly complementary. This means that the increase of the C - O bond with increasing coverage is connected with a decrease in the Pt - C bond.

The repulsion forces between the surface dipoles and the heterogeneity of the surface are supposed to weaken the metal carbon bond and this in turn strengthens the C - O bond and shifts the corresponding frequency towards higher wave numbers.

For the strong bonding of CO in metal carbonyls and in its chemisorbed state on transition metal surfaces the back donation of electrons from the metal into the 2π orbitals of the CO molecule is essential.

In the chemisorption of CO the influence of back donation on the bonding of the chemisorbed CO species can be studied in the series Pt, Pt^{2+}, Pt^{4+}, where the electron concentration in the d, p levels for back donation decreases. In the same sequence we find the CO stretching band shifting towards higher wave numbers, i.e. from about 2070 cm^{-1} for "Pt - CO", to 2120 cm^{-1} for "Pt^{2+} - CO" and, finally, 2170 cm^{-1} for "Pt^{4+} - CO".

The CO stretching bands of the first two species have been shifted towards lower wave numbers in comparison with gaseous CO (2143 cm^{-1}) (45) indicating back donation of electrons from the Pt and Pt^{2+}-sites. For "Pt^{4+} - CO"

the CO band is shifted to higher frequencies compared with gaseous CO. In this case there is no back donation. The comparatively weakly bound CO is obviously positively charged ($CO^{\delta+}$) and its CO stretching frequency is close to that in the CO^{+} species (2184 cm^{-1}) (45). This lack of back donation results in a relatively weak chemisorption of the CO species on the Pt^{4+}-sites.

In the case of Pt^{2+} the electron concentration in the d, p levels is higher compared with that in Pt^{4+} and back donation results. The bonding between Pt^{2+} and CO is very strong and of the same order as the bonding for the strongly chemisorbed CO on Pt metal, for which we would expect an even stronger chemisorption bonding according to its increased back donation. But as we have seen (chapter 1.5 and 1.10) a good deal of the chemisorbed CO can be quite easily pumped off the Pt surface, whereas the removability of CO on Pt^{2+} is relatively small.

In the bonding of CO by Pt and Pt^{2+} some other effects come into play. There are differences in the radii which in turn affect the overlapping of the orbitals concerned. Further, due to its charge the bonding between Pt^{2+} and CO might possibly be of less covalent character than in the case of Pt. Additionally there are the effects arising from differences in the metal and oxide surfaces.

A mathematical relationship between the frequency of the CO stretching vibration and the number of electrons in the chemisorbed CO species has been discussed by Gardner and Petrucci (44).

For a limited number of CO species on metal and metal oxide surfaces the CO stretching vibrations could be related to the number of valence electrons. These chemisorbed CO species have been called intermedions. They are weakly held on metallic and metal oxide surfaces possessing partially vacant orbitals. These species are in equilibrium with the gasphase and can be removed easily by pumping (61).

When we apply this mathematical treatment to CO chemisorbed on Pt^{4+}-ions which has the properties of an "intermedion", we should expect on Pt and its ions chemisorbed CO species with ... 8.82, 9.82, 10.82, 11.82 etc. valence electrons.

But the figure which we get from the CO stretching frequency of CO on Pt^{4+} (2170 cm^{-1}) according to this mathematical treatment is 9.47 valence electrons, i.e. very far from that proposed by Gardner's interpretation (61).

Gardner's mathematical interpretation lacks a well based relation to the main factors determining the bonding on surfaces, such as radii, electrostatic charges, surface fields. Due to this the application of this treatment seems to us very limited.

PART II

INFRARED SPECTROSCOPIC AND SURFACE POTENTIAL STUDIES OF THE OXIDATION OF CHEMISORBED CARBON MONOXIDE ON PLATINUM.

2.1 Introduction

The oxidation of CO has been studied on Pd (62, 63), Pt (4), Ag (62, 64) and Au (63). The reaction kinetics are different for different metals and with Pd and Ag even two different mechanisms have been suggested.

All these experiments had in common a gasphase consisting of CO and O_2 and the reaction mechanism was derived by means of the rate at which CO_2 was formed.

Experiments on the oxidation of chemisorbed CO on Pd and Ni films have recently been reported (65, 66).

In the present work we followed the oxidation reaction on the Pt surface directly by measuring the decrease of the intensity of the CO stretching band of the chemisorbed CO in the infrared region (1). During the S.P. measurements (2) we studied the oxidation by following the replacement process of the oxidized CO by oxygen.

2.2 Infrared spectroscopic studies of the kinetic of the oxidation of carbon monoxide chemisorbed on Aerosil supported platinum

2.2.1 Experimental

Our previous I.R. measurements have shown that the only CO species we have to deal with on the surface of the Aerosil supported Pt sample is the linearly chemisorbed CO. This fact simplifies the study as no equilibria between different chemisorbed species have to be considered.

Another advantage of the Pt-catalyst is, that at the end of an oxidation run the chemisorbed oxygen on the Pt surface is very easily replaced by carbon monoxide. This reaction takes place even more rapidly than the oxidation of the chemisorbed CO by gaseous O_2 in which we are mainly interested.

Hence, the reaction can be easily repeated without changing the catalytic activity by vigorous reduction in H_2 at high temperatures.

All experiments described in this part were carried out with the same Pt-sample which was also used during the

previous I.R. studies. By these previous experiments the sample has obtained a suitable and stable catalytic activity as indicated by the good reproducibility of the results.

The procedure in the oxidation experiments was as followed: first, the surface of the Pt-sample was exposed for a constant time (10 min) to an CO atmosphere of 2 mm Hg. The cell was then evacuated for another 15 min to remove all the gaseous and weakly chemisorbed CO (fig. 7).

The initial CO surface concentration C as well as its changes during the reaction were determined by using the apparent extinction coefficient k_a (fig. 6) which had been determined in the previous experiments:

$$k_a = 200 \times 10^{-20} \text{ cm}^2/\text{molecules}.$$

As the maximum initial CO concentrations are less than 45×10^{16} molecules per CM^2 geometric pellet area (we use $\underline{CM}^2$, when the CO concentration is referred to the geometric pellet area and $\underline{cm}^2$, when related to the actual Pt surface) we had not to consider the deviation of the intensity from linearity at higher surface concentrations (fig. 6).

Oxygen was then introduced into the cell at 0.9 mm Hg pressure. This oxygen pressure is high enough so that it can be assumed to be constant during the whole of the reaction, the decrease being less than 2%. At this

pressure the rate of the decrease can be conveniently followed.

Higher oxygen pressure was avoided since overheating of the sample might occur and would make it difficult to study the kinetics. Such an overheating was actually observed at p > 10 mm oxygen.

When determining the activation energy of this oxidation process it was necessary to study the reaction at different temperatures (40-82° C).

As the efficiency of the furnace in the cell was dependent on the gaspressure present, the right figures for the heating current were obtained in blank experiments with an O_2 gaspressure of 0.9 mm Hg.

In the higher temperature experiments the CO gas was also chemisorbed at the given reaction temperature, and also the removal of the gaseous and weakly bonded CO took place at that same temperature. 10 seconds before the oxygen was introduced into the cell the heating current was switched to the corresponding value.

The temperature of the pellet was measured by the installed thermocouple th (fig. 2) fixed at the metal tubing. There was a good mechanical contact between the pellet and the metal tubing as the pellet itself was actually pressed in this piece of tubing.

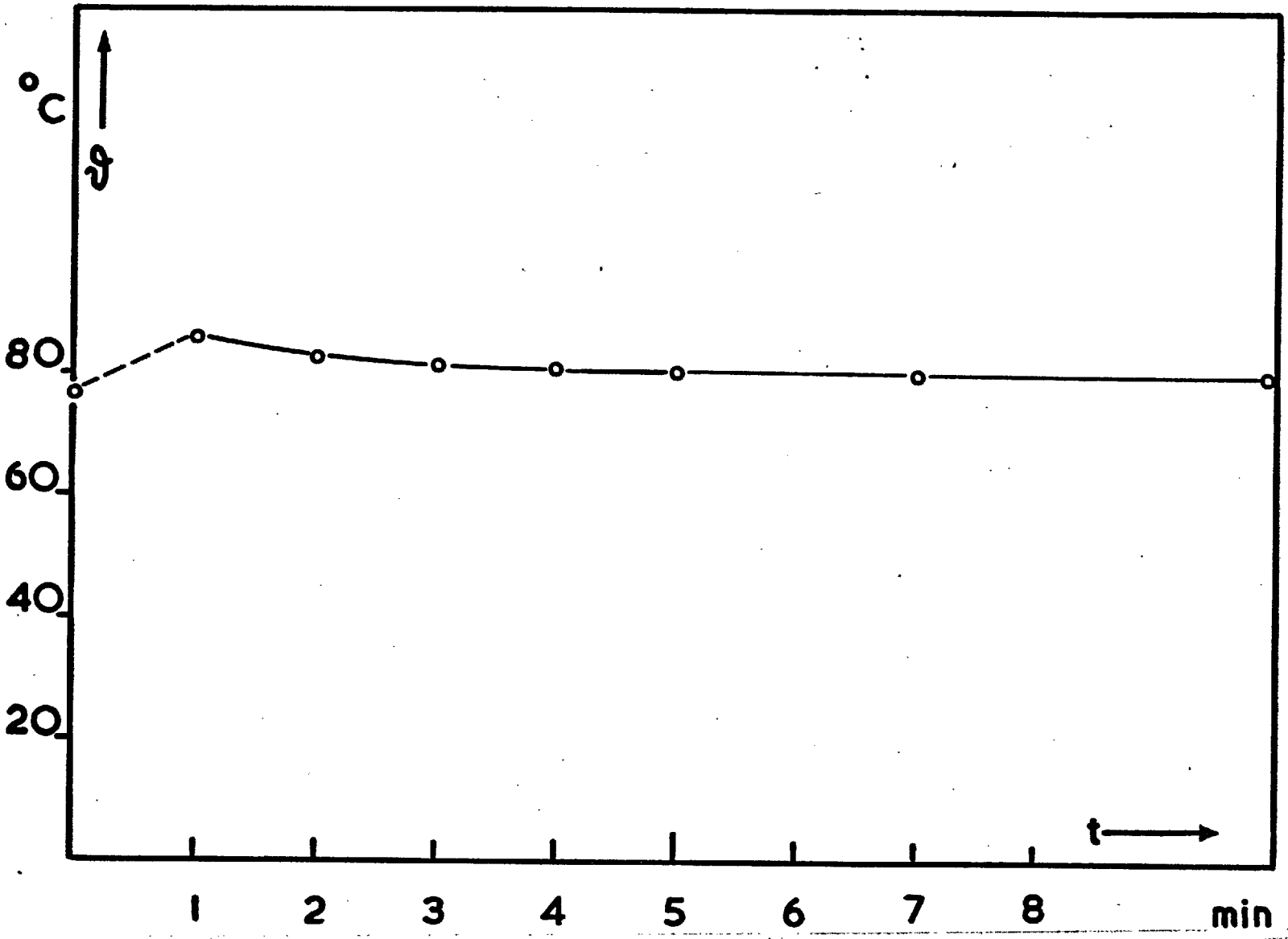


Fig.16. Temperature variation of the Pt-sample during the oxidation of the chemisorbed CO

Fig. 16 demonstrates the temperature variation of the sample during the reaction at 355° K.

The reproducibility of the experimental results was good and not affected by the conditions of the preceding oxidation run.

As the CO is removed by oxidation from the chemisorbed layer oxygen will rapidly be chemisorbed on the freed Pt-sites. After pumping off the oxygen gasphase the chemisorbed oxygen can be removed rapidly (< 30 sec) by exposure to CO ($p \sim 1$ mm) at room temperature due to formation of gaseous CO_2. Then CO is there again chemisorbed on the freed sites and the surface returns to the original condition of the first oxidation experiment.

The oxidation process was followed by the decrease in the concentration of the chemisorbed CO. The C - O stretching band of the linearly chemisorbed CO at about 2070 cm^{-1} was recorded at 1 minute intervals. The recording of the peak of the band was accurate to $\pm$ 5 sec.

During all the quantitative experiments the I.R. cell remained with its pellet in a fixed position in the I.R. apparatus and too, the Pt-sample was not exposed to air or other gases than CO and O_2 ($p \sim$ 2 mm).

In the tables 7, 8, and 9, are given the experimental results for three typical runs at three different temperatures (309° K, 316° K, and 355° K).

The following symbols are as:

T - Apparent I.R. intensity at the peak of the CO stretching band of the linearly chemisorbed CO.

T_o - Apparent I.R. intensity of the sample with no CO present on its surface, taken under $p_{O_2} = 0.9$ mm. T_o is taken at the same wave number as T.

E_a - Apparent extinction; $E_a = \log_{10} T_o/T$.

C - Concentration of the chemisorbed CO, calculated from the apparent extinction coefficient $k_n = 200 \times 10^{-20}$ cm^2/molecules. The concentrations in these tables are in terms of geometric pellet area (CM^2).

In the last two columns of these tables are given the values of $^1/C$ and log C, which are used in the following discussion.

Table 7

Oxidation experiment: $p_{O_2} = 0.9$ mm Hg; $T = 309^{\circ}$ K

t min	T	T_o	$E_a = \log \frac{T_o}{T}$	C $\frac{\text{molec.}}{CM^2}$	$^1/C$	log C
0	11	80.6	0.865	43.3×10^{16}	2.31×10^{-18}	17.636
1	14	80.4	0.758	37.9×10^{16}	2.64×10^{-18}	17.578
2	16	80.3	0.700	35.0×10^{16}	2.86×10^{-18}	17.544
3	19	80.1	0.625	31.3×10^{16}	3.20×10^{-18}	17.495
4	22	79.9	0.559	27.9×10^{16}	3.58×10^{-18}	17.445
5	24	79.8	0.521	26.1×10^{16}	3.83×10^{-18}	17.416
7	25	79.7	0.503	25.2×10^{16}	3.97×10^{-18}	17.401
10	35	79.2	0.354	17.7×10^{16}	5.65×10^{-18}	17.248
15	41	78.7	0.283	14.2×10^{16}	7.04×10^{-18}	17.152
20	47	78.2	0.221	11.1×10^{16}	9.00×10^{-18}	17.045
25	51	78.0	0.184	9.2×10^{16}	10.85×10^{-18}	16.963
30	54	77.5	0.156	7.8×10^{16}	12.81×10^{-18}	16.891

Table 8

Oxidation experiment: p_{O_2} = 0.9 mm Hg; T = 316° K

t min	T	T_o	E_a	log $\frac{T_o}{T}$	C $\frac{\text{molec.}}{CM^2}$	$^1/C$	log C
0	15	80.4	0.729	36.5×10^{16}	2.74×10^{-18}	17.550
1	25	79.8	0.504	25.2×10^{16}	3.97×10^{-18}	17.401
2	29	79.5	0.438	21.9×10^{16}	4.56×10^{-18}	17.340
3	33	79.3	0.381	19.1×10^{16}	5.24×10^{-18}	17.281
4	34	79.2	0.367	18.4×10^{16}	5.44×10^{-18}	17.265
5	36	79.1	0.342	17.1×10^{16}	5.85×10^{-18}	17.233
7	41	78.7	0.283	14.2×10^{16}	7.05×10^{-18}	17.152
10	45	78.4	0.240	12.0×10^{16}	8.33×10^{-18}	17.078
15	52	77.7	0.174	8.7×10^{16}	11.50×10^{-18}	16.939
20	53	77.6	0.166	8.3×10^{16}	12.05×10^{-18}	16.918
25	56	77.3	0.140	7.0×10^{16}	14.30×10^{-18}	16.844
30	59	76.8	0.114	5.7×10^{16}	17.55×10^{-18}	16.756

Table 9

Oxidation experiment: p_{O_2} = 0.9 mm Hg; T = 355° K

t min	T	T_o	E = log $\frac{T_o}{T}$	C $\frac{\text{molec.}}{CM^2}$	$^1/C$	log C
0	15	80.4	0.729	36.5×10^{16}	2.74×10^{-18}	17.562
1	35	79.2	0.354	17.7×10^{16}	5.65×10^{-18}	17.248
2	45	78.4	0.240	12.0×10^{16}	8.34×10^{-18}	17.078
3	50	77.9	0.192	9.6×10^{16}	10.42×10^{-18}	16.982
4	54	77.5	0.156	7.8×10^{16}	12.81×10^{-18}	16.892
5	56	77.3	0.140	7.0×10^{16}	14.30×10^{-18}	16.844
7	60	76.7	0.106	5.3×10^{16}	18.90×10^{-18}	16.724
10	62	76.4	0.090	4.5×10^{16}	22.20×10^{-18}	16.652

2.2.2 Discussion

The question whether the activation energy E varies with the surface concentration of the chemisorbed CO or not becomes vital for further discussion of any kinetics.

Previous I.R. results have given evidence (chapter 1.6) that the polarity of the C - O bond of the chemisorbed CO varies with its concentration on the Pt surface.

Hence, we should expect a change of the activation energy of the oxidation as the amount of chemisorbed CO decreases.

We have plotted C as a function of time and derived graphically the values of $-\frac{dC}{dt} \equiv V$ for different C at different temperatures (tab. 10) (C - concentration of the chemisorbed CO in molecules/CM^2).

In fig. 17 are plotted log V as a function of C at 309° K (i), 316° K (ii), and 355° K (iii).

As the activation energy is

$$E = R \times \frac{T_1 \cdot T_2}{T_1 - T_2} \times (\log_e V_{T_2} - \log_e V_{T_1})$$

for C = const, the variation of the intercept between two of these three plots would indicate the change of the activation energy E during the oxidation process.

Table 10

C x 10^{-16} [molec. CM^{-2}]	V x 10^{-13} [molec. cm^{-2} sec^{-1}]			log C	log V		
	T = 309°K	T = 316°K	T = 355°K		T = 309°K	T = 316°K	T = 355°K
8	3.38	5.00	27.0	16.903	0.528	0.699	1.432
10	5.98	7.66	42.0	17.000	0.777	0.884	1.623
12	8.14	11.20	56.3	17.079	0.910	1.049	1.750
14	10.25	15.45	91.2	17.146	1.011	1.189	1.960
16	13.20	19.32	111.0	17.204	1.120	1.286	2.045
18	19.00	24.30	139.8	17.255	1.279	1.386	2.145
20	24.65	35.62	183.2	17.301	1.392	1.551	2.262
22	29.50	45.00	250.0	17.343	1.470	1.653	2.398

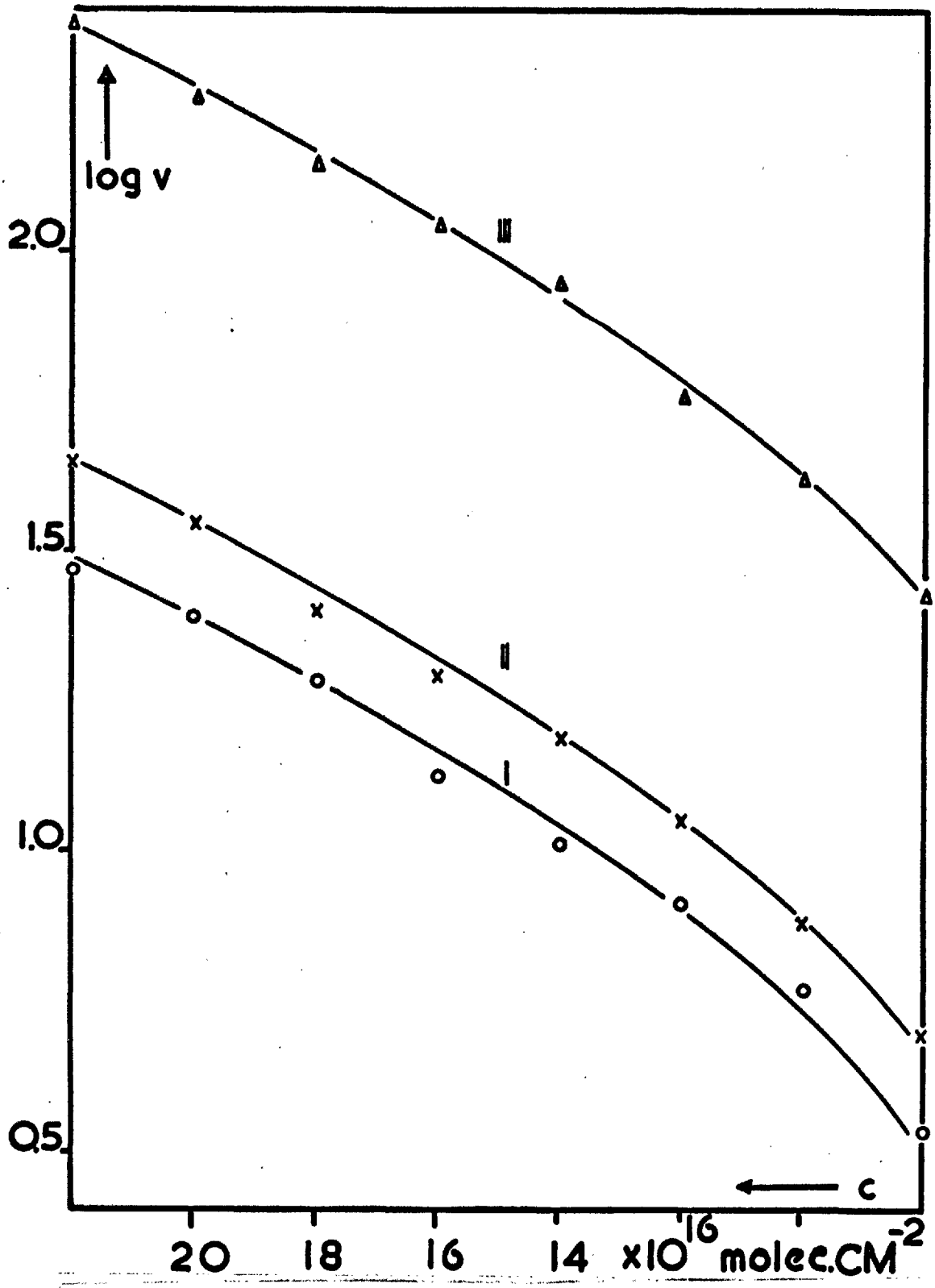


Fig.17. Oxidation of the chemisorbed CO; log (velocity) as a function of surface concentration.

All the three plots are parallel to each other over a large range, so that E = const.

For surface concentrations $C > 22 \times 10^{16}$ and $C < 8 \times 10^{16}$ molecules/CM^2 the changes of the surface concentrations become either too large or too small to provide us with reasonable reliable values for V.

The activation energy derived is

$$E = 9600 \text{ cal/mole} \quad \text{(fig. 18)}.$$

The reaction order n of the decrease of the chemisorbed CO during this oxidation process is given by the following equation

$$V = k \cdot C^n$$

so that

$$\log V = \log k + n \log C$$

In fig. 19 $\log V = f(\log C)$ is plotted for the three runs. The slope of these lines gives n = 2. Hence, there is a second order decrease of the chemisorbed CO during the oxidation, i.e.

$$-\frac{dc}{dt} = k'' \cdot c^2$$

$$\frac{1}{c} - \frac{1}{c_o} = k'' \cdot t$$

$$\frac{1}{c} = a \cdot t + b$$

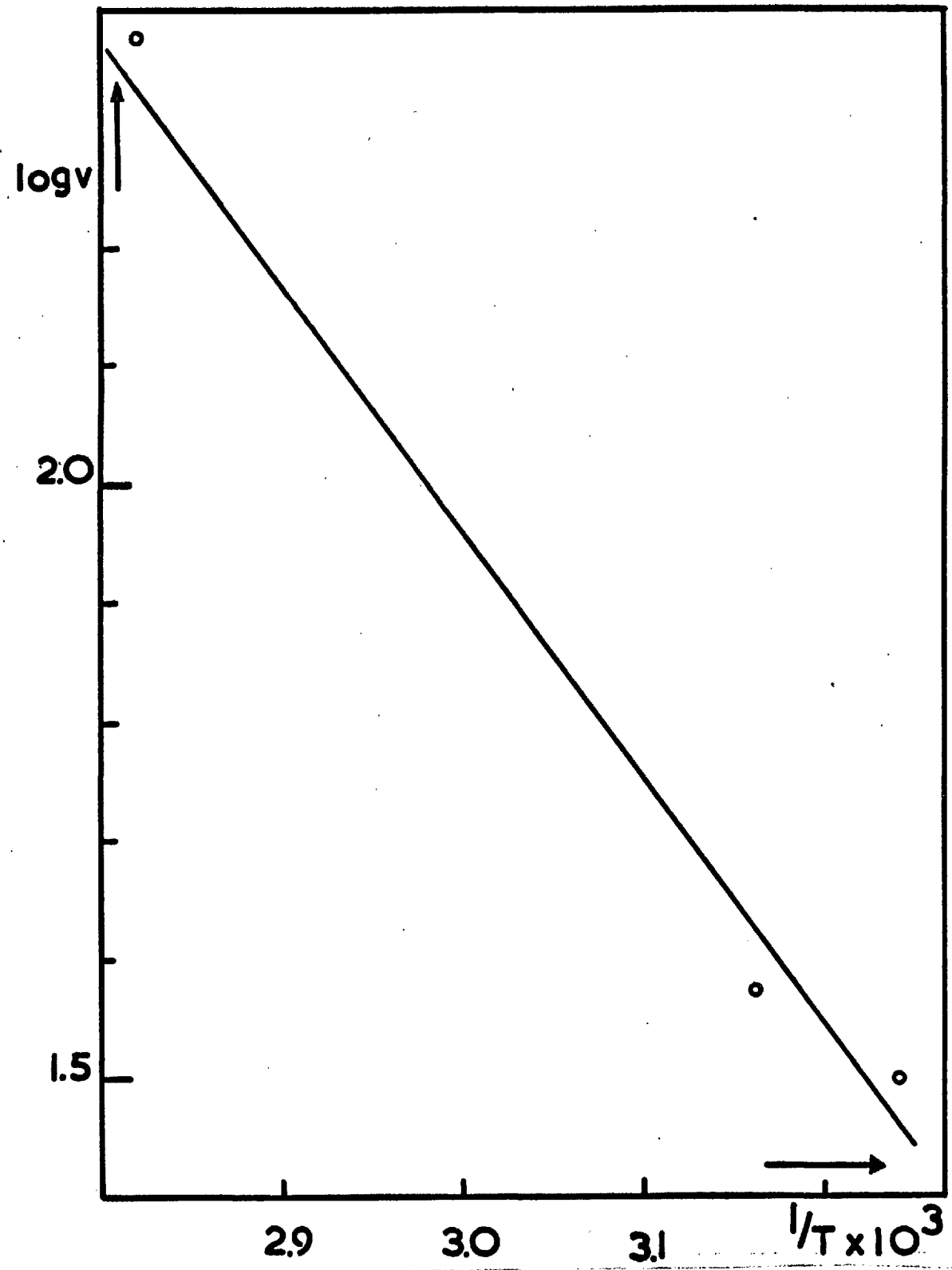


Fig.18. Oxidation of the chemisorbed CO; determination of the activation energy.

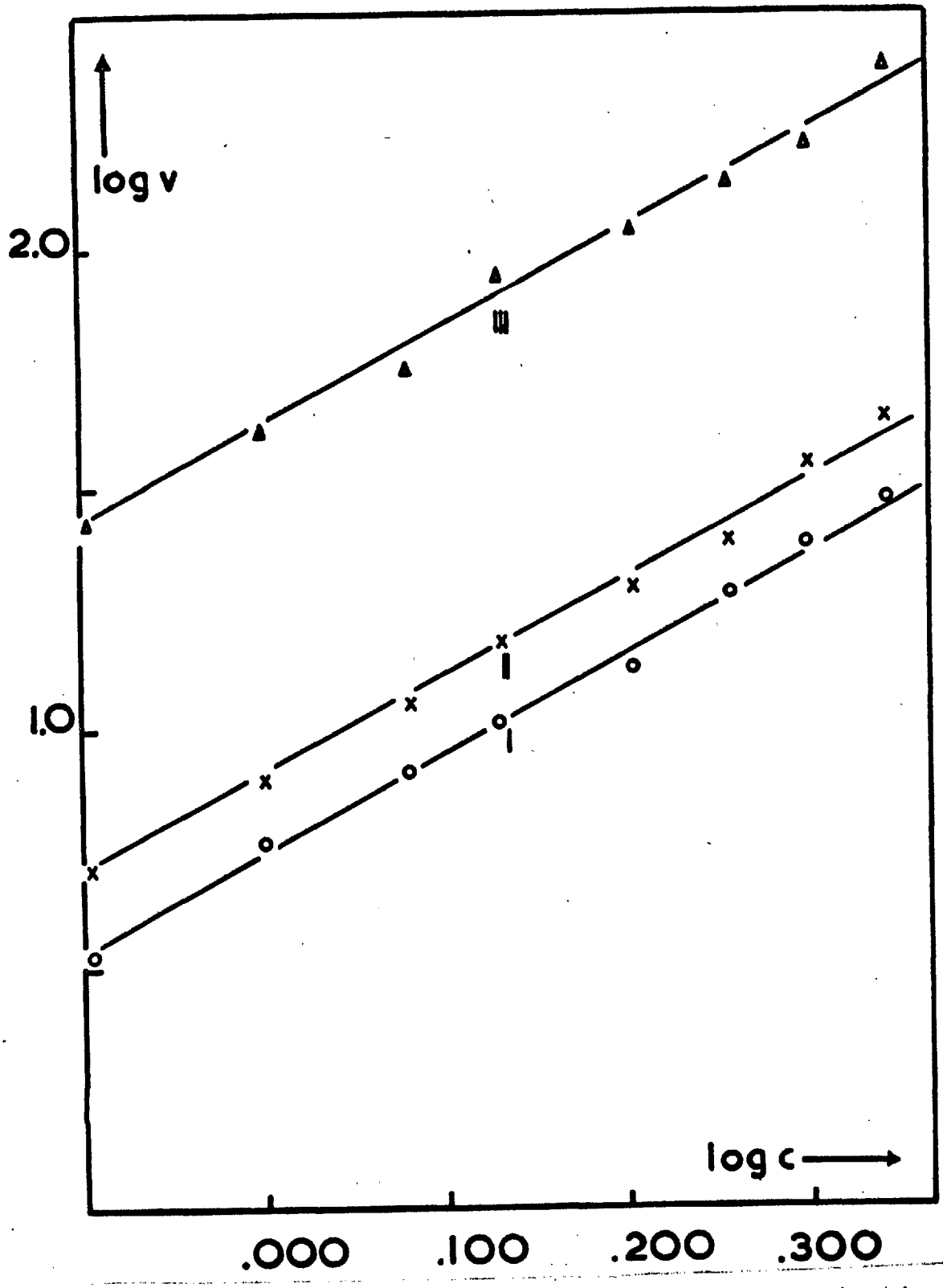


Fig.19. Oxidation of the chemisorbed CO; determination of the reaction order.

where

C is the concentration of the chemisorbed CO at time t,

C_o is the initial concentration at time t = 0,

a, b are constants, and

k'' the velocity constant.

For comparison we also show the decrease of CO according to a first order reaction. The corresponding equations are

$$-\frac{dc}{dt} = k'.c$$

$$\log_e c = -k't + \log_e c_o$$

$$\log c = -At + B$$

In fig. 20, 21, 22 are plotted $^1/C = f(t)$ and also $\log C = f(t)$.

The decrease in the CO concentration C is clearly described by a second order kinetic.

For the three different temperatures the velocity constants k'' turn out to be:

309^o K : $k'' = 0.56 \times 10^{-20}$ molec.$^{-1}$ CM^2 sec^{-1}

316^o K : $k'' = 0.81 \times 10^{-20}$ molec.$^{-1}$ CM^2 sec^{-1}

355^o K : $k'' = 3.83 \times 10^{-20}$ molec.$^{-1}$ CM^2 sec^{-1}

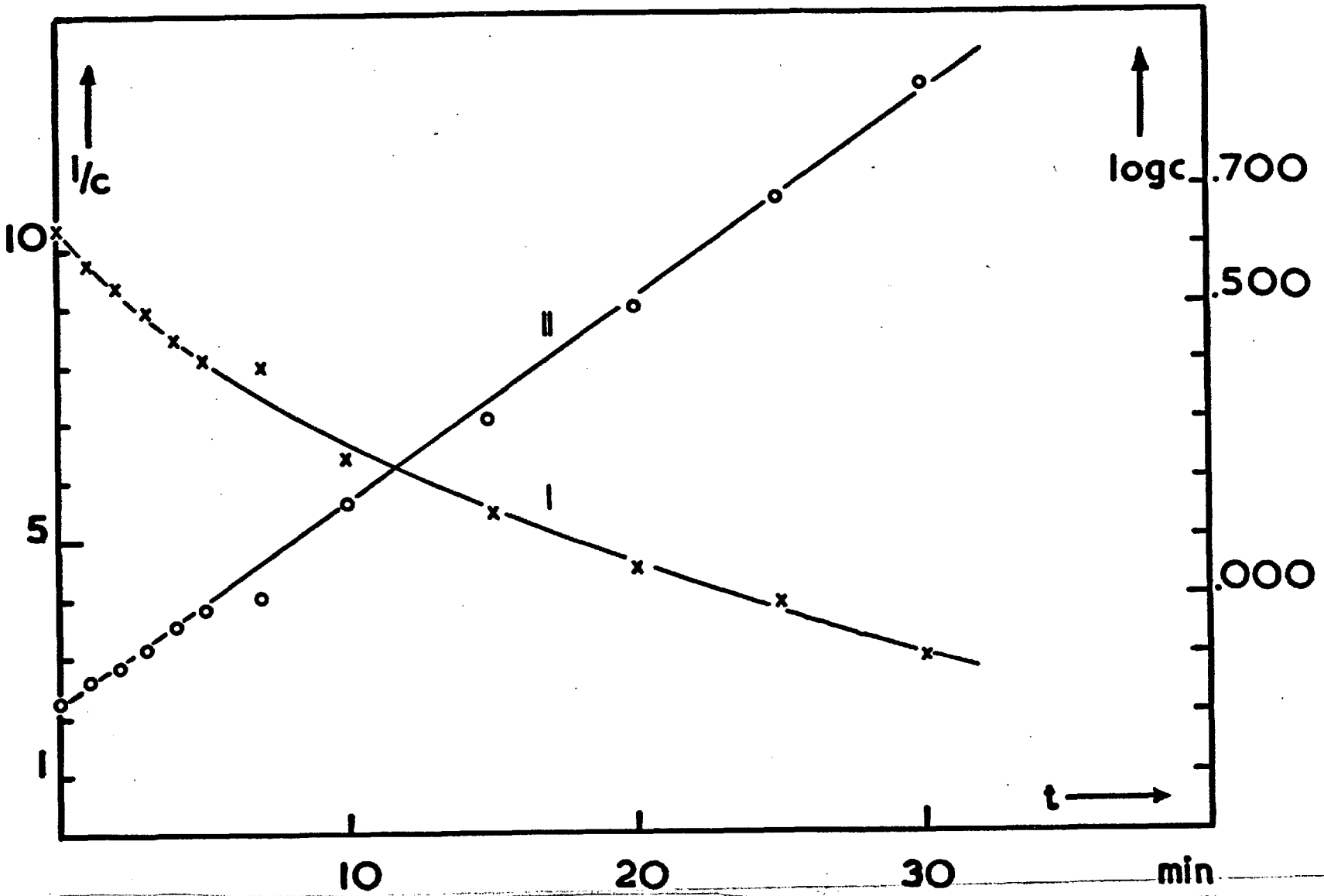


Fig.20. 1st-order (log c) and 2nd-order ($^1/c$) plots for the oxidation of the chemisorbed CO; p_{O_2} = 0.9 mm Hg; T = 309° K.

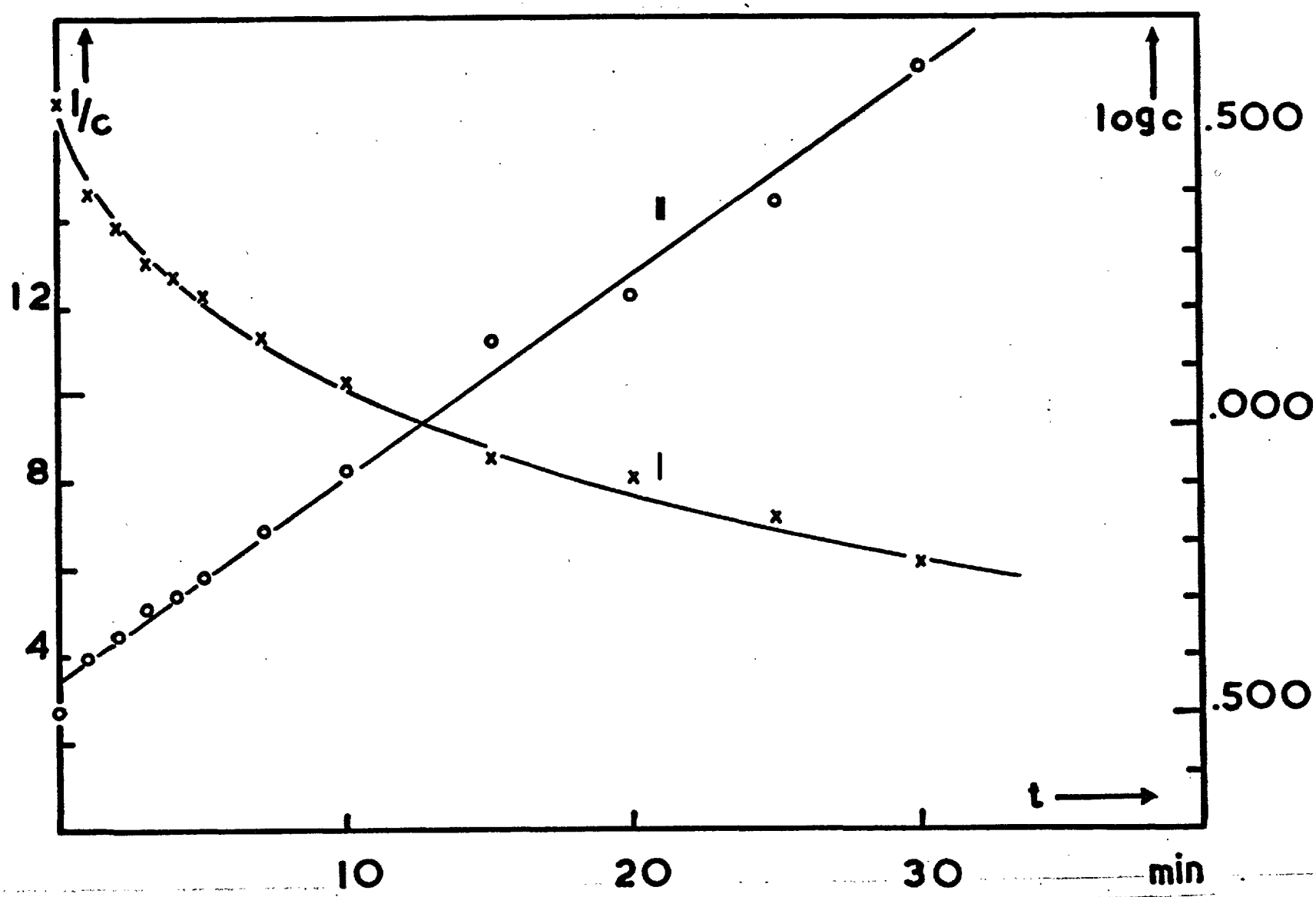


Fig.21. 1st-order (log c) and 2nd-order ($^{1}/c$) plots for the oxidation of the chemisorbed CO; p_{O_2} = 0.9 mm Hg; T = 316° K.

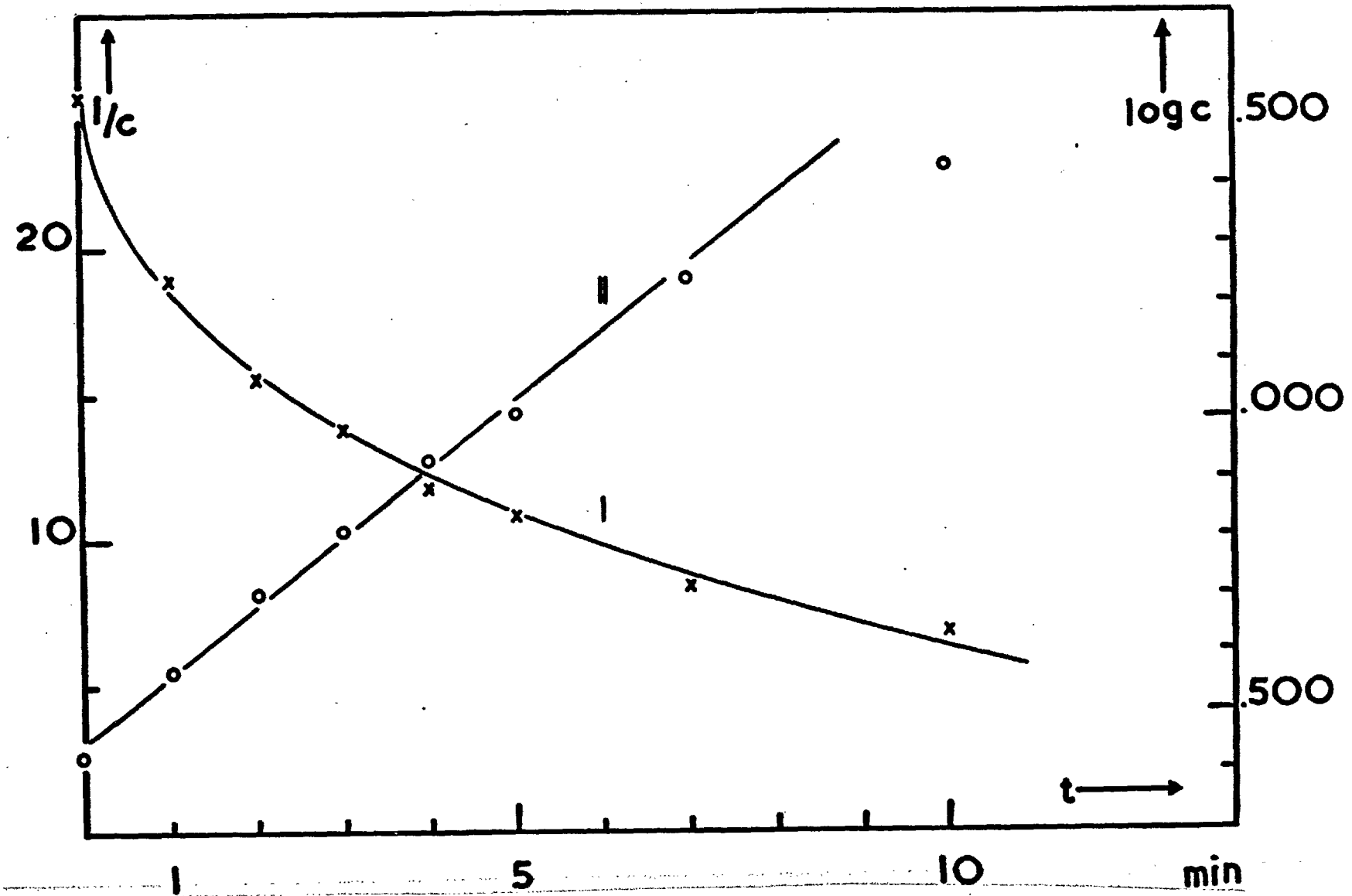


Fig.22. 1st-order (log c) and 2nd-order ($^{1}/c$) plots for the oxidation of the chemisorbed CO; p_{O_2} = 0.9 mm Hg; T = 355° K.

For applying these experimental figures to the process occurring on the Pt surface it is convenient to relate the rate to the concentration of the chemisorbed CO on the Pt-surface.

We assume that at p_{CO} = 2 mm Hg the apparent extinction E_a = 1.1 corresponds to a Pt surface covered by a monolayer of CO.

The number of CO molecules chemisorbed per CM^2 geometric pellet area is according to fig. 6

$$N = 70 \times 10^{16} \text{ molecules.}$$

We now assume that 1 CO molecule is chemisorbed by 1 Pt surface atom, so that the Pt-area (roughness factor = 1) per CM^2 pellet area is

$$\frac{70 \times 10^{16}}{1.25 \times 10^{15}} = 560 \text{ cm}^2 \text{ Pt area/CM}^2 \text{ pellet area}$$

if it is further assumed that equal areas of the three more prominent planes (111), (100), (110), are equally present on the surface.

To relate the experimental velocity constants k'' to the actual Pt-surface means multiplying the previous k'' figures by a factor of 560 (tab. 11).

The first figures K_a at each temperature refer to the runs in tab. 7-10 and fig. 20, 21, 22.

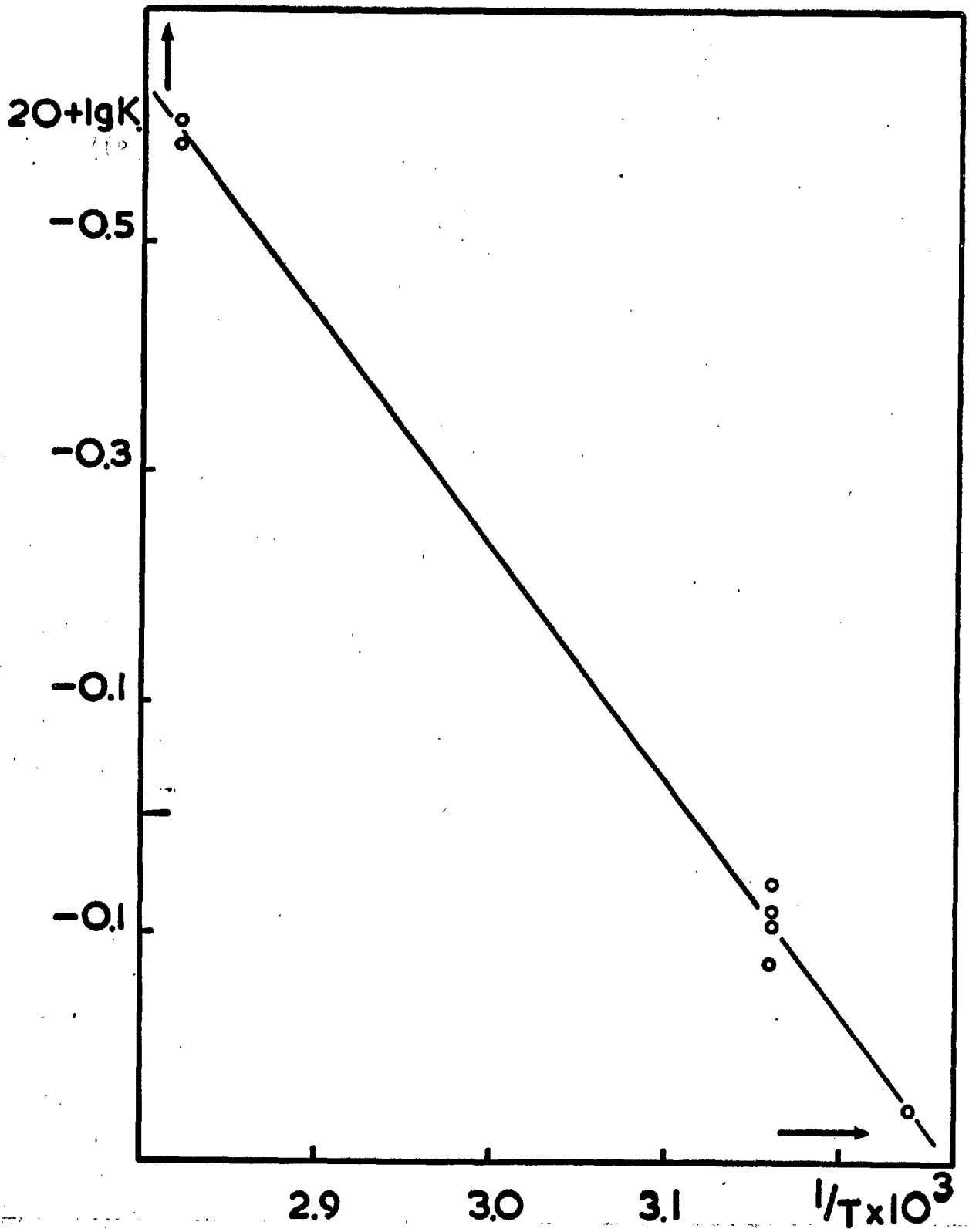


Fig.23. Oxidation of the chemisorbed CO; determination of the activation energy.

Table 11

T °K	$\frac{1}{T} \times 10^3$	$K_a \times 10^{18}$ [molec^{-1} cm^2 sec^{-1}]	18 + log K_a
309	3.24	2.91	0.464
316	3.16	4.21	0.624
	3.16	4.32	0.636
	3.16	3.90	0.591
	3.16	4.67	0.669
355	2.82	19.9	1.290
	2.82	21.0	1.322

The temperature dependency of K_a gives an activation energy of

$$E = 9350 \text{ cal/mole} \quad \text{(fig. 23, tab.11)}$$

compared with 9600 cal/mole deduced from the temperature dependence of the reaction velocity.

Assuming p_{O_2} = const the decrease of the chemisorbed CC can be described by a second order kinetics with respect to the chemisorbed CO, i.e.

$$-\frac{d[CO_a]}{dt} = K_a[CO_a]^2$$

or the complete oxidation is given by

$$+\frac{d[CO_{2g}]}{dt} = -\frac{d[CO_a]}{dt} = k[CO_a]^2 f(p_{O_2}) = K_a[CO_a]^2$$

K_a is an apparent velocity constant containing besides k the unknown function $f(p_{O_2})$.

The kinetics and particularly the dependency of the oxygen pressure is further discussed in connection with the S.P. results.

The activation energy is discussed in connection with the proposed mechanism in the final chapter.

It has been further demonstrated in separate experiments that the catalytic activity of the pellet is increased in the presence of a small pressure H_2 ($p = 10^{-2}$ mm Hg). The

presence of adsorbed mercury decreases the uptake of CO and also the rate of oxidation. After removing the adsorbed mercury (heating for several hours with evacuation) the catalytic activity was unexpectedly greatly increased, e.g. before Hg treatment about 90% CO was oxidized in 30 minutes, and after Hg treatment and its removal by heating, the process took now only 30 sec.

2.3 Surface potential studies of the chemisorption of carbon monoxide and oxygen on platinum films

2.3.1 Experimental

The surface potential measurements were carried out using the recently developed static capacitor technique (2).

A description of the cell used is given in the paper mentioned; further details about all the experimental procedure are given in (67).

The Pt[x]-films were evaporated from W-filaments. Experiments with spectralpure Pt-wire did not show any significant change in the S.P. results.

The films were deposited at pressures ranging from 5×10^{-9} mm Hg to 8×10^{-10} mm Hg at room temperature. The pressure after the deposition was always less than 10^{-9} mm Hg and usually about 5×10^{-10} mm.

The gases for the S.P. experiments, i.e. carbon monoxide and oxygen were obtained from British Oxygen Company, London, in sealed glass ampoules.

---

[x] Thermopure Pt (99.999 %)
Johnson, Matthey, Co., Ltd.,
73-83, Hatton Garden,
London, E.C.1.

2.3.2 Chemisorption of carbon monoxide on platinum films at 300° K and 77° K

Within 5-15 minutes after the deposition of the Pt-films CO was introduced in small doses to the film. The gas was chemisorbed and the resulting S.P. was found to be ± 0.0 Volts at $p_{CO} < 10^{-1}$ mm Hg. At p > 1 mm a decrease of the S.P. of + 0.02 Volts was observed. This effect probably due to a weak adsorption of CO could be completely removed by pumping.

The amount of CO chemisorbed by a Pt-film in a typical run at 300° K was

$$N = 1.27 \times 10^{18} \text{ molecules at } p_{CO} = 3.7 \times 10^{-2} \text{ mm Hg.}$$

For a ratio Pt:CO = 1, and 8.09 Å per Pt site, corresponding to equal distribution of (111), (100), (110) crystal planes in the Pt-surface, the covered surface area of the film would be

$$8.09 \times 1.27 \times 10^{18} \text{ Å} = 1030 \text{ cm}^2$$

Assuming at $p = 3.7 \times 10^{-2}$ that $\theta \sim 1$, this corresponds to a roughness factor of 4 to 5. This assumption is supported by the fact that the amount of oxygen atoms taken up by a Pt film at 300° K is very close to the CO value.

The S.P. of CO chemisorbed on Pt proved to be independent on the temperature of introduction of gas to the film.

A film deposited at room temperature was then cooled down to 77° K. The S.P. was ± 0.0 volt at $p_{CO} < 10^{-1}$ mm Hg. The amount of CO chemisorbed at 77° K was

$$N = 8.8 \times 10^{17} \text{ molecules at } p = 2 \times 10^{-3} \text{ mm Hg.}$$

At p_{CO} = 3.4 mm Hg the S.P. became + 0.01 volts. On warming to room temperature the S.P. of + 0.01 volts remained but became 0.00 volts after removal of CO by pumping at room temperature.

Surface potentials of ± 0.0 due to chemisorption on transition metal surfaces are very rare (68, 69).

Compared with the high S.P. figures for Ni-CO at 293° K of -1.09 volt (70) and Pd-CO (71) of - 0.84 volt at 300° K a S.P. of ± 0.0. volt for Pt-CO is unexpected, particularly because there are two quite different S.P. figures given in the literature (72, 73), thus Dorgelo and Sachtler (72) reported a S.P. for Pt-CO of - 0.24 volt and later Rootsaert, van Reijen and Sachtler a value of - 0.68 volt. The first figure was found by using a condensator method, the last figure emerged from F.E. work. No indication of which crystal plane used was given.

The effect of surface contamination could be studied in the case of a Pt-film which was evaporated at a pressure

of 2×10^{-8} mm Hg and was left for about 2 hours under $p \sim 1 \times 10^{-9}$ mm Hg before carbon monoxide gas was added. After the first CO dose an irreversible change of the S.P. of + 0.04 volt was observed.

This effect was most probably due to oxygen contamination of the Pt-surface which would give the film a negative S.P. (chapter 2.3.3). When CO was added afterwards the reaction between the gaseous CO and the chemisorbed oxygen took place and the removal of this oxygen contamination resulted in the observed positive change of the S.P. This explanation is strongly supported by those results which were obtained on oxygen covered Pt-surfaces (chapter 2.5).

The initial vacuum conditions in the actual S.P. investigations of Pt/CO were much better and also the time between deposition of the film and the first addition of CO was much shorter. Hence, surface contamination should be largely excluded.

Surface contamination seems also from another point of view unlikely. So in the case of the chemisorption of oxygen on Pt at room temperature S.P. figures were obtained which were very close to those figures which are listed in literature by two different authors (74, 75).

An important factor, which could effect the S.P.

results, were oxygen traces in the carbon monoxide gas.

We took special precautions against such kind of contamination, which would, however, give a negative S.P.

In the presence of a CO gasphase the chemisorbed oxygen should then be removed and a positive S.P. change is likely to occur.

For the theory of the bonding of CO on the Pt-surface two facts are essential: firstly that the S.P. of Pt/CO is $\pm$ 0.0 volt and independent of coverage and secondly that due to the I.R. results the CO group forms a dipole which decreases with increasing surface coverage.

By means of the wavemechanically derived dipole properties of the CO molecule (76) it is possible to connect these two experimental facts and develop a qualitative view of the bonding of CO which is chemisorbed on Pt.

The wavemechanical treatment by Moffit (76) shows that the lone pair of electrons occupying the 3δ m.o. of the CO molecule at the C atom contributes an atomic dipole in the sense $\overleftarrow{CO}$ which more than compensates the amount which arises from the electrons involved in the 1δ m.o. and 2δ m.o. (59).

The resulting effect is a moment of 2.1D with the negative end towards the C atom being slightly greater than the moment of 1.9D in the reverse sense arising from the polarity of the π bondings.

Assuming that the chemisorption of the CO takes place at the C atom and provided that the electronic structure of the CO molecule would not be affected at all during this process, we would expect a resulting dipole with its positive end directing away from the surface.

S.P. measurements on the chemisorption of CO on a series of transition metals indicate that the actual surface dipole has a reverse direction with its negative end on the O-atom (68, 69).

Calculated from S.P. results the surface dipole in the case of the chemisorption of CO on Ni turns out to be about 0.5D. This figure agrees well with that assumed for the Ni - C - O group by dipoleinvestigations of carbonyl compounds (77, 78).

It is most likely that this change in the dipole moment is mainly due to the electrons in the 3σ m.o. which are taking part in the Me - C bonding. This in turn would lead to a decrease in the negative charge at the C atom and the dipole moment of the CO group would be now outweighted by the effects arising from the polarity of the 1 π-bondings and the 1σ and 2σ m.o.'s of the CO. Some negative charge is transferred back to the carbon by filling of the 2 π orbitals of the CO molecules.

Due to the bonding of the carbon monoxide on the Pt surface a Pt - C dipole is formed. The S.P. ± 0.0 volt for Pt/CO indicates that this dipole decreases in the same way as the CO dipol/ decreases when the CO concentration increases on the Pt-surface. From the general view of the CO bonding in metal carbonyls, discussed in chapter 1.13 follows that both, i.e. the C - O dipol/ and the Pt - C dipol/ are directly connected with each other.

For the chemisorption of CO there seems to be some kind of relationship between the S.P. results on the three metals Ni, Pd, and Pt, the I.R. results and the values of their electroaffinity.

According to Nyholm (79) the electroaffinity of Pd and Ni atoms in their d^{10} state are fairly close (corresponding similar S.P. and I.R. results) whereas there is quite a big gap between these figures and the electroaffinity of Pt, which is almost twice as big.

These figures indicate that Ni and Pd tend to concentrate less negative charges around themselves compared with Pt. Due to their smaller electroaffinity Ni and Pd cannot therefore form a negative counterpart for the O atom in the CO which is big enough to compensate the C - O dipole. This could be the reason why we are measuring large and similar S.P. values for Ni and Pd and a S.P. ± 0.0 volt for Pt.

The lower electroaffinity of Ni and Pd could also result in a larger back donation effect (chapter 1.13) of electrons from the metal atom into the 2π orbitals of the CO, measurable by the shift of the CO stretching band to lower frequencies.

We know that the major C - O stretching bands are for Ni and Pd at lower frequencies compared with the C - O band on Pt (48, 34).

2.3.3 Chemisorption of oxygen on platinum films at 300° K

The chemisorption of oxygen on Pt surfaces has been studied at 300° K. The Pt-films were evaporated under similar vacuum conditions as reported for the chemisorption of CO on Pt. The oxygen was added in small doses to the film and the S.P. and its dependency on the amount of oxygen taken up by the film was studied.

The relationship of the S.P. to oxygen coverage is shown in fig. 24. Up to almost 40 x 10^{16} molecules oxygen there is a reasonable linear relationship. With increasing oxygen coverage the time increased until the final S.P. figure was reached in about 3 min at 39 x 10^{16} molecules for run A (O - O - O) and 32 x 10^{16} molecules for run B (Δ - Δ - Δ).

The final S.P. figures were obtained by exposing film A to an oxygen pressure of 2 x 10^{-3} mm Hg and film B to one of 2.3 x 10^{-2} mm Hg.

The final amounts of oxygen adsorbed by the films during the last stage differ, but the final S.P. figures are similar: - 1.05 volt; - 1.03 volt.

These figures are in good agreement with those previously reported in the literature - 1.19 volt (74) and - 1.1 to - 1.2 volt (75).

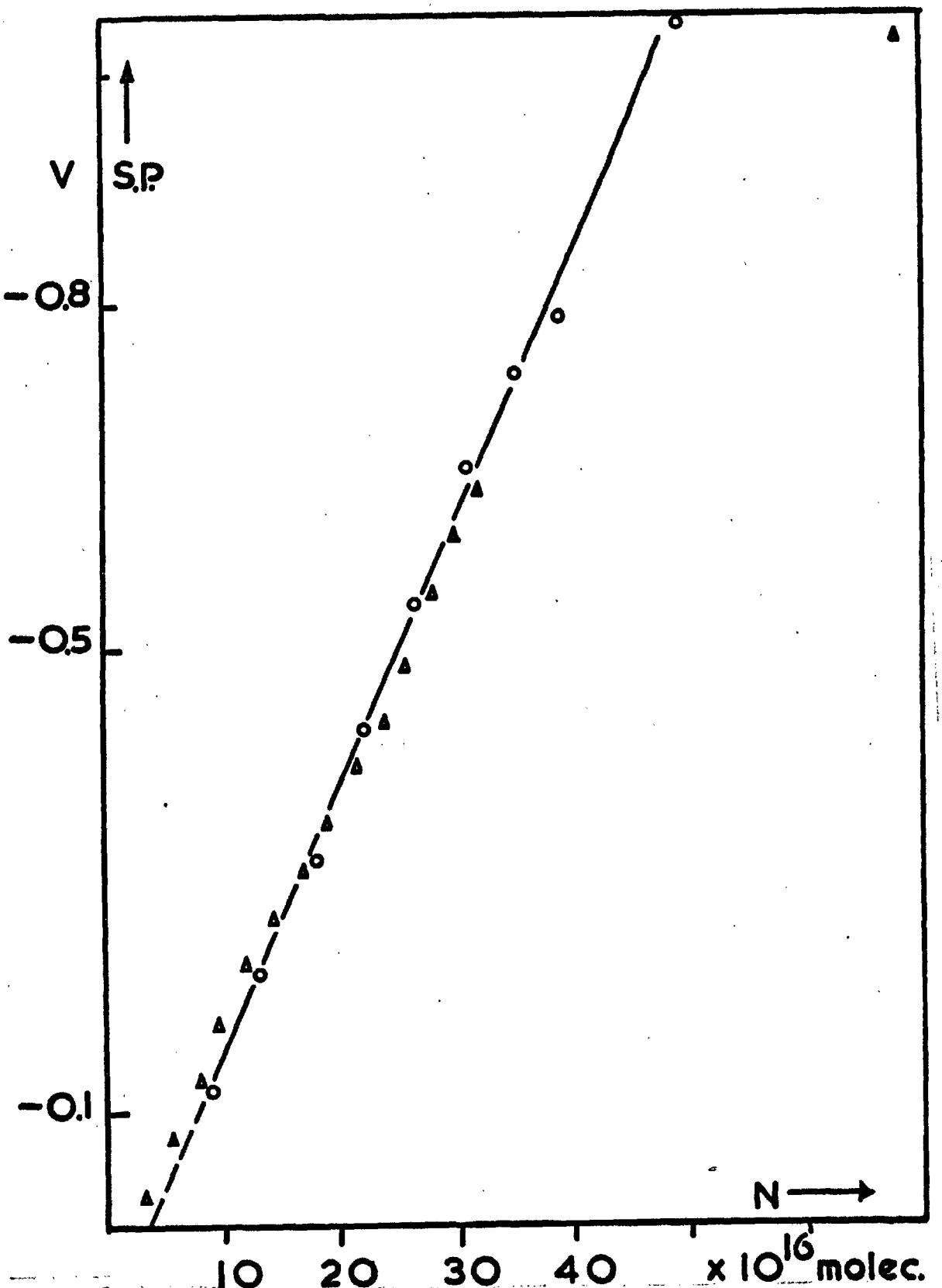


Fig.24. Chemisorption of oxygen on a Pt surface at 300° K; surface potential as function of coverage

In run B the deviation from the linear relationship at coverages > 32 x 10^{16} molecules could be due to additionally weakly adsorbed oxygen.

The number of oxygen atoms taken up by the Pt-films is close to the number of chemisorbed CO on Pt. This seems to indicate that the oxygen atoms and CO molecules may occupy the same sites on the Pt-surface.

The fact that in fig. 24 the plot does not go through the origin is probably due to the adsorption of oxygen on the metal parts of the cool ionization gauge etc.

The heat capacity of oxygen adsorbed on Pt at T > 250° K is 3.5 cal/mole. ° K, (80). From this result the picture of a two dimensional classical monoatomic O-gas on the Pt surface has been discussed. This idea seems to be in good agreement with the fact that the number of chemisorbed CO molecules and the number of O-atoms taken up are nearly the same on Pt. This result would also exclude a significant bulk oxidation of the Pt at room temperature.

Brennan, Hayward and Trapnell (81) who studied the adsorption heats of oxygen on various metals have shown that Pt together with Pd and Rh have a comparatively low heat of oxygen adsorption. There are also significant differences between these values and the heats of bulk oxide formation. With the other group of metals to which

Ni belongs there are much higher heats of oxygen adsorption and these generally reasonably close with those expected for the formation of the bulk oxide. For Ni the heat of adsorption of oxygen has been reported to be 107 K cal/mole and the heat of oxide formation to be 116 K cal/mole; for Pd the corresponding figures are 67 K cal/mole and 42 K cal/mole and for Pt 67 K cal/mole and 34 K cal/mole.

The differences in the heats of bulk oxide formation for Ni on one hand and Pd and Pt on the other can be related to the high 1. ionization potentials of Pd and Pt (8.11 and 8.55 V) and the comparable low figures for Ni (5.33 V) which indicates that much less energy is necessary to form a Ni ion (79).

The differences between the heat of oxygen adsorption and the heats of bulk oxide formation with Pd and Pt could also indicate different states of the oxygen species.

Lewis (39) recently studied the oxygen adsorption on Pt at different temperatures by means of the L_3 X-ray absorption edge of the Pt-sample. These results indicate a chemisorption of oxygen at room temperature on the Pt-surface and the formation of bulk Pt oxide at 350° K and $p_{O_2} = 0.5$ atm.

The different bonding states of oxygen on Ni on the one hand and Pd and Pt on the other is nicely demonstrated

by the highly different reactivity of oxygen species towards CO oxidation. Whereas at 0° C 89-92% of the adsorbed oxygen on Pd can be removed by reaction with CO (65) only 0.2-0.4% of the adsorbed oxygen is removed from a Ni surface (66). The corresponding figures of these authors for Pd are 65-95% (66).

For Pt we found 50-90% of the oxygen can be removed from the surface by adding CO ($p \sim 1$ mm Hg) at 300° K, the percentage depending on the activity of the Pt film.

From the heat capacity measurements (80) it was concluded that for $T < 250^{\circ}$ K the oxygen becomes increasingly chemisorbed in a molecular state.

Hence, depending on the temperature we have different oxygen species on the Pt surface.

2.4 Surface potential studies of the reaction between chemisorbed carbon monoxide and gaseous oxygen

After deposition under ultra high vacuum conditions the Pt-films were covered with CO, the gasphase and the weakly bonded species were pumped off and small doses of O_2 were added to the system at 300° K.

The reaction between the chemisorbed CO and the gaseous oxygen commenced with a measureable velocity only at $p_{O_2} > 1 \times 10^{-3}$ mm. By adding oxygen to a pressure 10^{-1} mm the S.P. changed from ± 0.0 volt for Pt/CO to - 0.93 volt; - 1.0 volt for Pt/O_2 at 300° K.

These S.P. figures are close to those obtained for oxygen on a clean Pt-surface at 300° K.

It is therefore reasonable to assume that practically all the chemisorbed CO has been oxidized and the resulting CO_2 has been replaced by chemisorbed oxygen.

The carbon dioxide evolved was frozen out. Its amount corresponded to the amount of chemisorbed oxygen, indicated by the S.P. change.

Hence, oxidation of the chemisorbed CO occurred on the film surface in a manner similar to that on the Aerosil supported Pt, where the vacuum conditions (10^{-5} to 10^{-6} mm Hg) were far from being satisfactory.

2.5 Surface potential studies of the reaction between chemisorbed oxygen and gaseous carbon monoxide

In contrary to the oxidation of chemisorbed carbon monoxide in an oxygen atmosphere the reaction between chemisorbed oxygen and gaseous carbon monoxide takes place almost instantaneously (< 5 sec) under similar pressure and temperature conditions.

This fact was expected from our I.R. results. Due to the comparatively low activation energy for the reaction between gaseous CO and chemisorbed oxygen it was convenient to follow the reaction over a wide range by means of the change in S.P.

A change of the original S.P. for Pt/O_2 to less negative figures occurred. In fig. 25 the dependency of the change in surface potential S.P. on the number N of CO molecules added to the film is shown.

In this particular case the change of S.P. was almost 0.73 volt, which indicated that almost three quarters of the chemisorbed oxygen could be removed by the reaction with CO.

In the initial stages of the process the slope is about

$$0.1 \text{ volt}/10^{17} \text{ molecules CO}$$

i.e. initially all CO molecules react according to

$$Pt\text{-}O + CO \rightarrow Pt + CO_2$$

and the amount of CO chemisorbed on the Pt-surface remains small.

When the reaction came finally to an end the CO could be very easily removed by exposing the film for some minutes to oxygen ($p_{O_2} \sim 1$ mm). After pumping off the gaseous oxygen it was possible to repeat the previous experiment, i.e. the reaction between chemisorbed oxygen and gaseous carbon monoxide.

Fig. 25 demonstrates one experiment of a sequence of five performed on the same Pt-film. The S.P. changes obtained in this sequence were 0.80 V; 0.78 V; 0.74 V; 0.73 V; 0.70 V.

The slope shown in fig. 25 was the same for the last four runs. In the first one, where Δ S.P. = 0.8 volt, the decrease of the initial slope was smaller.

During the following runs of similar nature a further decrease of Δ S.P. occurred until a "final" figure of 0.62 V was reached which then remained almost unchanged. These figures for Δ S.P. (final) varied from film to film indicating that the amounts of reactive surface on various

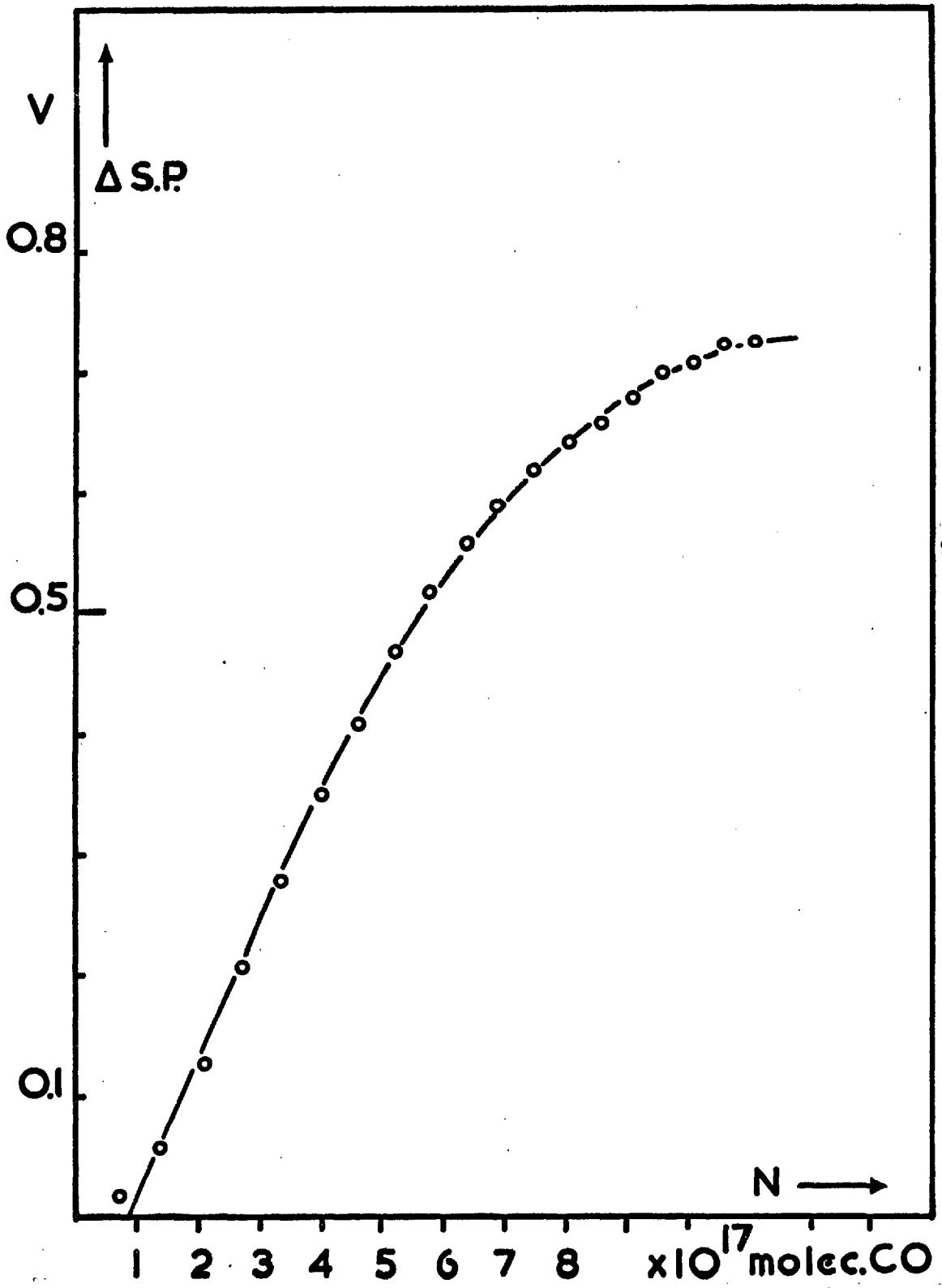


Fig.25. Surface potential study of the reaction between chemisorbed oxygen and gaseous carbon monoxide

films were different. For a series of Pt-films the figures of Δ S.P. (final) were about 0.5 $\pm$ 0.1 volt.

For another Pt-film the Δ S.P. figures of a sequence of reactions between chemisorbed CO and gaseous O_2 (I) and between chemisorbed oxygen and gaseous CO (II) are as

reaction	Δ S.P. volt
I	0.48
II	0.45
---	---
II	0.47
I	0.49
II	0.46

These figures indicate that the change in S.P. is independent of whether the oxidation of carbon monoxide takes place according to reaction (I) or reaction (II).

The amount of CO_2 evolved during each of these processes correspond to

0.09 to 0.1 volt per 10^{17} molecules CO_2 formed,

in good agreement with the previously mentioned figures of 0.1 volt per 10^{17} molecules CO added (fig. 25) and the slope of fig. 24 which corresponds in its linear section to

0.1 volt per 10^{17} O-atoms.

By means of the S.P. technique it was possible to study the oxidation of carbon monoxide according to reaction (I) or reaction (II) at low temperatures.

The results showed that the oxidation of chemisorbed CO in an oxygen atmosphere ($p_{O_2} \sim$ 1 mm) starts about 195° K and has a reasonably high velocity at about 0° C.

The reaction between oxygen chemisorbed at 300° K and gaseous CO is completed even at 77° K at < 5 sec. This fact makes it clear that the activation energy of this process must be very low. It is therefore reasonable to assume that a 'sticking probability' for CO on Pt-O is in the order of almost 1.

Stephens (65) studied the oxidation of CO on Pd according to reaction (I) and reaction (II). His results concerning the reaction (II) between chemisorbed oxygen and gaseous carbon monoxide are of interest for the interpretation of our results on Pt-films. He determined for this reaction the ratio of CO_2 formed to CO added to the Pd. film to be 0.49 over almost the whole of the reaction. Hence, he could assume the following reaction to occur on Pd.:

$$Pd.\text{-}O + 2CO_g \rightarrow CO_{2g} + Pd\text{-}CO$$

Our results on a Pt surface are at variance with these. We find for a large part of reaction (II) a ratio 1, which gradually decreases (fig. 25). This would mean that the reaction takes place in the initial stages as

$$Pt\text{-}O + CO_g \rightarrow CO_{2g} + Pt$$

and the freed Pt-sites remain mostly unoccupied.

We can explain these differences by means of different sticking probabilities of CO on Pt-, PtO-sites and on Pd-, PdO-sites.

Let the velocity with which CO reacts with the 'Pt-O' be V_1 and the velocity at which it is chemisorbed on Pt be V_2, then

$$\frac{V_1}{V_2} = \frac{S_1}{S_2} = \frac{\theta_1 \cdot e^{-E_1/kT}}{\theta_2 \cdot e^{-E_2/kT}}$$

where S is the sticking probability,

E the activation energy, and

θ the fraction of the surface which is involved in the process concerned.

The reaction between gaseous CO and chemisorbed oxygen atoms is treated as a kind of adsorption process.

θ_1 and θ_2, i.e. the fraction of the surface covered with chemisorbed oxygen and the uncovered fraction of the Pt surface, can be calculated at different stages of the

CO addition by means of the amount of CO added and the corresponding changes of S.P. which indicate the amount of CO which has reacted with the chemisorbed oxygen.

The surface involved in the reaction is assumed to correspond to 7.3×10^{17} sites according to a total change of S.P. of 0.73 V. The first 1×10^{17} molecules CO are not considered in the calculation of the θ figures as these molecules only cause a very small change of the S.P. They are obviously adsorbed as parts of the surface /on which are not involved in the measured reaction.

At $N = 7 \times 10^{17}$ molecules (fig. 25) when the slope of the curve indicates equal velocities for the chemisorption of CO on freed Pt sites (V_2) and the reaction of CO with the chemisorbed oxygen to form CO_2 (V_1) the corresponding figures for θ_1 and θ_2 are 0.07 and 0.63 (Pt-CO:$\theta_3 = 0.3$).

Hence,

$$e^{-(E_1 - E_2)/RT} = 9.$$

Assuming $E_1 = 0$ K cal mole^{-1}, the activation energy for the chemisorption of CO E_2 would turn out to be 1-2 K cal/mole. In other words, for $\theta_1 = \theta_2$ the sticking probability of CO on Pt(S_2) is only about one tenth of that for CO on Pt-O(S_1) leading to the reaction and formation of CO_2. Presuming $S_1 = 1$, i.e. every collision of a CO molecule with a chemisorbed oxygen atom leads to the

formation of CO_2, the sticking probability of CO on Pt(S_2) would be in the order of 0.1 and similar to those figures on other metals (82).

When we extend the discussion to the experimental results on Pd which we mentioned above (65) then a reaction according to

$$Pd\text{-}O + 2CO_g \rightarrow CO_{2g} + Pd\text{-}CO$$

would mean that V_1, the velocity for the reaction of CO with PdO is over the whole of the reaction much smaller than V_2, the velocity of chemisorption of CO on Pd. For the oxygen covered surface the reaction between PdO and CO_g becomes the rate-determining process.

As it is reasonable to assume sticking probabilities for CO on Pd and Pt to be about the same, there should be a significant difference between the 'sticking probabilities' of CO on oxygen-covered Pt- and oxygen covered Pd-sites.

In other words, the oxidation of CO on an oxygen covered Pd surface needs a greater activation energy than for Pt.

For the catalytic oxidation of olefins on various metal films (83) the higher activity of Pt compared with Pd has been demonstrated.

2.6 Surface potential studies of the kinetic of the oxidation of carbon monoxide chemisorbed on platinum films

Our previous S.P. studies have shown that the surface area of the Pt-films taking part in following two processes:

i $CO_a + O_{2g} \rightarrow CO_{2g} + O_a$

ii $O_a + 2\,CO_g \rightarrow CO_{2g} + CO_a$

at first continuously decreases but finally reaches an almost constant value.

The "reactive" part of the surface is measured by the absolute value of the change of the S.P. and is found to be one half of the whole film surface.

It was generally necessary to repeat the reactions i and ii one after the other several times before reproducible results could be obtained.

In this chapter we are mainly concerned with the kinetic of process i. We are using reaction ii only to replace the chemisorbed O_a at the end of reaction i again by CO_a, i.e. chemisorbed carbon monoxide.

In any run the Pt surface was covered with CO (P 1 mm Hg, T = 300° K, t = 5-10 min), the CO gasphase was then pumped off and the cell was evacuated down to 10^{-7} mm.

The S.P. was recorded before the oxygen was admitted at various pressures ranging from about 0.5 to about 5 mm Hg. The temperature range was 250° to 310° K, depending on the catalytic activity of the film.

The oxygen pressures were always so high that there was no decrease over the whole of the reaction.

The oxidation of the chemisorbed CO to form gaseous CO_2, which was condensed in the cold trap, and its replacement on the surface by an equivalent amount of chemisorbed oxygen adatoms was monitored by the increase of the negative S.P. which was displayed on the chart of the recorder. The reaction was substantially complete in about 2 to 5 minutes, depending on the reaction conditions and the activity of the film concerned.

When we are using the chemisorption of oxygen on the freed Pt sites as a monitoring device for the velocity of the evolution of CO_2 we are presuming that the chemisorption velocity of the oxygen on Pt is extremely rapid and independent of temperature and pressure. This is reasonable as this chemisorption takes place with almost no activation

energy, and the velocity of the chemisorption is virtually limited by the collision frequency at p (in the order of 1 mm) and T (about 273° K). This rate is about a factor 10^7 bigger than the observed velocities of CO_2 evolution. Hence, the evolution of CO_2 becomes the rate limiting process.

No chemisorption of CO_2 on Pt has be-n observed at about 300° K (24).

Although this monitoring process

iii $\quad Pt_2 + O_{2g} \rightarrow 2\ PtO$

gives the velocity of the evolution of the CO_2 and, thus, the velocity of the oxidation of the chemisorbed CO, it is independent on the kinetic of the CO oxidation.

It was found, that the rate of change of S.P. at time t is directly proportional to the difference d between the negative $S.P._{\infty}$ at the end of the reaction and $S.P._t$ at time t.

Hence,

(1) $\quad \frac{d\ S.P.}{dt} \propto (S.P._{\infty} - S.P._t)$

We are presuming that

(2) $\quad S.P. \propto (O_a)$

which we have previously proved to be true up to relatively

high oxygen coverages (fig. 24). Combining (1) and (2) we are getting

$$(3) \qquad + \frac{d(CO_2)}{dt} = + \frac{d(O_a)}{dt} = K_b((O_{a,\infty}) - (O_{a,t}))$$

In tab. 12, 13, 14 we have listed for one of the Pt films (film B) the S.P. data, given in volts.

The three runs were taken at different temperatures and oxygen pressures.

For calculating the concentration of the O_a atoms on the surface a factor of

$$10^{18} \text{ O adatoms} \quad \mathbf{x} \quad \text{volts}^{-1}$$

as deduced from the calibration curve can be used. The effective area of the Pt films is about 500 cm^2.

In fig. 26 the function

$$\log \frac{d\ S.P.}{dt} = n.\ \log\ (S.P._{\infty} - S.P._t)$$

has been plotted for the three runs and indicates that $n = 1$ or 1st order with respect to $d \equiv S.P._{\infty} - S.P._t$ (In fig. 26 V stands for $\frac{d\ S.P.}{dt}$).

Table 12: Film B; $T = 253^{\circ}$ K; $P_{O_2} = 24.5 \times 10^{-1}$ mm Hg

t units *	$S.P._t$ volts	$d = S.P._\infty - S.P._t$ volts	$1/d$	1 + log d
0	0.00	0.54	1.85	0.73
5	0.10	0.44	2.27	0.64
10	0.15	0.39	2.56	0.59
15	0.20	0.34	2.94	0.53
20	0.23	0.31	3.22	0.49
25	0.27	0.27	3.70	0.43
30	0.31	0.23	4.35	0.36
35	0.34	0.20	5.00	0.30
40	0.36	0.18	5.55	0.26
45	0.38	0.16	6.25	0.20
50	0.40	0.14	7.15	0.15
60	0.44	0.10	10.0	0.00
70	0.46	0.08	12.5	
80	0.49			
∞	0.54			

* 17 time units = 60 seconds;

Table 13: Film B; $T = 273^{\circ}$ K; $P_{O_2} = 20.5$ mm Hg

t units *	$S.P._t$ volts	$d = S.P._\infty - S.P._t$ volts	$1/d$	1 + log d
0	0.00	0.57	1.75	0.76
2	0.11	0.46	2.18	0.66
5	0.21	0.36	2.78	0.56
7	0.26	0.31	3.22	0.49
10	0.34	0.23	4.35	0.36
12	0.37	0.21	5.00	0.30
15	0.41	0.16	6.25	0.20
17	0.43	0.14	7.15	0.15
20	0.46	0.11	9.10	0.04
25	0.50	0.07		
30	0.52	0.05		
∞	0.57	0		

* 17 time units = 60 seconds;

Table 14: Film B; $T = 299^{\circ}$ K; $P_{O_2} = 4.1 \times 10^{-1}$ mm Hg

t units *	$S.P._t$ volts	$d = S.P._{\infty} - S.P._t$ volts	$1/d$	1 + log d
0	0.00	0.65	1.54	0.81
5	0.10	0.55	1.82	0.74
10	0.20	0.45	2.22	0.65
15	0.32	0.33	3.03	0.52
20	0.40	0.25	4.00	0.40
25	0.45	0.20	5.00	0.30
30	0.50	0.15	6.66	0.17
35	0.54	0.11	9.1	0.04
40	0.58	0.07		
50	0.62	0.03		
∞	0.65			

* 17 time units = 60 seconds;

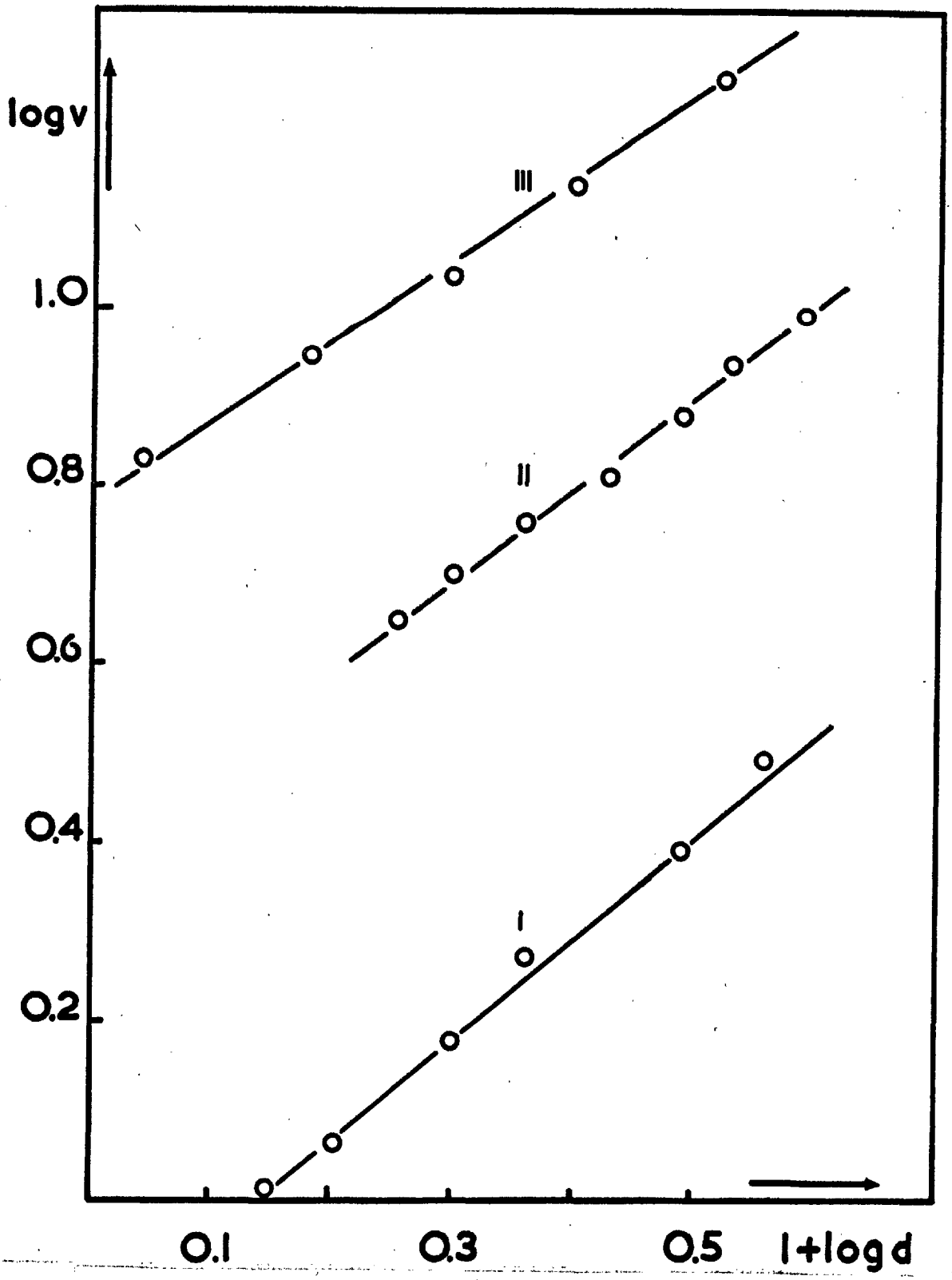


Fig.26. Determination of reaction order from surface potential results

In fig. 27, 28, 29 log d = f(t) and $\frac{1}{d} = f(t)$ have been plotted according to a first order and second order kinetic.

The velocity constants for the three runs according to a first order kinetic are

T [°K]	P_{O_2} [mm Hg]	K_b [sec^{-1}]
253	24.5×10^{-1}	0.75×10^{-2}
273	20.5×10^{-1}	2.34×10^{-2}
299	4.1×10^{-1}	1.61×10^{-2}

For the two runs at 253° K and 273° K, which were carried out at comparable oxygen pressures we have plotted $\log \frac{d\ S.P.}{dt} = f(d)$ in fig. 30; (V stands for $\frac{d\ S.P.}{dt}$ in fig. 30). This figure demonstrates how the activation energy of the evolution rate of the CO_2 varies with coverage.

Similarly to our I.R. results the evolution of CO_2 is occurring with a constant activation energy over the major region of the reaction.

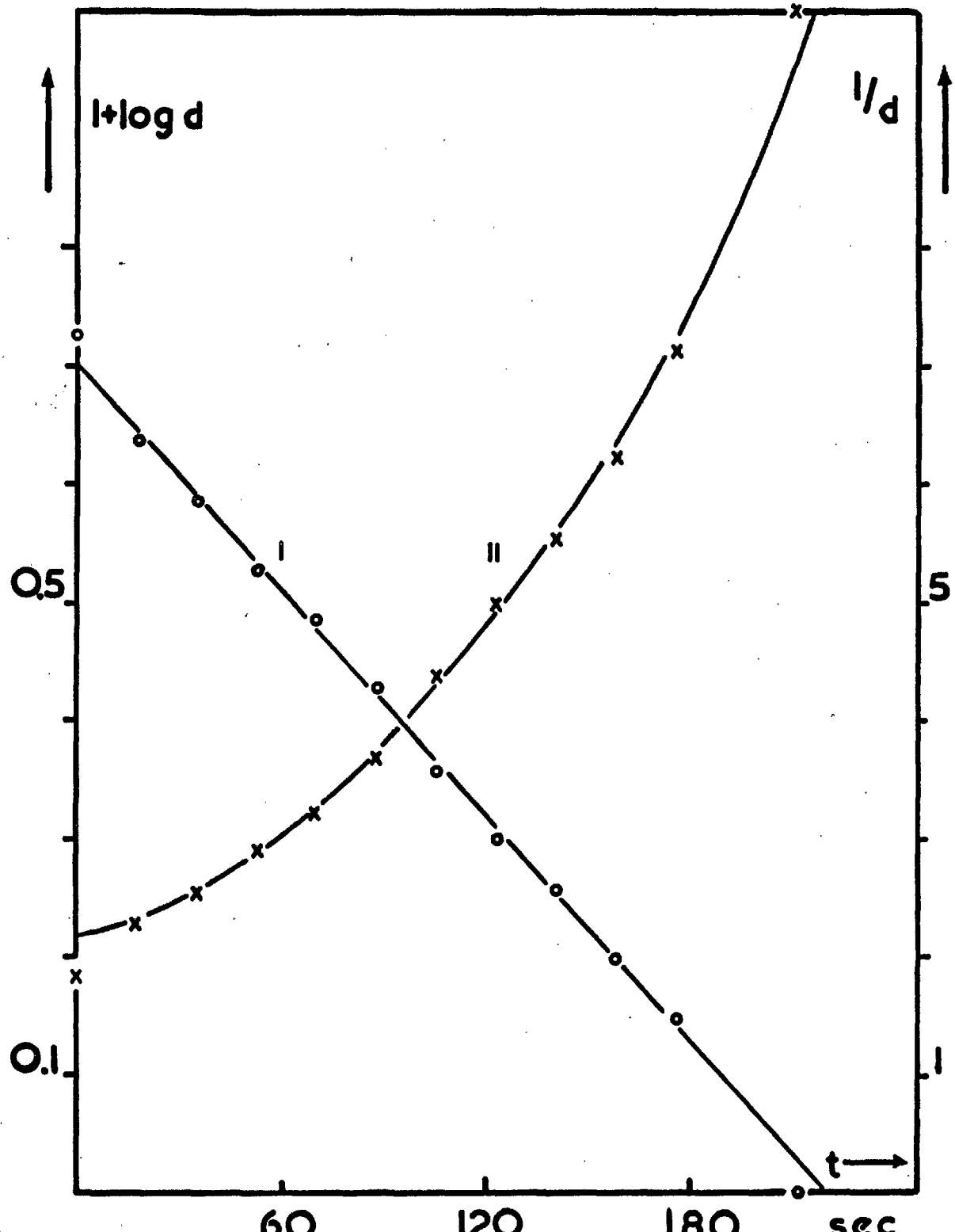


Fig.27. Kinetics of the reaction from S.P. measurements; plot of 1st-order (log d) and 2nd-order (1/d) equations; p_{O_2} = 24.5 x 10^{-1} mm Hg; T = 253°K.

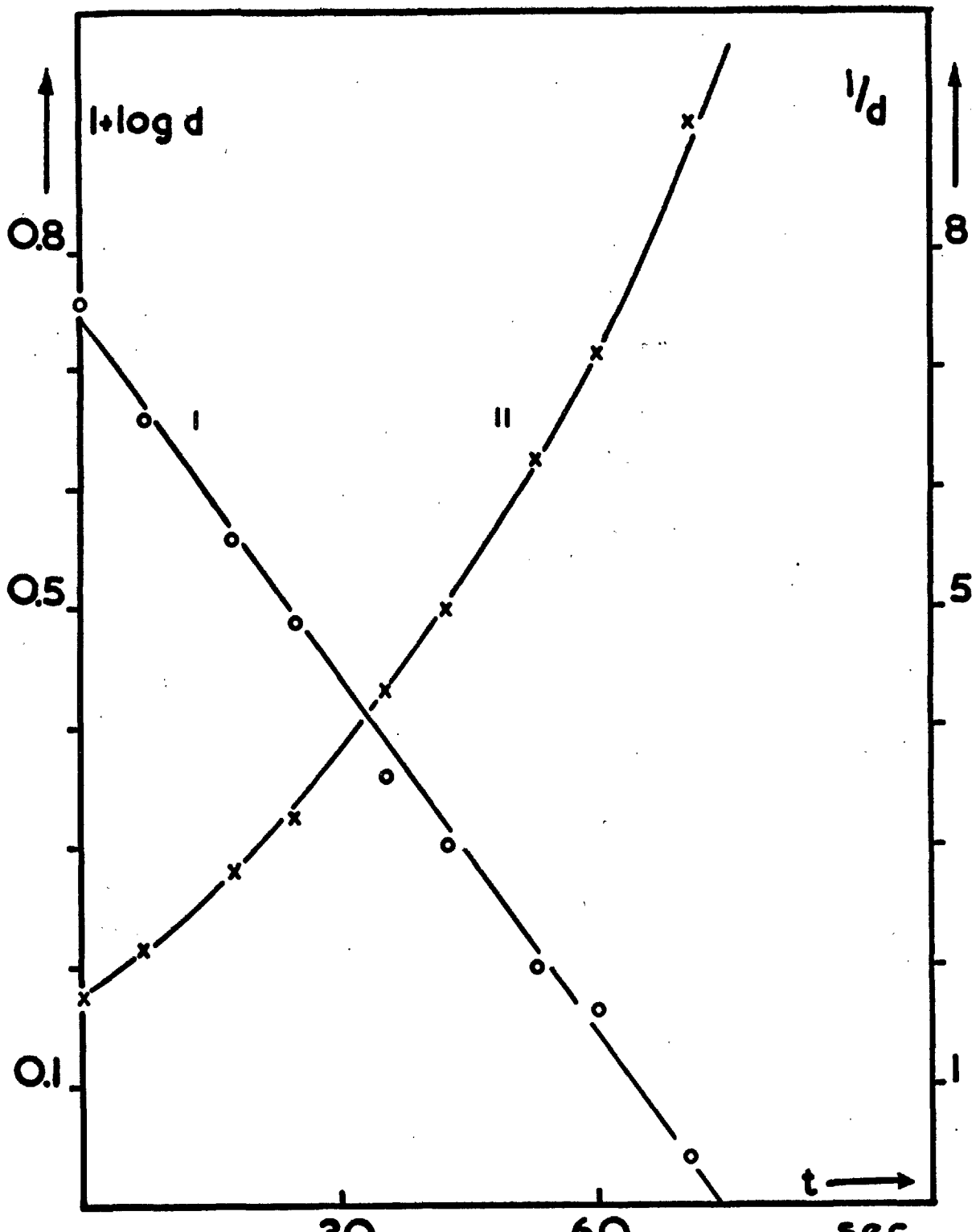


Fig.28. Kinetics of the reaction from S.P. measurements; plot of 1st-order (log d) and 2nd-order (1/d) equations; $p_{O_2} = 20.5 \times 10^{-1}$ mm Hg; T = 273°K.

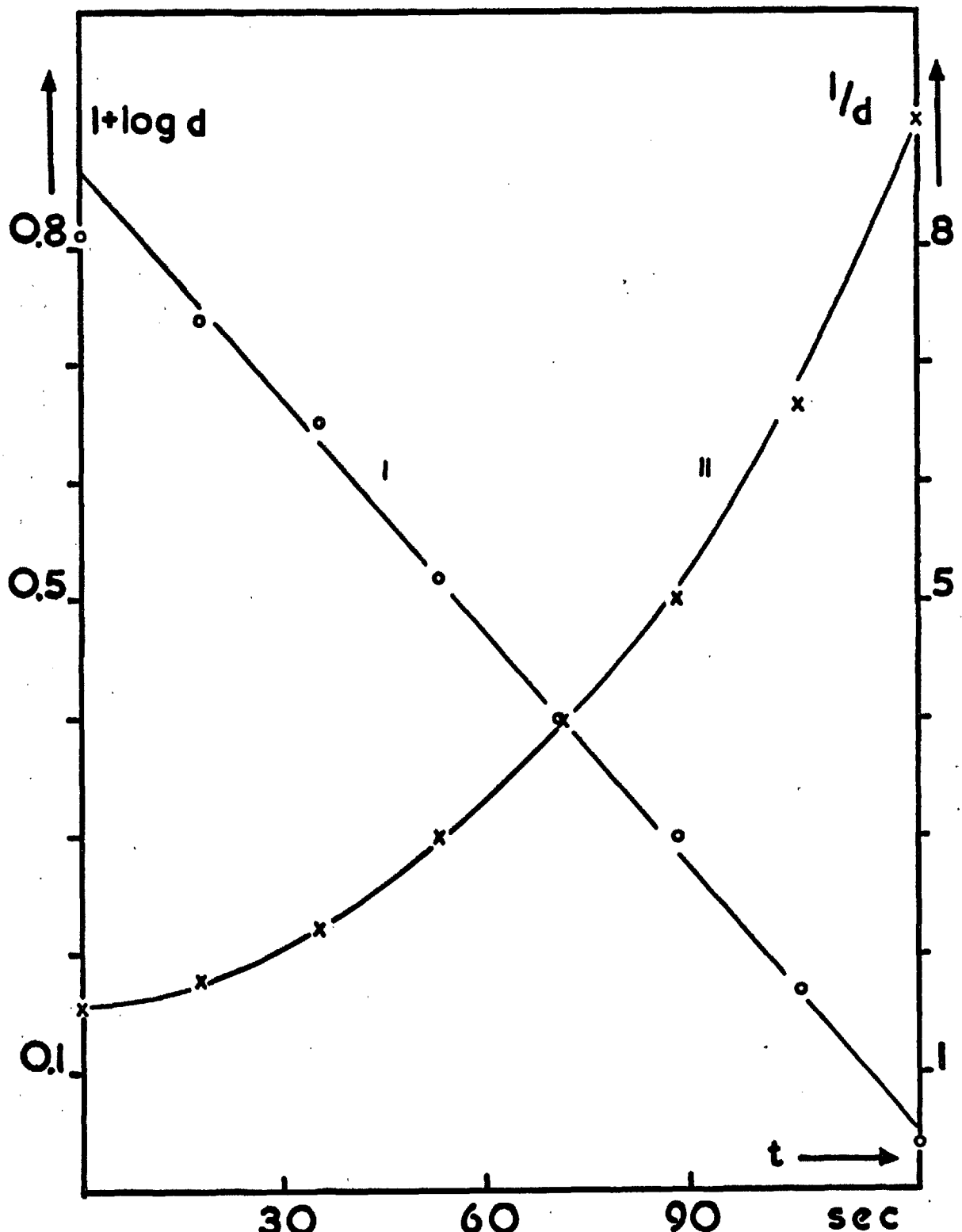


Fig.29. Kinetics of the reaction from S.P. measurements; plot of 1st-order (log d) and 2nd-order (1/d) equations; p_{O_2} = 4.1 x 10^{-1} mm Hg; T = 299° K.

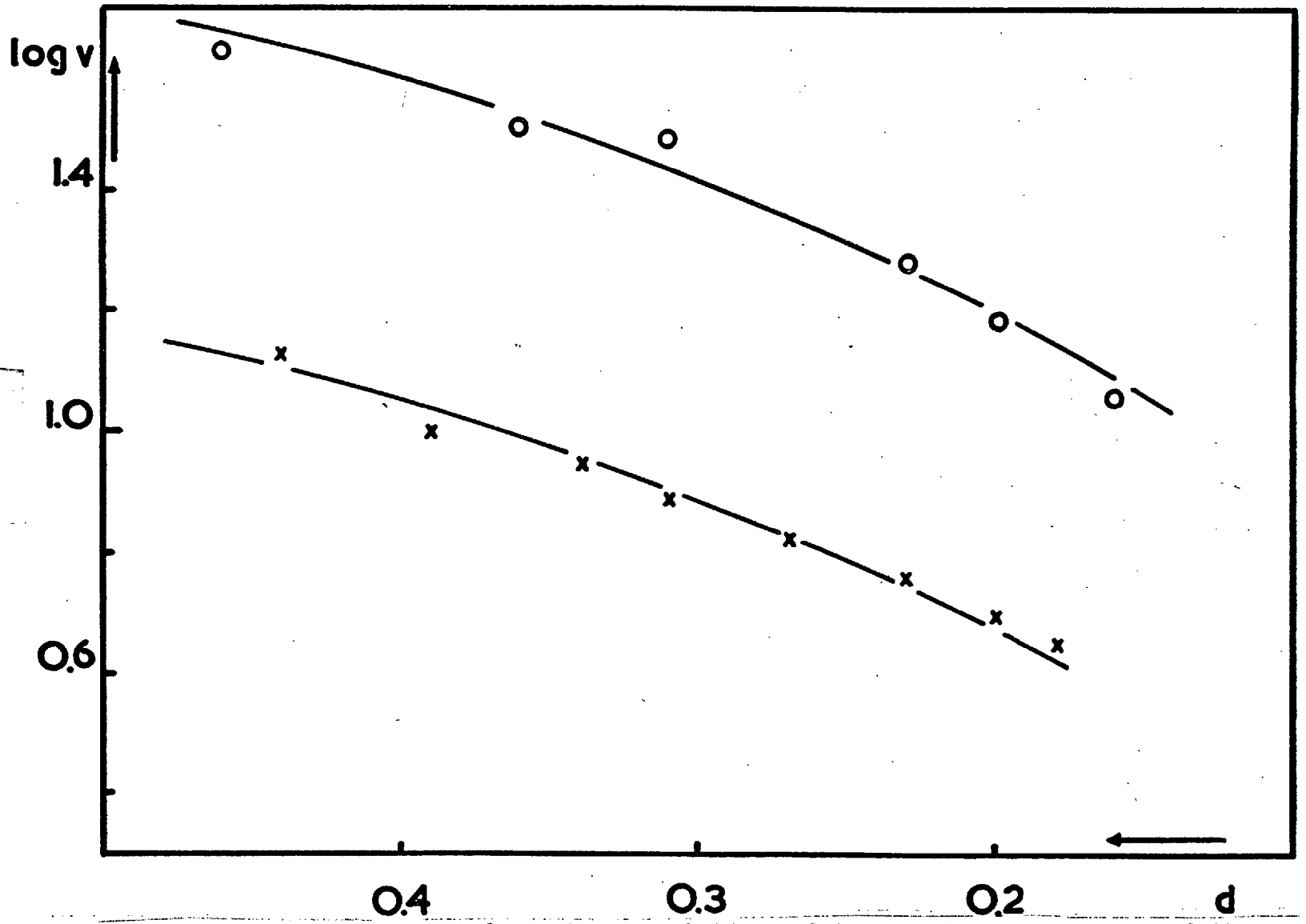


Fig.30. Surface potential study; variation of the activation energy of the oxidation with decreasing CO coverage.

The pressure dependency of the rate of CO_2 formation is demonstrated in fig. 31 where the specific velocity K_b is plotted versus oxygen pressure for various temperatures (film B). At low pressures the specific rate of evolution of CO_2 increases almost linearly with pressure, but with increasing pressure the plot becomes concave to the pressure axis. At higher temperatures the linear part extends to higher pressures of oxygen.

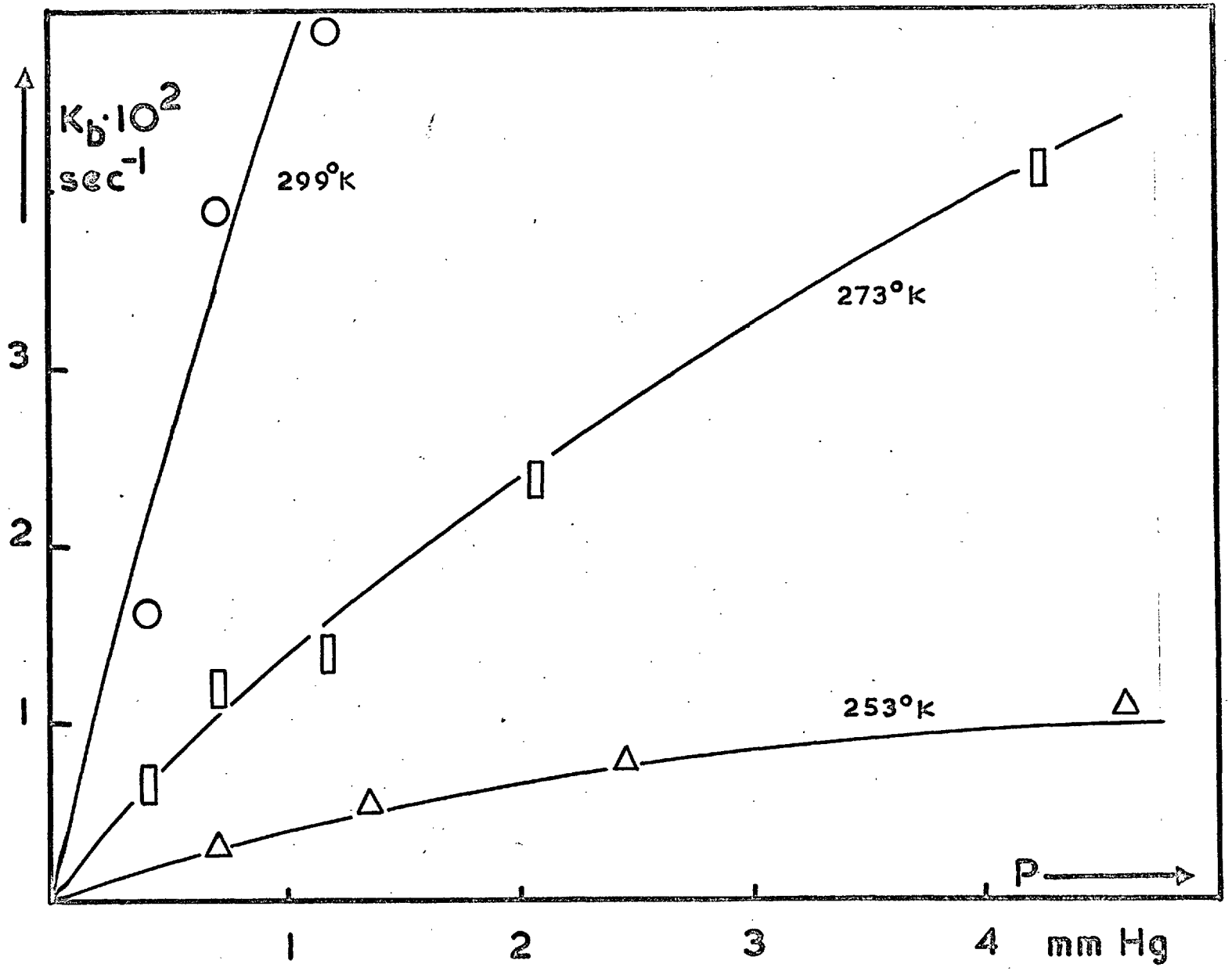


Fig. 31. Surface potential study; pressure dependency of the specific rate of the oxidation of the chemisorbed carbon monoxide.

2.7. Discussion of the kinetic results and the mechanism of the oxidation of carbon monoxide chemisorbed on platinum

In considering the primary step of the surface reaction leading to the oxidation of the chemisorbed CO, four possible main reactions are considered.

i $\quad CO_a + \frac{1}{2} O_{2\,g} \rightarrow CO_{2\,g}$

ii $\quad CO_a + \frac{1}{2} O_{2\,ad}^{*} \rightarrow CO_{2\,g}$

iii $\quad CO_g + O_a \rightarrow CO_{2\,g}$

iv $\quad CO_a + O_a \rightarrow CO_{2\,g}$

The relevant thermodynamical equations are

$CO_g \rightarrow CO_a \qquad \Delta H = -48$ K cal/mole falling with coverage (84)

$\frac{1}{2} O_{2g} \rightarrow O_a \qquad \Delta H = -35$ K cal/g-atom falling with coverage (81)

* $O_{2\,ad}$ - molecular oxygen adsorbed on top of the chemisorbed layer

$CO_g + \frac{1}{2} O_{2\,g} \rightarrow CO_{2\,g}$ $\quad \Delta H = -67.5$ K cal/mole

$O_{2\,g} \rightarrow 2\,O_g$ $\quad \Delta H = +117$ K cal/mole

$O_{2\,g} \rightarrow O_{2\,ad}$ $\quad \Delta H_a \sim \Delta H_{sublimation}$

According to ref. 4, 81 CO_2 is not adsorbed on a Pt surface at 300° K and we are presuming that the desorption of the CO_2 formed requires only a small amount of energy corresponding to its heat of physical adsorption.

Hence

i $CO_a + \frac{1}{2} O_{2\,g} \rightarrow CO_{2\,g}$ $\quad \Delta H = -19.5$ K cal/mole; $\theta = 0$

ii $CO_a + \frac{1}{2} O_{2\,ad} \rightarrow CO_{2\,g}$ $\quad \Delta H = -(19.5 + \Delta H_a)$ K cal/mole; $\theta = 0$

iii $O_a + CO_g \rightarrow CO_{2\,g}$ $\quad \Delta H = -32.5$ K cal/mole; $\theta = 0$

iv $O_a + CO_a \rightarrow CO_{2\,g}$ $\quad \Delta H = +15.5$ K cal/mole; $\theta = 0$

All processes become increasingly negative with increasing coverage θ. It follows that since the activation energy is about 10 K cal/mole all these processes are possible.

From the viewpoint of ease of formation of the surface transition complex, iii and iv are more probable since they do not involve the high energy of dissociation of the O_2 molecule.

We have found experimentally that iii is very rapid compared with i or ii, and iv is very slow because if an oxidation is interrupted by removing O_2 from the gasphase, i.e. when both CO_a and O_a are present on the surface, the reaction ceases but commences immediately at the same rate if the same pressure of oxygen is reintroduced as that preceeding the interruption.

This conclusion was unexpected. Thus for a typical run, we may assume that 20% of the effective Pt surface is covered with chemisorbed oxygen O_a and the remainder with CO_a, i.e. chemisorbed carbon monoxide. Then the probability that a CO_a and an O_a species are adjacent to each other on the surface is $0.8 \times 0.2 = 0.16$, and full coverage corresponds to 1.25×10^{15} species per cm^2 Pt. If the activation energy of about 10 K cal/mole for the reaction is derived from the vibrational energy of the adsorbent, the rate of CO_2 formation is at 273° K.

$$0.16 \times 1.25 \times 10^{15} \times 10^{13} \times \exp\left(-\frac{10000}{2 \times 273}\right) \frac{\text{molecules}}{\text{cm}^2 \times \text{sec}}$$

$$2 \times 10^{19} \text{ molecules/cm}^2\text{.sec}$$

and hence by a factor of 10^6 - 10^7 higher than the observed highest initial rate of CO_2 evolution.

In order for this reaction iv to be rate determining

the activation energy of the reaction must be therefore almost 20 K cal/mole.

For process i we can calculate the rate of reaction assuming that each molecular collision of an O_2 molecule from the gasphase leads to a reaction provided the necessary activation energy of about 10 K cal/mole is available.

The number of collisions per cm^2 and sec is

$$Z = 3.52 \times 10^{22} \frac{P}{M^{1/2}\, T^{1/2}} \left[\frac{1}{sec.cm^2}\right]$$

where P is the oxygen pressure in mm Hg,

M is the molecular weight, and

T is the absolute temperature.

At 273° K and P = 1 mm Hg the rate of collisions is 3.9×10^{20} sec^{-1} cm^{-2} and with E about 10000 cal this is reduced to an effective rate

$$Z_{eff} = 3.9 \times 10^{20} \times 10^{-8} = 3.9 \times 10^{12} \text{ sec}^{-1} \text{ cm}^{-2}$$

compared with the experimental figures of 1.6×10^{13} molec.sec^{-1} cm^{-2} (S.P. result; film B; $T = 273^{\circ}$ K; $P = 1$ mm Hg; $\theta_{CO} = 1$) and 6.6×10^{11} molecules sec^{-1} cm^{-2} (I.R. result; Pt-pellet; $T = 273^{\circ}$ K; $P = 0.9$ mm Hg; $\theta_{CO} = 1$).

Hence, the collision theory provides a simple model which would explain the experimental figures satisfactorily. But for an oxidation reaction by means of a direct collision between an oxygen molecule from the gasphase and a chemisorbed carbon monoxide molecule the reaction velocity should be directly proportional to the oxygen pressure.

According to fig. 31 the rate of the oxidation velocity with the oxygen pressure gradually decreases as the pressure rises.

We, therefore, conclude that the oxygen forms a second molecularly adsorbed layer on top of the chemisorbed carbon monoxide and that the reaction with the underlying carbon monoxide takes place from this adsorbed oxygen layer.

We postulate for the oxidation of the chemisorbed carbon monoxide the following mechanism

$$(1,2)\quad O_2\,g \underset{2}{\overset{1}{\rightleftharpoons}} O_2\,ad \qquad V_1,\ V_2;\ E_1,\ E_2$$

$$(3,4)\quad O_2\,ad + CO_a \underset{4}{\overset{3}{\rightleftharpoons}} CO_3\,a \qquad V_3,\ V_4;\ E_3,\ E_4$$

(5,6) $CO_{3\,a} + CO_a \underset{6}{\overset{5}{\rightleftharpoons}} 2\ CO_{2\,g}$ $\qquad V_5,\ V_6;\ E_5,\ E_6$

Hence

(7) $$\frac{d(CO_{3a})}{dt} = k_3(O_{2ad})(CO_a) - k_4(CO_{3a}) + k_6(CO_{2g})^2 - k_5(CO_{3a})(CO_a)$$

As the formed CO_2 is continually frozen out during the reaction it is

(8) $$k_6(CO_{2\ g})^2 \ll k_5(CO_{3\ a})(CO_a)$$

Assuming steady state conditions

(9) $$\frac{d(CO_{3\ a})}{dt} = 0$$

we get

(10) $$k_3(O_{2\ ad})(CO_a) = (CO_{3\ a})\left[k_4 + k_5(CO_a)\right]$$

and

(11) $$(CO_{3\ a}) = \frac{k_3}{k_4 + k_5(CO_a)} \times (CO_a) \times (O_{2\ ad})$$

Inserting (11) in

(12) $$\frac{d(CO_{2\ g})}{dt} = k_5(CO_a)(CO_{3\ a})$$

we get

(13) $$\frac{d(CO_{2\ g})}{dt} = \frac{k_5 \cdot k_3}{k_4 + k_5(CO_a)} \times (CO_a)^2\ (O_{2\ ad})$$

Assuming that the velocity of decomposition of the $CO_{3\ a}$ complex V_4 is much bigger than the reaction velocity V_5 between a $CO_{3\ a}$ and a neighbouring CO_a species we can impose the restriction

(14) $$k_5(CO_a) \ll k_4$$

and we get

(15) $$\frac{d(CO_{2\ g})}{dt} = \frac{k_5 \cdot k_3}{k_4} \times (CO_a)^2 \times (O_{2\ ad})$$

In our further discussion the dependency of the concentration of the adsorbed oxygen on its gasphase pressure is of major importance, i.e. whether the oxygen adsorption takes place on a homogeneous surface of chemisorbed carbon monoxide in a Langmuir type of isotherm or whether the oxygen is adsorbed on a heterogeneous surface according to a Freundlich or Temkin type of isotherm.

Since the activation energy for the reaction remains constant over the major part of the process a discussion of the oxygen adsorption in terms of a Langmuir type of surface seems favourable.

Since the pressure dependency on a Langmuir isotherm requires that θ should be significant with respect to unity, one may calculate that the heat of molecular adsorption

must be ca. 10 K cal/mole, which value would be considerably greater than be expected, and moreover, the experimental value deduced from the curvature of the K_b versus $p(O_2)$ plots leads to a value of only 1-3 K cal/mole. We therefore conclude that the decreasing adsorption with coverage is not due to exclusion of sites by occupation of sites by adsorbed molecules (Langmuir hypothesis) but due to a decreasing heat of adsorption as the coverage increases.

If we assume an average heat for the physical adsorption of oxygen of 2 K cal/mole the surface coverage θ at p_{O_2} = 1 mm Hg and $T = 273^{\circ}$ K is

$$(16) \quad Z(1-\theta)\left[\frac{\text{molec}}{\text{cm}^2.\text{sec}}\right] = \theta.\exp\left(-\frac{q_a}{RT}\right)\nu N\left[\frac{\text{molec}}{\text{cm}^2.\text{sec}}\right]$$

where Z is the number of oxygen collisions with the surface,

θ the surface coverage,

q_a the heat of adsorption,

ν the frequency factor of 10^{13} sec^{-1}, and

N the number of sites/cm^2, assumed to be $1.25 \times 10^{15}/\text{cm}^2$.

At p_{O_2} = 1 mm and T = 273° K the collision rate is

$$Z = 3.8 \times 10^{20} \text{ molec.sec}^{-1}.\text{cm}^{-2}$$

Hence

$$3.8 \times 10^{20}(1 - \theta) = \theta \times 10^{-1.6} \times 10^{13} \times 1.25 \times 10^{15}$$

$$\theta = 1.2 \times 10^{-6}$$

The number of adsorbed O_2 molecules/cm² is then

$$N_{O_2} = 1.25 \times 10^{15} \times 1.2 \times 10^{-6} = 1.5 \times 10^{9}$$

This calculation demonstrates that only a minute part of the surface formed by the chemisorbed carbon monoxide is covered by oxygen.

In terms of the proposed mechanism the relationship between the concentration of the adsorbed oxygen $O_{2\,ad}$ and the gasphase pressure is given by

$$(17) \qquad (O_{2\,ad}) = \frac{k_1}{k_2} (O_{2\,g}) \times f(p,T)$$

where the term f(p,T) measures the deviation of the adsorption on a heterogeneous surface from that of a homogeneous one. This term also describes the deviation of the oxidation velocity from a direct proportionality to the oxygen pressure.

Inserting (17) into (15) we end with the following rate equation

$$(18) \qquad \frac{d(CO_{2\,g})}{dt} = \frac{k_5 \cdot k_3 \cdot k_1}{k_4 \cdot k_2} (CO_a)^2 (O_{2\,g}) \cdot f(p,T)$$

During the I.P. experiments the evolution of CO_2 was studied by observing the decrease of the chemisorbed CO at a constant oxygen pressure (0.9 mm). The kinetic of this reaction could be described by

$$(19) \qquad + \frac{d(CO_2)}{dt} = - \frac{d(CO_a)}{dt} = K_a (CO_a)^2$$

In the S.P. measurements the velocity of the evolution of CO_2 was investigated by the subsequent rapid reaction, during which the two Pt-sites freed from CO_2 were covered by oxygen according to

$$(20) \qquad Pt_2 + O_2 \rightarrow 2\ Pt\ O$$

Assuming that reaction takes place instantaneously the evolution of the CO_2 can be monitored by the surface potential and can be described by

$$(21) \qquad + \frac{d(CO_2)}{dt} = - \frac{d(CO_a)}{dt} = K_b((O_{a\,\infty}) - (O_{a\ t}))$$

(chapter 2.6).

Consistency between the first order term of the surface concentration in (21) and the square term in (19) is achieved because the oxidation process involves a reaction between two adjacent sites, i.e. between a $CO_{3\ a}$ and a CO_a species, whereas the subsequent chemisorption of the oxygen (20) on those two sites takes place in one single step.

From the temperature dependency of the velocity ν (I.R. results) we derived an apparent activation energy (chapter 2.2.2.)

$$E_{exp} = 9.6 \text{ K cal/mole.}$$

We are using this apparent activation energy figure to calculate in terms of the basic collision theory

$$(22) \qquad V_{theo} \equiv Z_{eff} = Z.\exp(-\frac{E_{exp}}{RT})$$

the theoretical reaction velocity. A comparison of the experimental velocities V_{exp} with these derived theoretical velocities provides then the steric factor P for this reaction

$$(23) \qquad P \equiv \frac{V_{exp}}{V_{theo}}$$

In tab.12 are listed the experimental reaction velocities of the I.R. results for $\theta_{co} = 1$, $p_{O_2} = 0.9$ mm Hg for various temperatures; the figure for 273° K is extrapolated by using $E_{exp} = 9.6$ K cal mole^{-1}. Additionally are listed the corresponding figures for V_{theo} and also P.

Table 12

(I.R. results)

T [° K]	V_{exp} [molec.cm^{-2}.sec^{-1}]	V_{theo}	P
273	6.6×10^{11}	7.2×10^{12}	9×10^{-2}
309	4.6×10^{12}	5.8×10^{13}	8×10^{-2}
316	6.8×10^{12}	8.8×10^{13}	8×10^{-2}
355	32×10^{12}	39×10^{13}	8×10^{-2}

In comparison with the experimental results obtained on an Aerosil supported Pt pellet are listed the corresponding figures of the four Pt-films in tab. 13. at T = 273° K and p_{O_2} = 1 mm Hg. For the calculation of the theoretical velocities V_{theo} were used the individual figures of the experimental activation energy obtained from the temperature dependency of the velocity constant K_b.

Table 13

(S.P. results)

Film	E_{exp} [K cal.mole^{-1}]	V_{exp} [molec.cm^{-2}.sec^{-1}]	V_{theo}	P
A	10	9.8×10^{13}	3.8×10^{12}	(2 6)
B	8	1.6×10^{13}	1.5×10^{14}	11×10^{-2}
C	12	0.4×10^{13}	9.5×10^{10}	42×10^{-2}
D	8	1.4×10^{13}	1.5×10^{14}	9×10^{-2}

With the exception of film A the figures of P are all in the order of 10^{-1}. The average of P taken from the results of the films B, C, D is 21×10^{-2} and rather close to the P figure of 8×10^{-2} derived from the I.R. results on the Aerosil supported Pt-pellet.

The reason why we obtained for film A a steric factor

much bigger than for the other films and the Pt-pellet is not quite clear. It could be due to the fact that this Pt film has been treated with hydrogen in an earlier stage, and it has been shown that this treatment accelerates the reaction (2.2.2).

This discussion has shown that good agreement between the experimental velocities V_{exp} and the derived figures of V_{theo} can be achieved by using a steric factor P in the order of 0.1 and the individually determined apparent activation energy E_{exp} (Tab. 12, 13).

This activation energy consists of various energy terms according to the proposed mechanism. It is

(24) $$E_5 - \left(E_4 - E_3\right) - \left(E_2 - E_1\right) = E_{exp}$$

where $E_2 - E_1$ is the heat of the adsorption of molecular oxygen on top of the layer of chemisorbed carbon monoxide,

$E_4 - E_3$ the heat of formation for the CO_3 complex, and

E_5 the activation energy for the reaction between a $CO_{3\,a}$ and a neighbouring CO_a species.

It has been shown (chapter 2.2.2 and 2.6) that these apparent activation energies remain constant over the major part of the reaction, which means that on the heterogeneous Pt catalyst surface compensation within the various

activation energy terms takes place. Equation 24 would also provide the explanation why differences in the activation energy are likely to occur depending on the activity of the Pt-catalyst.

Langmuir (4) studied the kinetic of the reaction

$$2\ CO + O_2 \rightarrow 2\ CO_2$$

on platinum, using mixed gases. His experiments were carried out at lower gas pressures (10^{-3} to 10^{-1} mm Hg) and at higher temperatures (500 to 750° K). An electrically heated Pt-wire was used as catalyst in these experiments.

It was found that the reaction velocity was proportional to the oxygen pressure and inversely proportional to the pressure of carbon monoxide.

Hence, at T = 572° K the reaction rate was found to be

$$r = 7.10 \times 10^{14}\ \frac{O_{2\,g}}{CO_g}\ \text{molecules cm}^{-2}.\text{sec}^{-1} \qquad (25)$$

This reaction rate is also proportional to the rate of desorption of carbon monoxide, the temperature coefficient of which corresponds to an activation energy of 31,800 cal/mole.

Of basic interest for the solution of Langmuir's and the present experimental results are the following two equations

$$(26)\quad \theta Z_1 = \nu \exp\left(-\frac{q_1}{RT}\right)\theta_1 N + Z_2 \cdot \theta_1 \cdot \exp\left(-\frac{E_1}{RT}\right)$$

$$(27)\quad \theta Z_2 = \nu \exp\left(-\frac{q_2}{RT}\right)\theta_2 N + Z_1 \cdot \theta_2 \cdot \exp\left(-\frac{E_2}{RT}\right)$$

$$(28)\quad V_1 = Z_2 \cdot \theta_1 \cdot \exp\left(-\frac{E_1}{RT}\right)$$

$$(29)\quad V_2 = Z_1 \cdot \theta_2 \cdot \exp\left(-\frac{E_2}{RT}\right)$$

where

ν is the frequency factor 10^{13} sec^{-1},

N is the number of sites/cm^2, assumed to be 10^{15} sites/cm^2,

θ is the bare fraction of the surface,

θ_1, θ_2 are the fractions of the surface covered by carbon monoxide and oxygen,

q_1, q_2 are the heats of chemisorption of carbon monoxide and oxygen,

E_1, E_2 are the apparent activation energies for the reaction between gaseous oxygen and carbon monoxide (V_1) and for the reaction between gaseous carbon monoxide and chemisorbed oxygen (V_2),

Z_1, Z_2 are the collision frequencies measured in molec.cm^{-2}.sec^{-1} for gaseous carbon monoxide and oxygen.

The equations 26 and 27 correspond more or less to those used by Langmuir (4) in his first approach to the solution of his kinetic problem.

The model used in these two basic equations contains various assumptions. We are assuming that the activation energies for the chemisorption of carbon monoxide and oxygen on platinum are zero, that both gases have the same sticking probability and that both gases require each one single site on the Pt surface during the course of the reaction.

No further assumptions are made towards the bonding of the chemisorbed species. The reaction rates V_1 and V_2 are described in terms of collision rates using overall, i.e. apparent activation energies E_1 and E_2 and assuming steric factors of 1 for both rates.

As no detailed assumptions are made concerning the reaction mechanism in this rigid model we do not take into account the factor 2 coming into the first and second term of equation 26 and the third term in equation 27.

Assuming that CO_2 instantaneously desorbs as it has been formed we can further state

$$\theta + \theta_1 + \theta_2 = 1 \qquad (30)$$

From the results of his experimental work carried out

at relatively high partial pressures in the order of 10^{-1} mm Hg Langmuir (4) concluded that at oxygen pressures in the order of 10^{-3} mm Hg the third term in equation 26, i.e. the reaction velocity V_1 becomes very small compared with the first and second term, i.e. the rate of chemisorption and desorption of carbon monoxide. So equation 26 is simplified to

$$(31) \quad \theta Z_1 = \nu \cdot \exp\left(-\frac{q_1}{RT}\right) \cdot \theta_1 \cdot N = \theta_1 \cdot H_1,$$

and equation 27 can be simplified to

$$(32) \quad \theta Z_2 = Z_1 \cdot \theta_2,$$

because of the high heat of chemisorption of oxygen the rate of desorption of oxygen becomes negligible compared with the rate of chemisorption of oxygen and the reaction rate V_2.

We transform equation 31 and 32 into

$$(33) \quad \theta_1 = \theta \cdot Z_1/H_1$$

and

$$(34) \quad \theta_2 = \theta \cdot Z_2/Z_1$$

Inserting these equations into equation 30 we then get

$$(35) \quad 1 = \theta \left(1 + {}^{Z_1}/_{H_1} + {}^{Z_2}/_{Z_1}\right)$$

or

$$(36) \qquad \theta = \frac{H_1 \cdot Z_1}{H_1 Z_1 + Z_1^2 + Z_2 \cdot H_1}$$

According to equation 32 the rate of reaction V_2 then becomes

$$(37) \qquad Z_1 \cdot \theta_2 = Z_2 \cdot \theta = \frac{Z_2 \cdot H_1 \cdot Z_1}{H_1 \cdot Z_1 + Z_1^2 + Z_2 \cdot H_1}$$

In order to get the Langmuir's pressure dependency we have to make the two restrictions, that

$$(38) \qquad Z_1^2 \gg H_1 Z_1$$

$$(39) \qquad Z_1^2 \gg Z_2 \cdot H_1$$

Since $p_{co} \quad p_{o_2} = 10^{-3}$ mm Hg, then $Z_1 = Z_2 = 10^{17}$ molecules $cm^{-2}.sec^{-1}$ and using $q_1 = 31.8$ K cal.mole^{-1} (4) we get for H_1 at 500^{o} K

$$(40) \quad H_1 = 10^{13} \cdot 10^{-14} \cdot 1 \cdot 10^{15} = 10^{14} \text{ molecules } cm^{-2}.sec^{-1}$$

and, hence,

$$(41) \qquad Z_1 \gg H_1$$

It follows that

$$(42) \qquad \frac{\theta_1}{\theta} = \frac{Z_1}{H_1} = 10^3 ,$$

and

$$(43) \qquad \frac{\theta_2}{\theta} = \frac{Z_2}{Z_1} = 1$$

Assuming $\theta_1 \sim 1$, for $p_{co} \sim 10^{-3}$ mm and T = 500° K,

$$(44) \qquad \theta_2 = \theta = 10^{-3}$$

At steady state conditions the surface concentrations of chemisorbed carbon monoxide N_{co}, chemisorbed oxygen N_o, and that of the bare surface sites N_b are

$$(45) \qquad \begin{aligned} N_{co} &= 10^{15} \text{ molecules cm}^{-2} \\ N_o &= 10^{12} \text{ molecules cm}^{-2} \\ N_b &= 10^{12} \text{ sites.cm}^{-2} \end{aligned}$$

When we evaluate now the reaction velocity V_2 according to equation 29 we use for the activation energy of this reaction E_2 = 0 K cal mole^{-1}, since we know from our S.P. results (chapter 2.5) that the reaction between chemisorbed oxygen and carbon monoxide from the gasphase is extremely fast even at 77° K.

Assuming $p_{co} \sim p_{o_2} = 10^{-3}$ mm Hg, and then $Z_1 = Z_2 = 10^{17}$ molecules cm^{-2}.sec^{-1} the derived reaction velocity V_2 at 500° K is

$$(46) \quad V_2 = \theta_2 . Z_1 = 10^{-3} . 10^{17} = 10^{14} \text{ molec.cm}^{-2}.\text{sec}^{-1}$$

compared with the experimental velocity figure at 506° K which is

(47) $V_{exp} = 2.6 \times 10^{13}$ molec.cm^{-2}.sec^{-1}

($p_{co} = 2.6 \times 10^{-3}$ mm; $p_{o_2} = 1.5 \times 10^{-3}$ mm Hg)

For p_{co} p_{o_2} this experimental figure would then be by a factor of 2.6/1.5 = 1.7 higher.

Hence,

(48) $V_{exp} = 4.3 \times 10^{13}$ molec.cm^{-2}.sec^{-1},

which agrees well with the derived figure V_2 for the reaction velocity.

Since E_2 / 0 K cal.mole^{-1}, V_2 is extremely rapid except when θ_2 is extremely small. On introducing equal pressures of CO and O_2 the value of θ_2 would at $t_i = 0$, be $\frac{1}{2}$. Hence, the time which the reaction requires to reach steady state concentrations (45) on the platinum surface, and the amount of CO_2 formed during this initial period are of considerable interest; should these be large compared with the total time of experiment (10 min) and total CO_2 produced, then Langmuir's measurements do not subscribed to the steady state considerations required in the mathematical treatment above (equation 45).

We are assuming that the rate at which the concentration

of oxygen on the Pt surface decreases by the reaction with the carbon monoxide from the gasphase to its steady state value is proportional to the reaction velocity V_2 (equation 29). Then,

$$(49) \qquad -\frac{d(N.\Theta_2)}{dt} = Z_1 \cdot \Theta_2 = V_2$$

and

$$(50) \qquad \frac{d\Theta_2}{\Theta_2} = -\frac{Z_1}{N} \cdot dt$$

The integration of equation 50 between $\Theta_{2,i}$ at time $t_i = 0$ and the steady state figure $\Theta_{2,f}$ at time t_f brings us to

$$(51) \qquad \log \frac{\Theta_{2,i}}{\Theta_{2,f}} = -\frac{Z_1}{2.3.N} (t_i - t_f)$$

Assuming that at $t_i = 0$ half of the Pt surface is covered by chemisorbed oxygen, i.e. $\Theta_{2,i} = 0.5$, the time required to reach steady state conditions is then

$$(52) \qquad t_f = + \log \frac{0.5}{\Theta_{2,f}} \times \frac{2.3.N}{Z_1}$$

and taking

$$\Theta_{2,f} = 10^{-3}$$
$$N = 10^{15} \text{ sites cm}^{-2}$$
$$Z_1 = 10^{17} \text{ molec.cm}^{-2}.\text{sec}^{-1}$$

the time t_f is 6×10^{-2} sec, which means that in about one tenth of a second steady state conditions are achieved.

The amount of CO_2 formed during this time is almost 5×10^{14} molecules.cm^{-2}, when a figure of $\theta_{2,i} = 0.5$ and oxygen chemisorbed in atoms is assumed.

This amount would be big enough to have effect on the few experiments with low reaction velocity figures of Langmuir's work (4), but it should be hardly detectable when the reaction takes place with high velocities, since the pressure readings were made in Langmuir's experiments in one-minute-time intervals.

As we have pointed out before, the rigid model which we have been using in the previous discussion assumes single site chemisorption for oxygen and carbon monoxide molecules.

Hence, this model apparently disagrees with the experimental evidence from the present work that carbon monoxide is chemisorbed in a linear structure on platinum and occupies at 300° K only half as many sites as the chemisorbed oxygen molecule. Thus, both species occupy under normal conditions at least, when the surface is covered by one species only, different numbers of sites and not the same as required by the model.

But reasonable agreement can be achieved, when we

assume that the oxygen molecule is chemisorbed during the reaction as such on a single site without further dissociation.

This assumption would necessarily involve a two step mechanism for the reaction between this kind of molecular oxygen species and the carbon monoxide.

One possibility would be that a $CO_{3\ a}$ complex is formed as intermediate as the gaseous CO molecule hits the chemisorbed $O_{2\ a}$ species. The further reaction of this complex could then take place with an adjacent CO_a species forming two CO_2 molecules which desorb.

This kind of mechanism would change equation 32 into

$$\theta Z_2 = Z_1 \cdot \theta_2 \cdot \theta_1 \tag{53}$$

But as θ_1, i.e. the coverage of the chemisorbed CO is practically unity the introduction of θ_1 would not essentially alter the further derivation according to the proposed single site mechanism (equation 26 to 46).

For this model the heat of chemisorption of undissociated oxygen molecules has to be assumed to be smaller than that of dissociated oxygen and, hence, the rate of desorption would become more important as for the dissociated oxygen species. But this would not affect equation 53 as long as the heat of chemisorption of

molecular oxygen is about that of carbon monoxide, i.e. > 30 K cal $mole^{-1}$.

To maintain this type of mechanism the additional restriction has to be made that the number of double sites does not increase during the reaction. This can be achieved by assuming surface mobility of the chemisorbed CO on Pt at $T > 500^{\circ}$ K.

We are discussing now the experimental results of the present work on the basis of the same model in terms of which we could derive the reaction velocity V_2 in good agreement with the experimental figures given by Langmuir (4).

In table 14 are compared the conditions at which Langmuir's experiments were carried out with those for the present work. This table also contains the pressure dependency of the reaction and the figures of the activation energies for both sets of experiments.

When we assume thermal equilibrium for the carbon monoxide on the Pt catalyst at 300° K the equilibrium pressure in the gasphase during the I.R. and S.P. experiments would be extremely small and according to Langmuir (4) in the order of 10^{-17} mm Hg.

At this very low CO pressure the rate of chemisorption in equation 26 becomes negligible. Negligible is also the rate of desorption of the chemisorbed CO which is in the order of 10^5 molec.cm^{-2}.sec^{-1} at 300° K and $q_1 = 31.8$ K cal $mole^{-1}$ (4).

Table 14

Langmuir results (4)	Results of present work
T: 500-750° K	T = 250-370° K
$P_{co} \sim P_{o_2} \sim 10^{-3} - 10^{-1}$ mm Hg	$P_{o_2} \sim 1$ mm Hg $P_{co} \sim 10^{-17}$ mm Hg according to (4) for T = 300° K
$\theta_{co} \sim 1$, almost constant $\theta_o = 10^{-3}$, almost constant (T = 500° K, p_{co} p_{o_2} = 10^{-3} mm Hg)	$\theta_{co} = 1$, decreasing to $\frac{1}{6}$ to $\frac{1}{10}$ $\theta_o = 0$, increasing, so that $\theta_{co} + \theta_o = 1$
rate $\propto H_{co} \frac{P_{o_2}}{P_{co}}$ H_{co} - rate of desorption of CO for $\theta_{co} = 1$	rate $\propto CO_a^2 \cdot P_{o_2} \cdot f(T, P_{o_2})$ CO_a - concentration of chemisorbed CO
E_{exp} = 31.8 K cal/mole	E_{exp}: 8-12 K cal/mole, depending on the activity of the surface.

Under the experimental conditions of the present work, i.e. pressure of oxygen in the order of 1 mm Hg, the last term in equation 26, i.e. the reaction velocity V_1 becomes now important. This velocity has been found to be in the order of 10^{13} molecules $cm^{-2}.sec^{-1}$ at p_{O_2} = 1 mm Hg and T = 273° K.

As the Pt sites are getting freed from carbon dioxide, which has been formed, they are subsequently covered by chemisorbed oxygen, the rate of which in equation 27 was assumed to be equal to the rate of reaction V_1.

The two other terms in equation 27, i.e. the rate of desorption and the reaction velocity V_2 become negligible under the experimental conditions of the present work, the first because of the high heat of chemisorption for oxygen, the latter due to the extremely low partial pressure of carbon monoxide in the gasphase.

When we use for E_1 in equation 28 our experimental figure of 10 K cal $mole^{-1}$ to calculate V_1 under the experimental conditions of Langmuir's work, i.e. $p_{O_2} \sim 10^{-3}$ mm Hg and T = 500° K, this comes out to be according to equation 28

$$V_1 = 10^{17} \cdot 1 \cdot 5 \times 10^{-5} = 5 \cdot 10^{12} \text{ molec.cm}^{-2}.\text{sec}^{-1}$$

Hence, V_1 comes out to be only $^1/_{20}$ of the figures of the major velocities in equation 26 and 27, i.e. the rate of

chemisorption of oxygen, and the rate of reaction between CO from the gasphase and chemisorbed oxygen. These figures are all about the same, i.e. 10^{14} molec.cm^{-2}.sec^{-1} ($T = 500^{o}$ K, $p_{co} \sim p_{o_2} = 10^{-3}$ mm Hg, $q_1 = 31.8$ K cal $mole^{-1}$ and $E_2 = 0$ K cal.$mole^{-1}$). Hence, an increase of both partial pressures by a factor of 20 would bring up the reaction velocity V_1 in the same order as V_2.

This conclusion agrees well with the experimental dependency of the overall reaction velocity on the oxygen partial pressure which Langmuir described (4). So, Langmuir found that at 200^{o} C the velocity V_1 would equalize V_2 when both partial pressures are increased from p 10^{-3} mm Hg to about 3×10^{-2} mm Hg, i.e. by a factor of 30.

During this discussion the same model and the same basic equations 26 and 27 have been successfully used to derive the reaction velocities V_1 and V_2 in terms of the basic collision theory and in good agreement with the experimental results of Langmuir's and the present work.

Hence, consistency has been achieved between different rate equations for the oxidation of carbon monoxide on a platinum catalyst which are solely due to different reaction

mechanism working under different conditions of pressure and temperature.

REFERENCES

1. R. P. Eischens, W. A. Pliskin, and S. A. Francis
J. Chem. Phys. 22, 1786 (1954)

2. T. Delchar, A. Eberhagen and F. C. Tompkins
J. Sci. Instr. 40, 105 (1963)

3. F. Bloyart, L. D'Or and J. C. P. Mignolet
J. Chim. Phys. 54, 53 (1957)

4. I. Langmuir
Trans. Farad. Soc. 17, 621 (1922)

5. V. Crawford
Quart. Revs. 14, 378 (1960)

6. A. V. Kislev and V. I. Lygin
Russ. Chem. Revs. 31, 175 (1962)

7. G. Blyholder and D. O. Bowen
J. Phys. Chem. 66, 1288 (1962)

8. G. Blyholder and L. D. Neff
J. Phys. Chem. 66, 1464 (1962)

9. G. Blyholder and L. D. Neff
J. Catal. 2, 138 (1963)

10. R. P. Eischens and W. A. Pliskin
Adv. Catal. 10, 2 (1958)

11. R. P. Eischens and W. A. Pliskin
Actes II^{ieme} Congr. Intern. Catal. 1961 TOME 1, 789

12. R. P. Eischens and W. A. Pliskin
Z. phys. Chem. N.F. 24, 11 (1960)

13. R. P. Eischens and J. Jacknow
Proc. 3rd Int. Congr. Catal. Amsterdam (1964), 1, 627

14. N. N. Kavtaradze and N. P. Sokolova
Russ. J. of Phys. Chem. (Transl.) 36, 1529 (1962)

15. R. J. Irving and E. A. Magnusson
J. Chem. Soc. 1958, pg. 2283

16. K. Noack
Helv. Chim. Act. 45, 1847 (1962)

17. G. Ewing
J. Chem. Phys. 37, 2250 (1962)

18. H. A. Benesi and A. C. Jones
J. Phys. Chem. 63, 179 (1959)

19. N. G. Yaroslavsky and A. N. Terenin
Doklady Akad. Nauk. SSSR 66, 885 (1949)

20. R. McDonald
J. Am. Chem. Soc. 79, 850 (1957)

21. G. J. C. Frohnsdorff and G. L. Kington
Trans. Farad. Soc. 55, 1173 (1959)

22. A. Eberhagen, D. O. Hayward and F. C. Tompkins
to be published

23. D. O. Hayward, C. McManus and F. C. Tompkins
to be published

24. A. C. Collins and B. M. W. Trapnell
Trans. Farad. Soc. 53, 1476 (1957)

25. E. Lippert and R. Mecke
Z. Elektrochem. 55, 366 (1951)

26. D. A. Ramsay
J. Am. Chem. Soc. 74, 72 (1952)

27. G. Blyholder
IIIrd Int. Congr. on Cat. Amsterdam 1964, I, 38

28. G. Blyholder
J. Phys. Chem. 68, 2772 (1964)

29. M. V. C. Sastri and T. S. Viswanathen
J. Am. Chem. Soc. 77, 3967 (1955)

30. W. F. Edgell and R. Summit
J. Am. Chem. Soc. 83, 1772 (1961)

31. W. Beck, W. Hieber and G. Braun
Z. anorg. und allg. Chem. 308, 23 (1961)

32. H. J. Emeleus and J. S. Anderson
Modern Aspects of Inorganic Chemistry 1960, pg. 268

33. A. C. Yang and C. W. Garland
J. Phys. Chem. 61, 1504 (1957)

34. N. N. Kavtaradze and V. I. Lygin
Doklady Akad. Nauk. SSSR. 138, 618 (1961)

35. R. P. Eischens and W. A. Pliskin
Adv. Cat. 9, 664 (1957)

36. C. Weissmantel, K. Schwabe and G. Hecht
Werkstoffe und Korrosion 12, 353 (1961)

37. L. Brewer
Chem. Revs. 52, 1 (1953)

38. L. Wöhler
Z. anorg. Chem. 40, 423 (1904)

39. P. H. Lewis
J. Phys. Chem. 67, 2151 (1963)

40. W. E. Garner, F. S. Stone and P. F. Tiley
Proc. Roy. Soc. (London) A 211, 472 (1952)

41. R. Rudham and F. S. Stone
in "Chemisorption", Proc. Chem. Soc. Symposium, 1956
(W. E. Garner, ed), p. 205

42. R. M. Dell and F. S. Stone
Disc. Farad. Soc. 50, 501 (1954)

43. F. S. Stone
Adv. Cat. 13, 1 (1962)

44. R. A. Gardener and R. H. Petrucci
J. Phys. Chem. 67, 1376 (1963)

45. G. Herzberg
Molecular Spectra and Molecular Structure
I. Spectra of Diatomic Molecules
D. Van Nostrand Co. Inc., Princeton, N.Y., 1955,
pg. 522

46. J. H. Taylor and C. H. Amberg
Can. J. Chem. 39, 535 (1962)

47. L. H. Little and C. H. Amberg
Can. J. Chem. 40, 1997 (1962)

48. R. P. Eischens, S. A. Francis and W. A. Pliskin
J. Phys. Chem. 60, 194 (1956)

49. J. W. Cable and R. K. Sheline
Chem. Rev. 56, 1 (1956)

50. G. Blyholder
J. Chem. Phys. 36, 2036 (1962)

51. L. E. Orgel "Transition Metal Chemistry"
Methuen and Co., Ltd., London

52. L. O. Brockway and P. C. Cross
J. Chem. Phys. 3, 828 (1935)

53. W. Sutton and J. B. Bentley
Nature, 130, 314 (1932)

54. J. Ladell, B. Port and I. Fankuchen
Acta Cryst. 5, 795 (1952)

55. L. E. Orgel
Inorg. Chem. 1, 25 (1962)

56. L. E. Orgel
Int. Conf. on Coordination Chemistry, London 1959, 93
Special Publication No. 13, The Chemical Society,
Burlington House, London, W.1.

57. C. J. Ballhausen "Introduction to Ligand Fieldtheory"
McGaw Hill Book Co., N.Y. 1962

58. J. W. Richardson "Organometallic Chemistry"
H. Zeiss, Ed., Reinhold Publishing Corp., N.Y. 1960

59. C. A. Coulson
Valence, Oxford University Press 1961

60. E. W. Abel
Quart. Rev. 17, 133 (1963)

61. R. A. Gardner
J. Cat. 3, 7 (1964)

62. G. M. Schwab and K. Gossner
Z. phys. Chem. N.F. 6, 39 (1958)

63. A. G. Daglish and D. D. Eley
Proc. 2nd Int. Congr. Cat. Paris 1960, 1615

64. A. F. Benton and R. T. Bell
J. Am. Chem. Soc. 56, 501 (1934)

65. S. J. Stephens
J. Phys. Chem. 63, 188 (1959)

66. E. G. Alexander and W. W. Russel
J. Phys. Chem. 68, 1615 (1964)

67. T. Delchar
Thesis 1963, Imperial College, London

68. L. V. Culver and F. C. Tompkins
Adv. Cat. 11, 67 (1959)

69. A. Eberhagen
Fortschr. d. Phys. 8, 245 (1960)

70. F. Bloyart, L. D'Or, J. C. P. Mignolet
J. Chim. Phys. 54, 53 (1957)

71. unpublished data

72. G. J H. Dorgelo and W. M. H. Sachtler
Naturwissenshaften 46, 576 (1959)

73. W. J. M. Drotsaert, L. L. van Reijen and
W. M. H. Sachtler
J. Cat. 1, 416 (1962)

74. J. Giner and E. Lange
Naturw. 40, 506 (1953)

75. C. W. Oatley
Proc. Phys. Soc. 51, 318 (1936)

76. W. Moffit
Proc. Roy. Soc. (Lond) 196 A, 524 (1949)

77. E. O. Fischer
Int. Conf. Coord. Chem., London 1959, pg. 87
Special publ. No. 13, The Chemical Society,
Burlington House, London W.1.

78. J. Chatt and F. A. Hart
J. Chem. Soc. 1960, pg. 1378

79. R. S. Nyholm
Proc. Roy. Soc. 1961, pg. 273

80. H. Chou, R. A. Fischer, E. Tomezsko and J. G. Aston
Act. IIieme Cong. Int. Cat. 1961, I, 217

81. D. Brennan, D. O. Hayward and B. M. W. Trapnell
Proc. Roy. Soc. A 256, 81 (1960)

82. G. Ehrlich
J. Chem. Phys. 34, 39 (1961)

83. W. R. Patterson and C. Kemball
J. Cat. 2, 465 (1963)

84. D. Brennan and F. G. Hayes
Phil. Trans. Roy. Soc. to be published